Electronic Supplementary Information

†Preparation of $Ru_3(CO)_8$-pyridine-alcohol cluster and its use for selective catalytic transformation of primary to secondary amines

Ajeet Singh,[a] Shaikh M. Mobin*[,a,b,c] and Pradeep Mathur*[,a]

[a]Discipline of Chemistry, [b]Discipline for Biosciences and Bio-Medical Engineering, and [c] Discipline of Metallurgy Engineering and Materials Science, Indian Institute of Technology Indore, Simrol, Khandwa Road, Indore 453552, India

Email address: Shaikh M. Mobin (xray@iiti.ac.in) and Pradeep Mathur (director@iiti.ac.in)

Content:

Table S1. Selected bond lengths (Å) and bond angles (°)

Bond Lengths for 1						
Atom	Atom	Length/ **Å**		Atom	Atom	Length/ **Å**
Ru1	Ru2	3.0697(3)		Ru1	N1	2.211(2)
Ru1	Ru3	2.8130(3)		Ru1	C16	1.860(3)
Ru2	C18	1.860(3)		Ru1	C15	1.854(3)
Ru2	Ru3	2.8147(3)		O1	C7	1.422(3)
Ru1	O1	2.1178(16)		O4	C16	1.159(3)
Ru1	O2	2.1558(16)				

Bond Angles for 1							
Atom	Atom	Atom	Angle/ °	Atom	Atom	Atom	Angle/ °
Ru3	Ru1	Ru2	56.972(7)	N1	Ru1	Ru2	113.08(5)
O1	Ru1	Ru2	44.15(5)	O2	Ru1	Ru3	82.35(5)

Bond Lengths for 2						
Atom	Atom	Length/ **Å**		Atom	Atom	Length/ **Å**
Ru2	Ru1	3.0307(4)		Ru1	O1	2.096(3)
Ru2	Ru3	2.7919(5)		Ru1	N1	2.243(4)
Ru2	O2	2.104(3)		Ru1	C17	1.845(5)
Ru2	O1	2.116(3)		Ru1	C18	1.838(4)
Ru2	N2	2.251(3)		Ru3	C23	1.940(5)
Ru2	C19	1.840(5)		Ru3	C21	1.936(5)
Ru2	C20	1.840(5)		Ru3	C24	1.910(6)
Ru1	Ru3	2.8038(5)		Ru3	C22	1.928(6)
Ru1	O2	2.112(3)				

Bond Angles for 2							
Atom	Atom	Atom	Angle/ °	Atom	Atom	Atom	Angle/ °
Ru3	Ru2	Ru1	57.398(13)	N1	Ru1	Ru2	110.35(10)
O2	Ru2	Ru1	44.14(8)	N1	Ru1	Ru3	167.29(10)
O2	Ru2	Ru3	85.19(8)				

Bond Lengths for 3						
Atom	Atom	Length/ **Å**		Atom	Atom	Length/ **Å**

Ru1	Ru2	3.0448(9)		Ru2	N2	2.239(6)
Ru1	Ru3	2.7808(9)		Ru2	C17	1.845(10)
Ru1	O1	2.084(5)		Ru2	C18	1.830(9)
Ru1	O3	2.135(5)		Ru3	C19	1.942(10)
Ru1	N1	2.215(6)		Ru3	C22	1.921(11)
Ru1	C16	1.858(10)		Ru3	C20	1.912(10)
Ru1	C15	1.823(9)		Ru3	C21	1.937(10)
Ru2	Ru3	2.7651(10)		O1	C6	1.412(8)
Ru2	O1	2.140(5)		O3	C13	1.410(8)
Ru2	O3	2.081(5)		Ru2	N2	2.239(6)

Bond Angles for 3							
Atom	Atom	Atom	Angle/°	Atom	Atom	Atom	Angle/°
Ru3	Ru1	Ru2	56.45(2)	N1	Ru1	Ru2	101.03(18)
O1	Ru1	Ru2	44.61(13)	N1	Ru1	Ru3	156.97(19)
O1	Ru1	Ru3	81.62(13)				

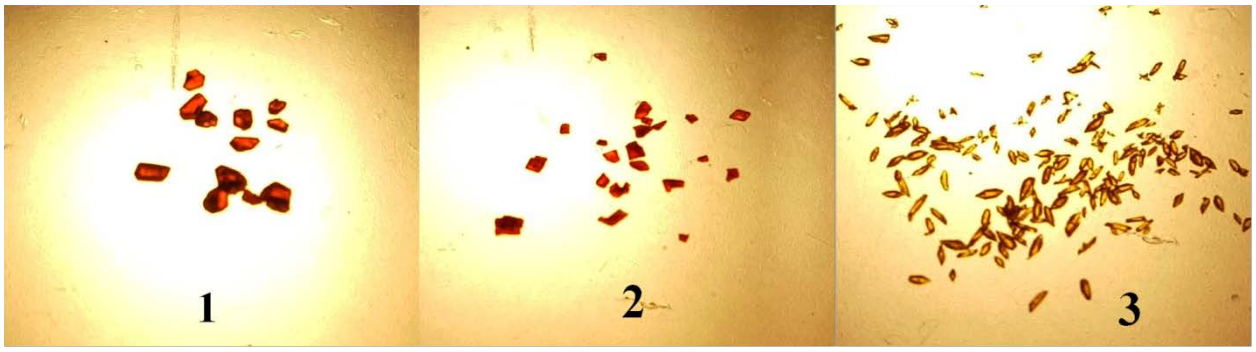

Fig. S1. Image of complexes **1–3** obtained after re-crystallizing from toluene

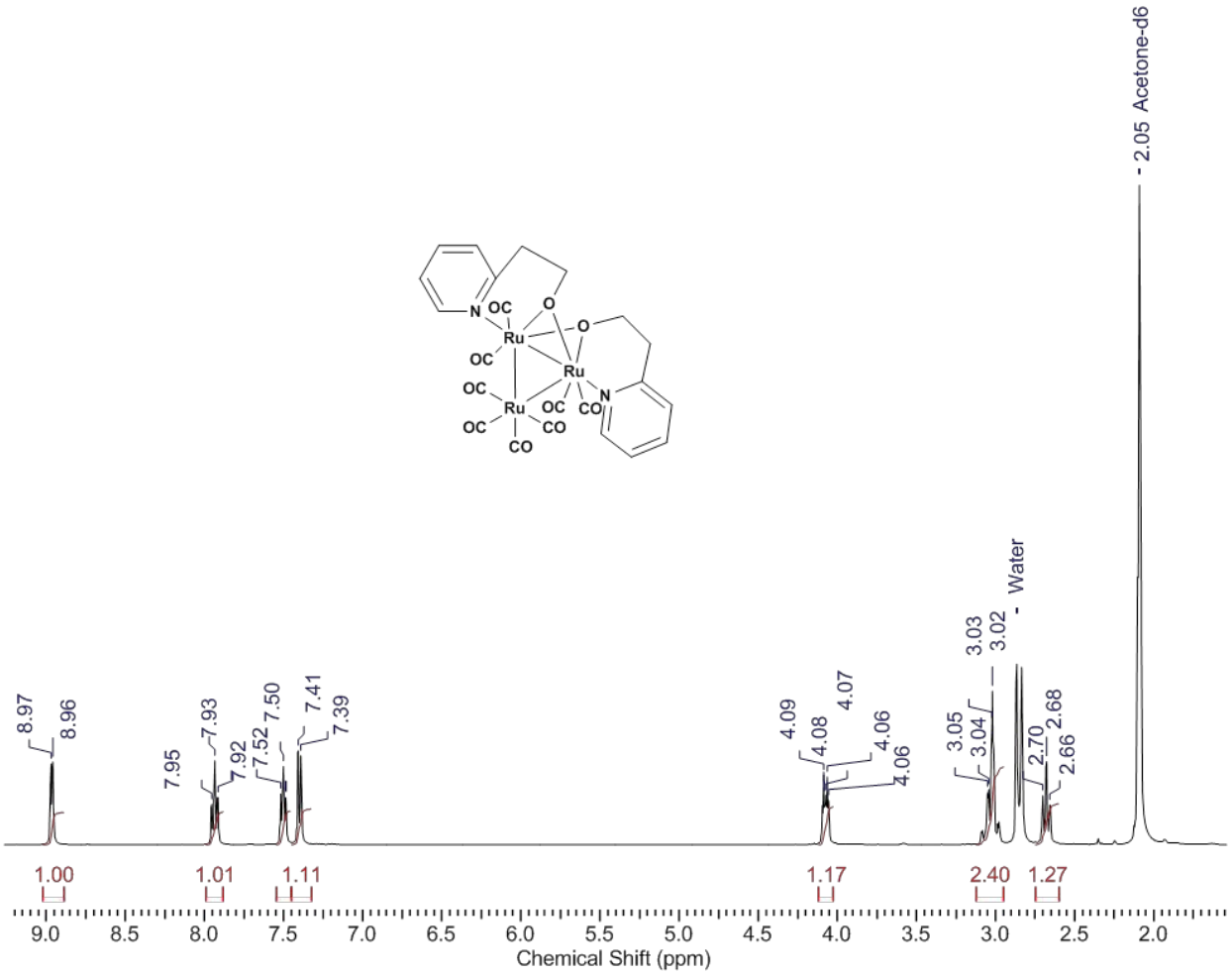

Fig. S2. ^{1}H NMR of **1**

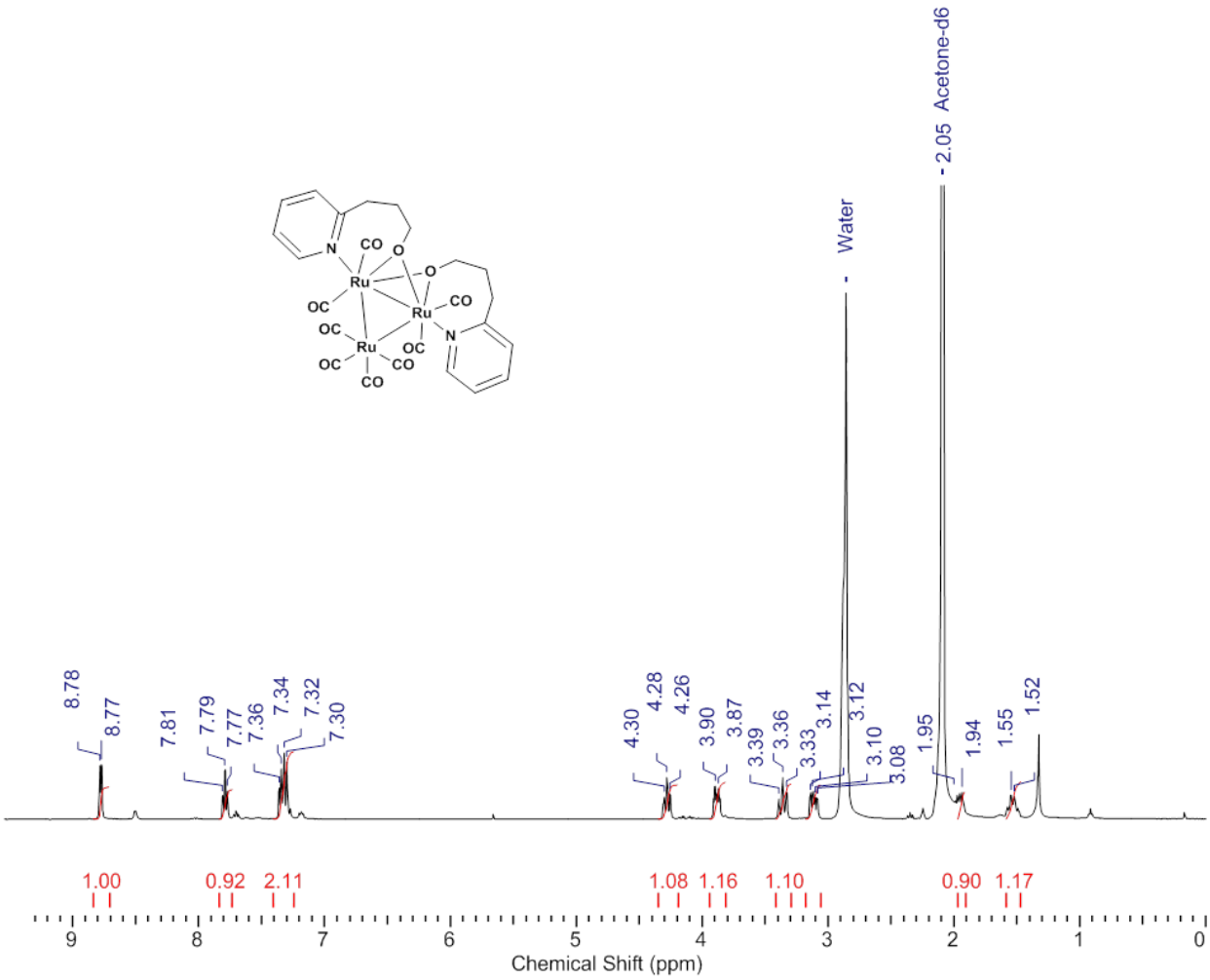

Fig. S3. ^{1}H NMR of **2**

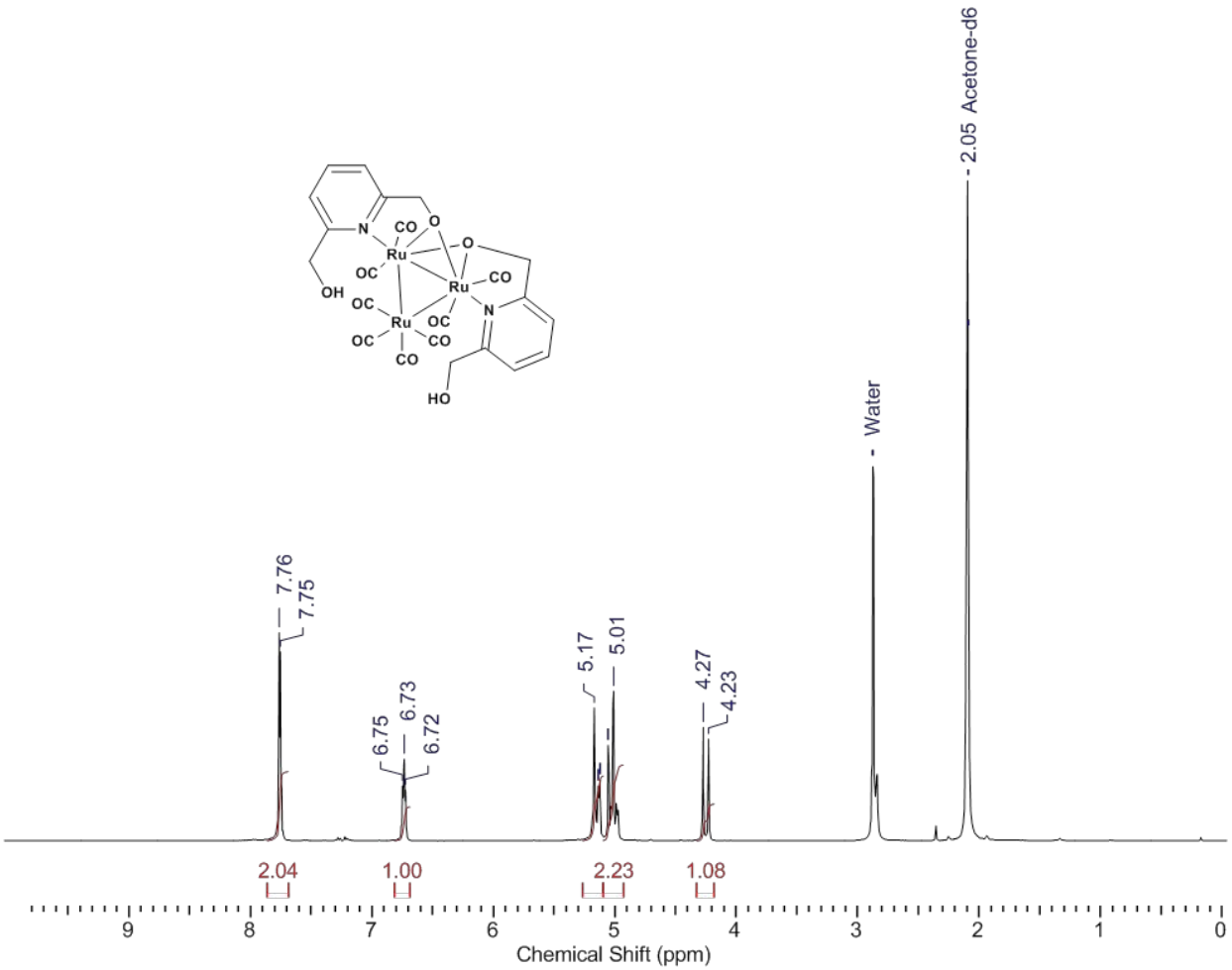

Fig. S4. ^{1}H NMR of **3**

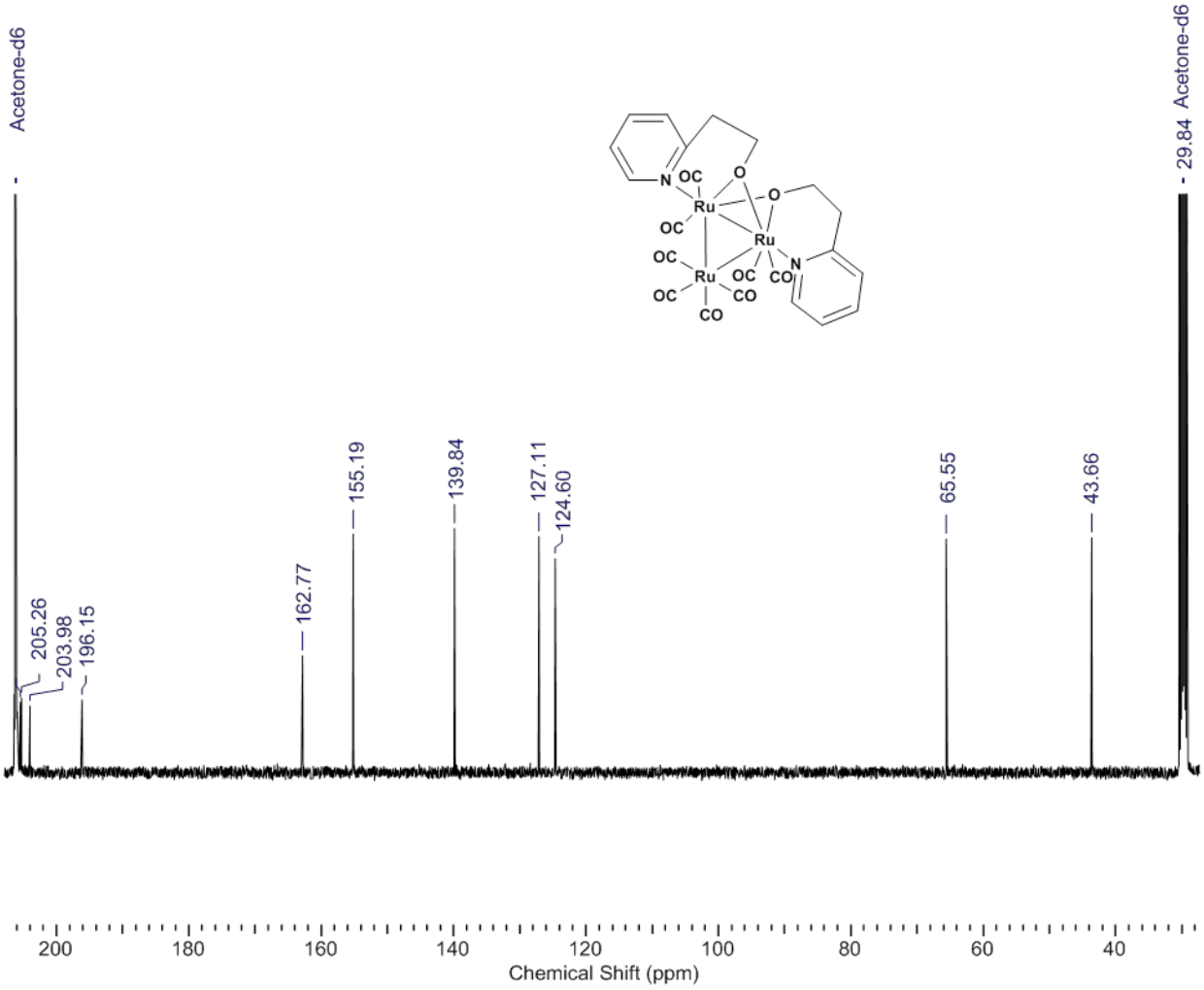

Fig. S5. ^{13}C NMR of **1**

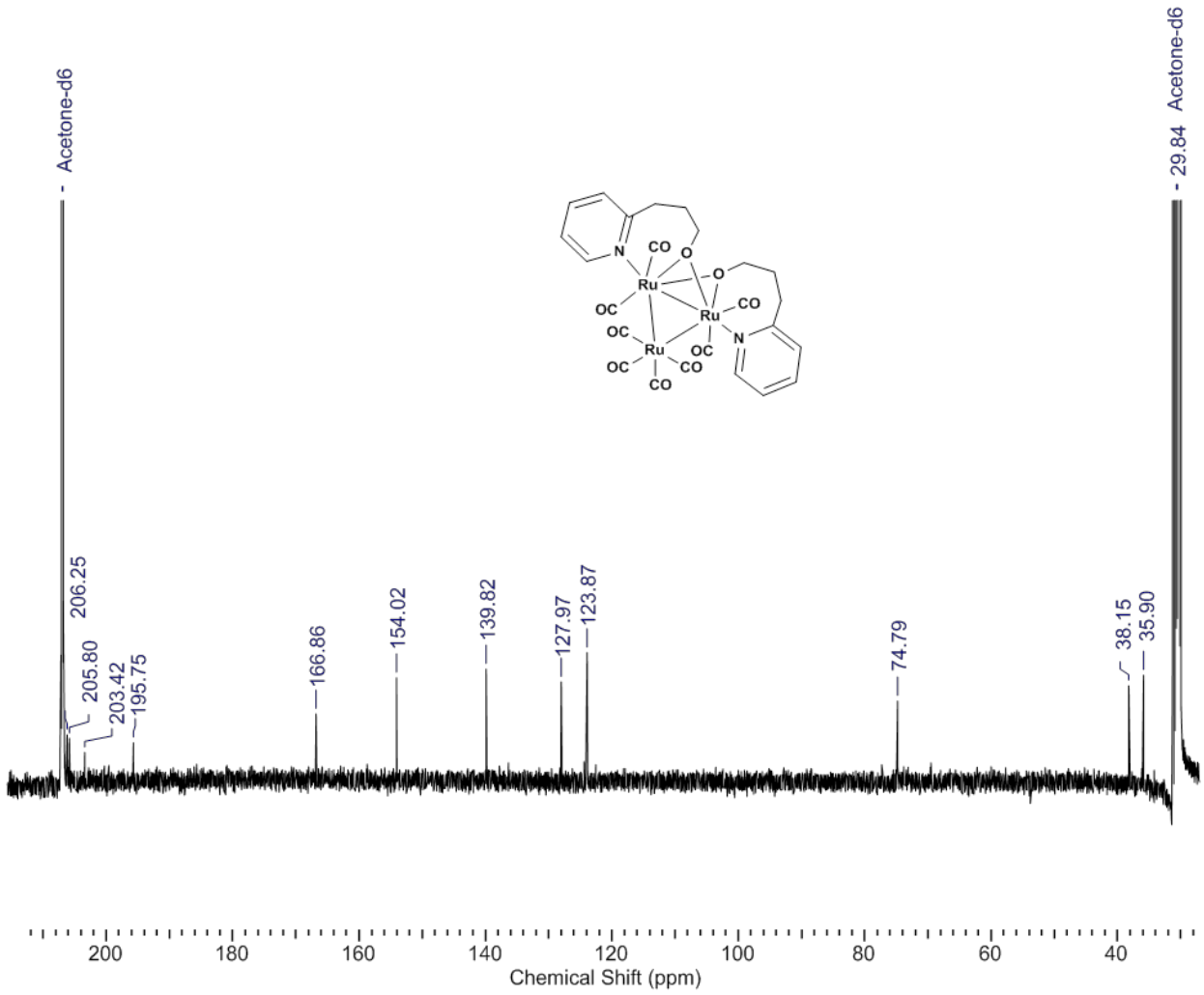

Fig. S6. ^{13}C NMR of **2**

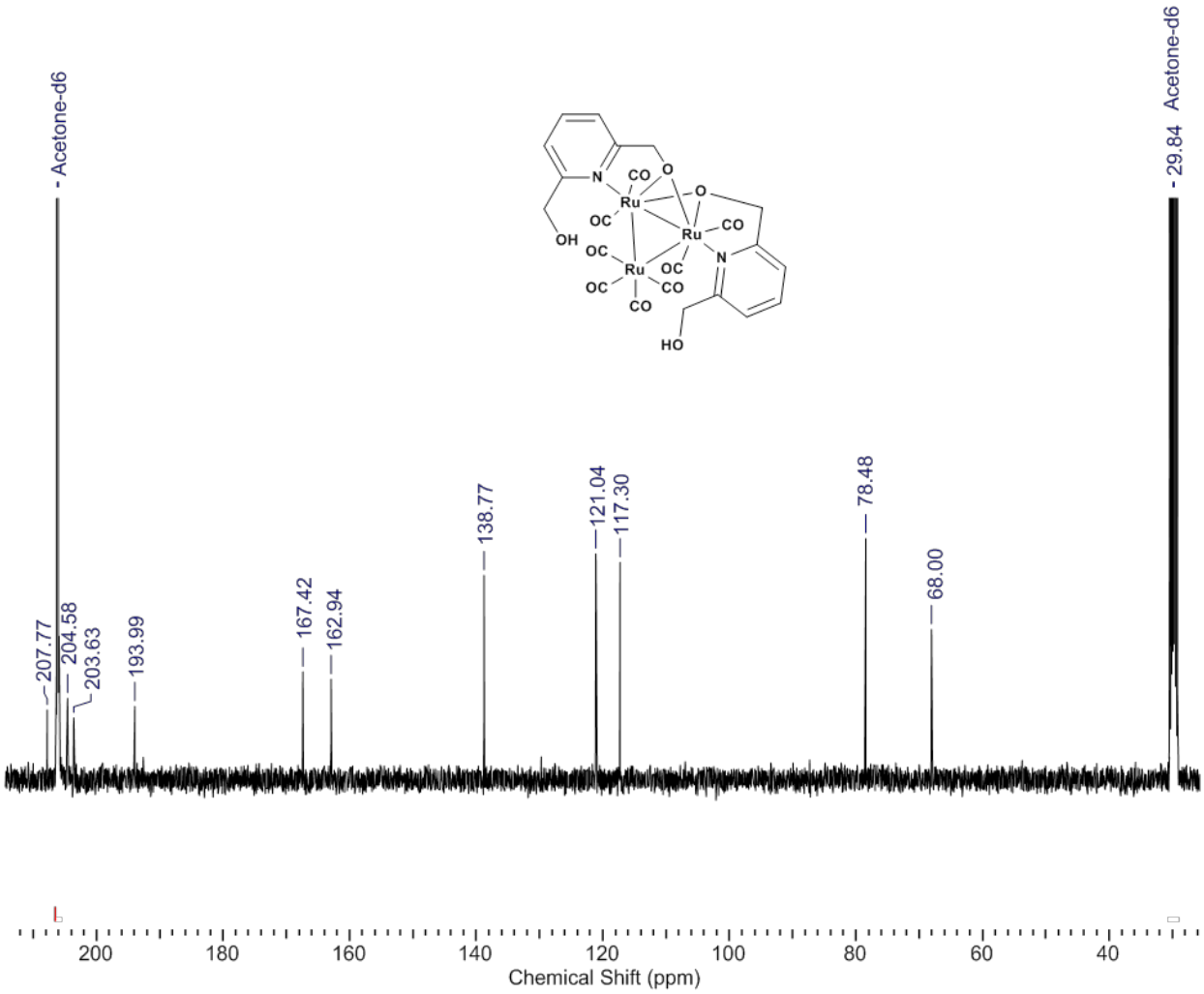

Fig. S7. ^{13}C NMR of **3**

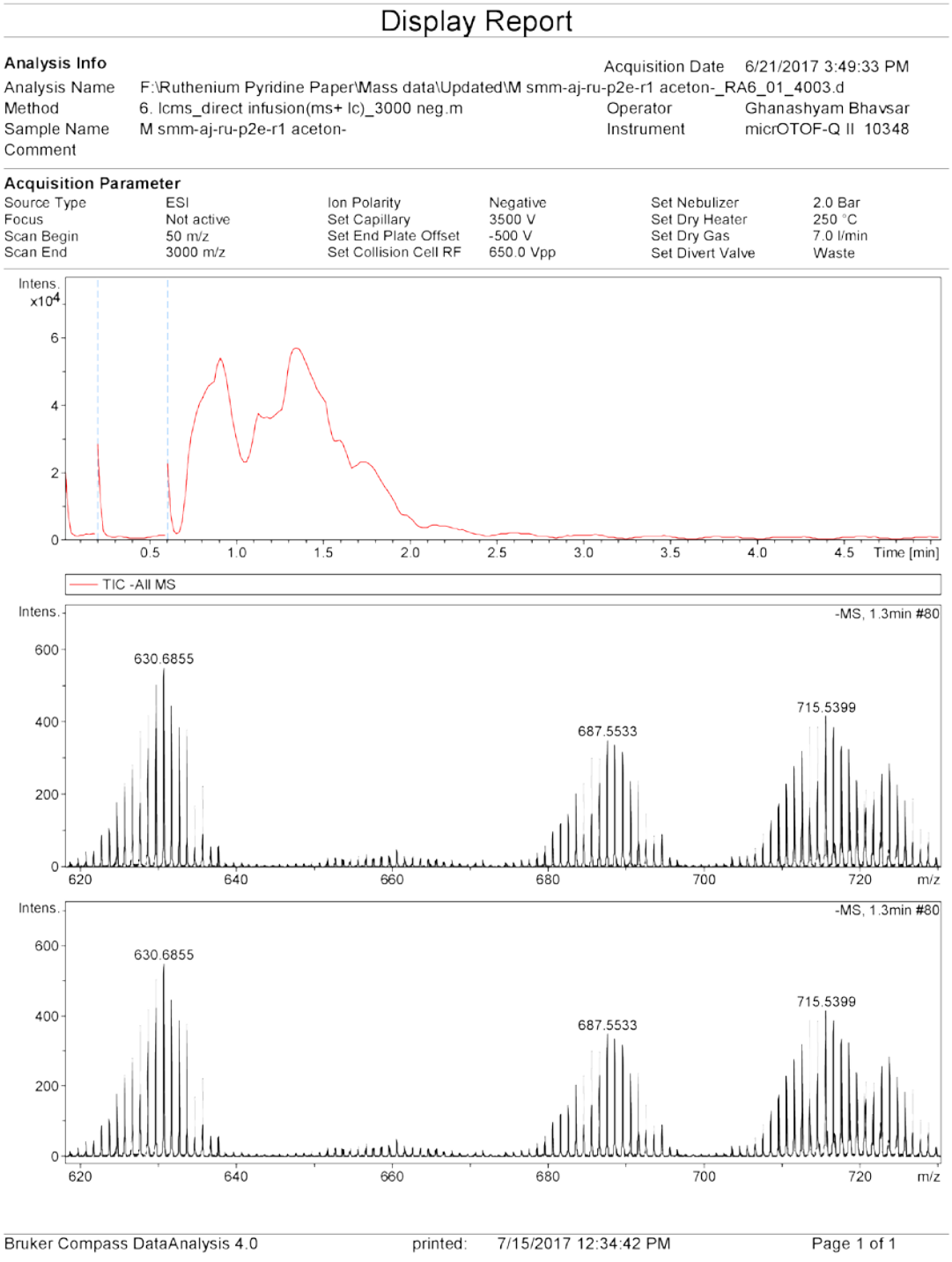

Fig. S8. LCMS of **1**

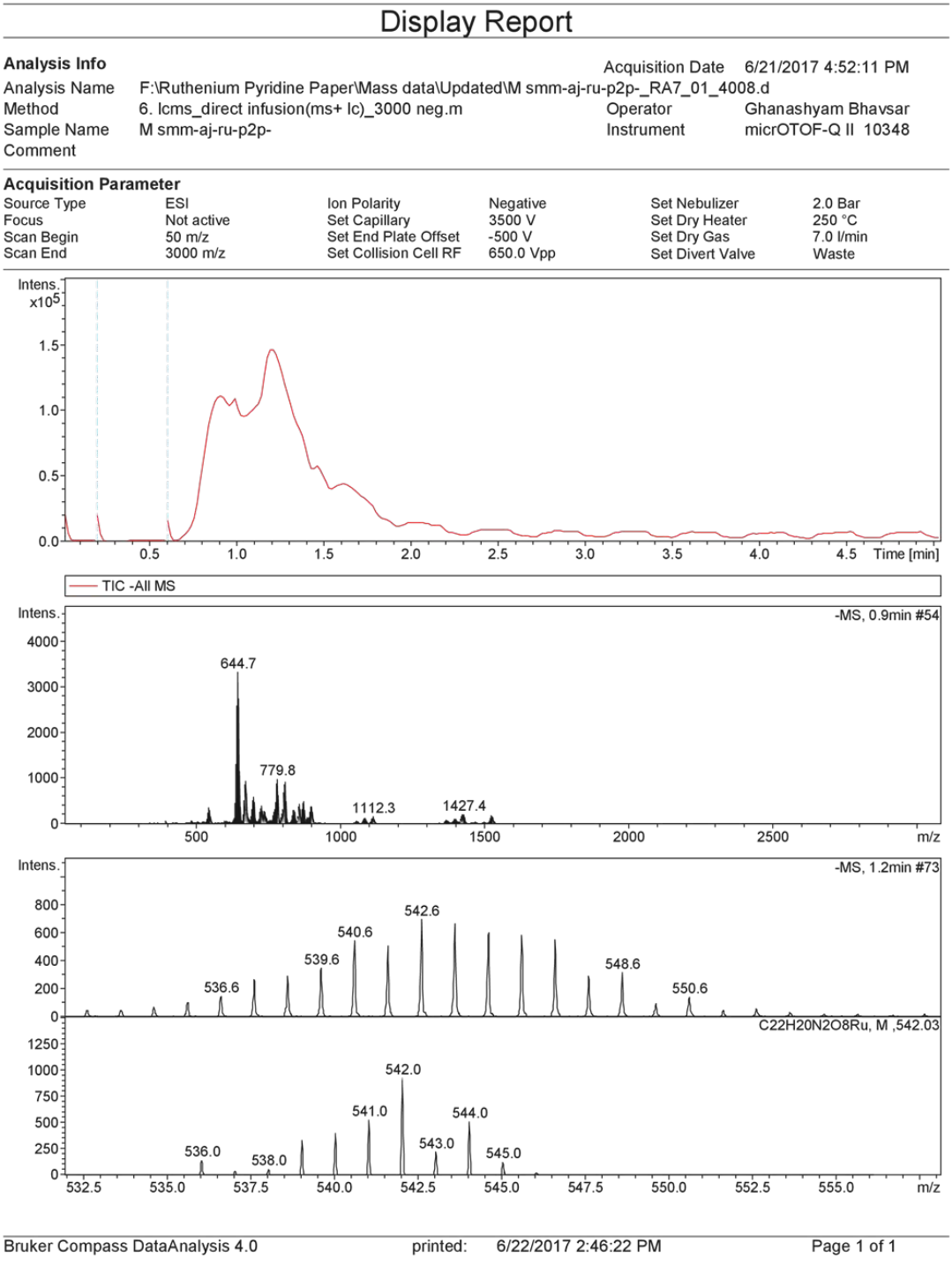

Fig. S9. LCMS of **2**

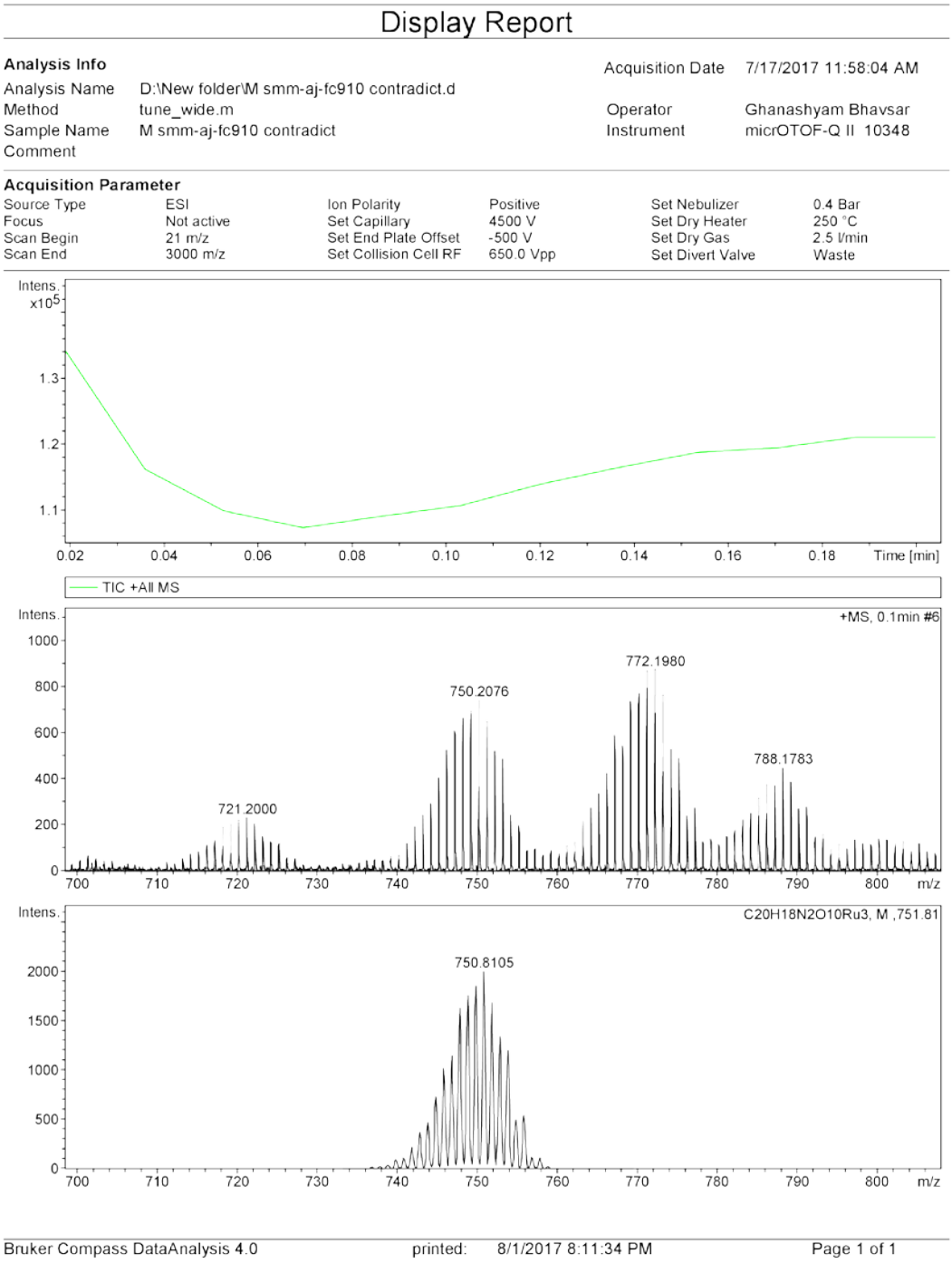

Fig. S10. LCMS of **3**

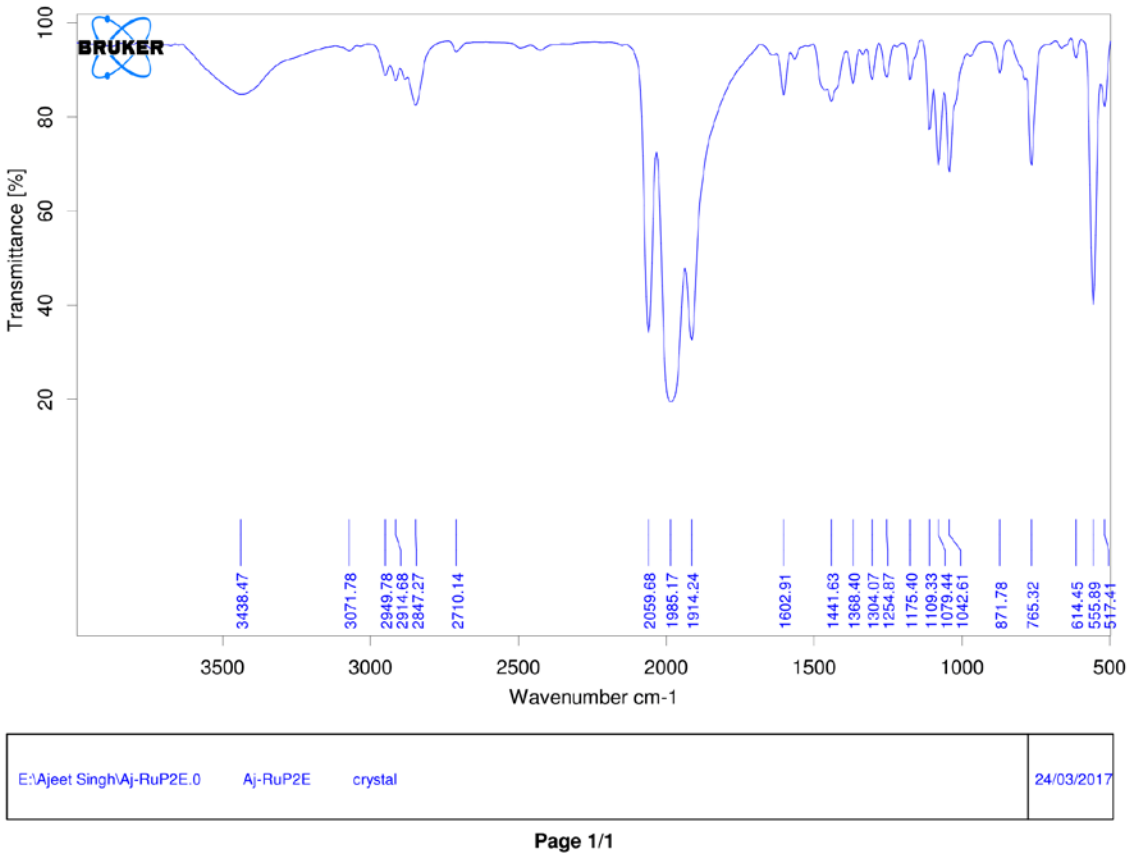

Fig. S11. IR of **1**

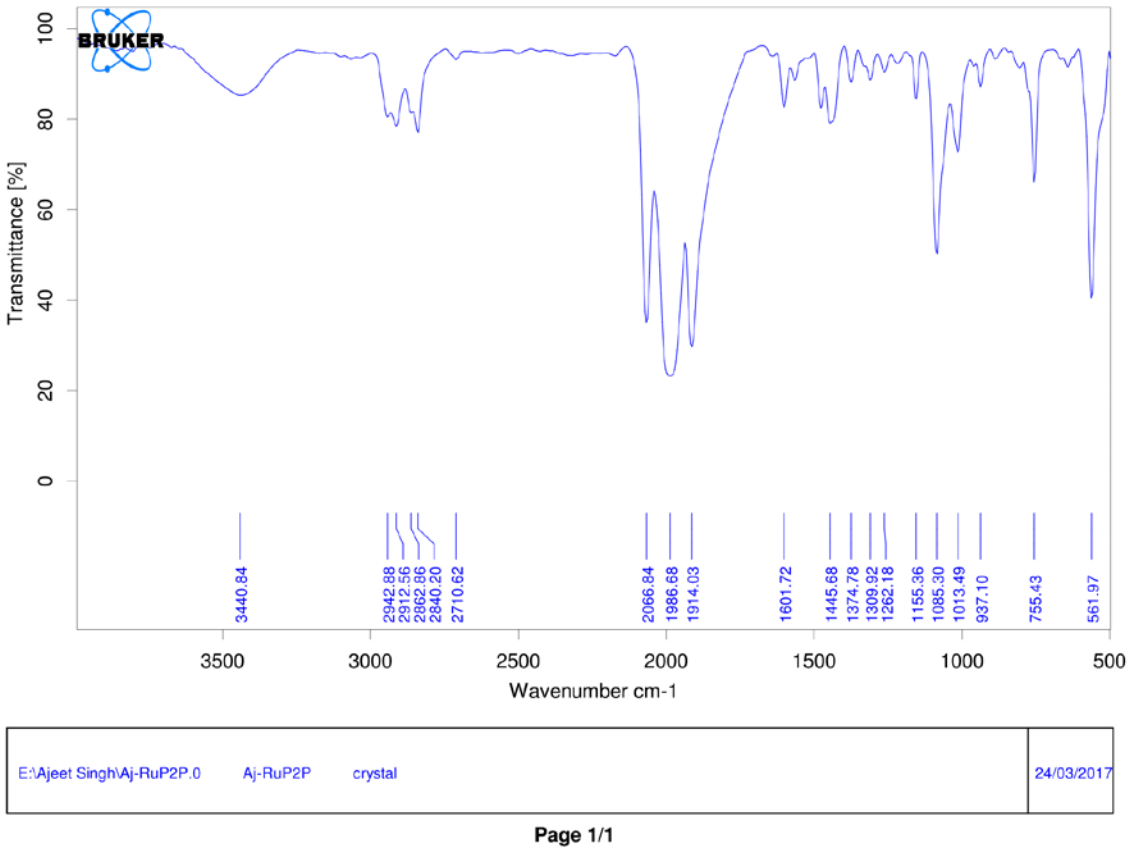

Fig. S12. IR of **2**

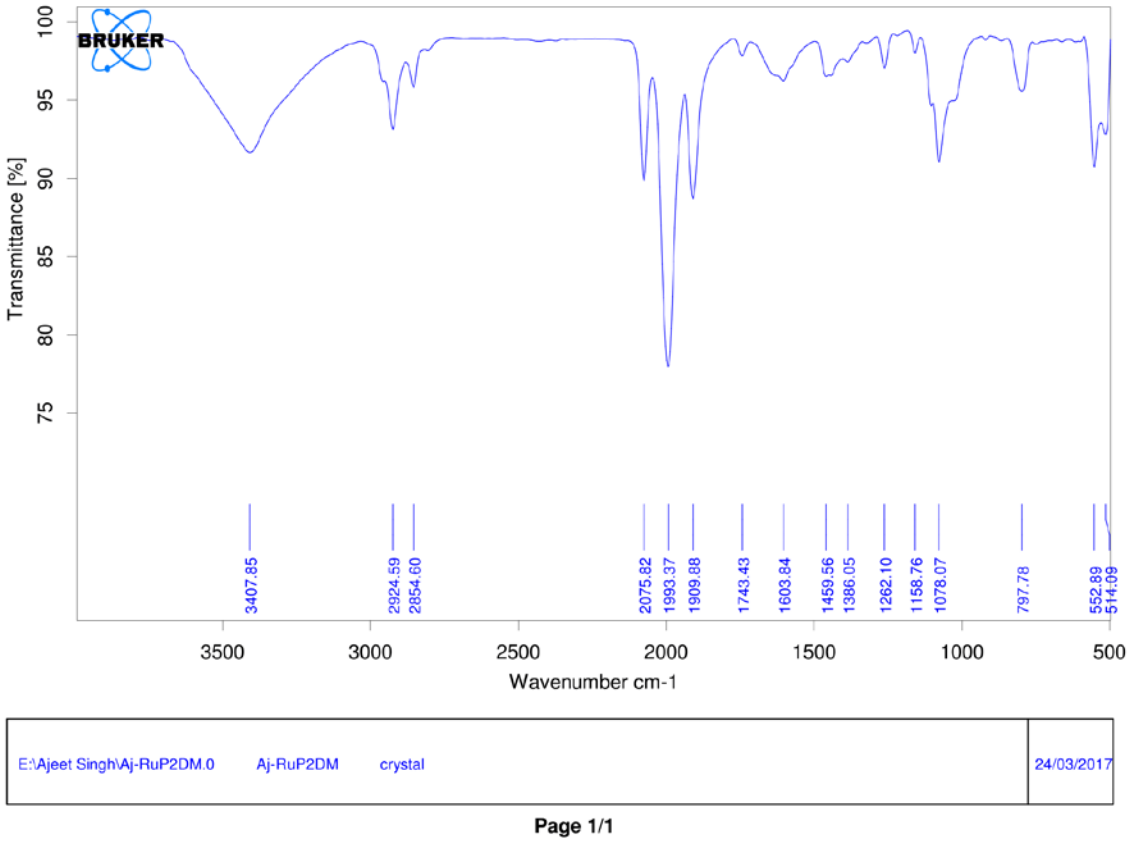

Fig. S13. IR of **3**

Description of polymeric chains present in the clusters 1–3

The presence of C-H···O interaction between H7a and O7 with the bond length 2.684 Å gives rise to the 1D polymeric chain (see Fig. S14).[1] The H3···O2 interactions with bond length 2.711 Å give rise to the 2D polymeric chain (see Fig. S22). This also looks like inverted nest facing towards each other, if observed from 'tilted c' axis. The presence of C-H…C interaction along with C-H···O between C11···H17 i.e. C11 from carbonyl and H17 from pyridine ring gives rise to the 3D polymeric chain (see Fig. S23). The bond length is 2.779 Å.

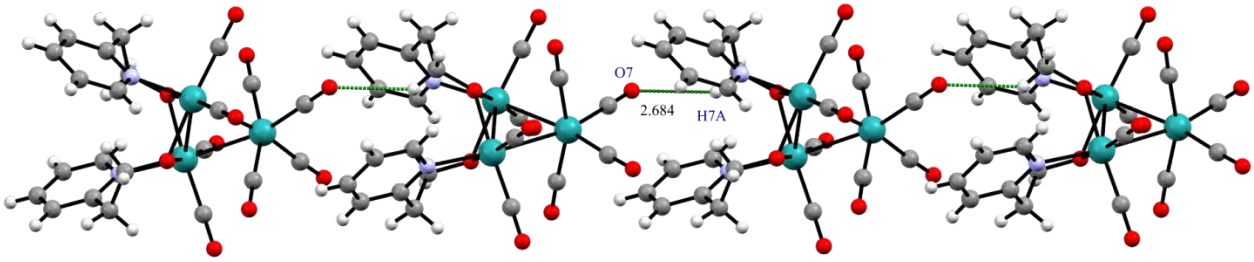

Fig. S14. 1D polymeric chain of complex **1**

The presence of C-H···O interaction between H2 and O10 with the bond length 2.513 Å gives rise to the 1D polymeric chain (see Fig. S15). The C1···O4 interactions with bond length 3.194 Å give rise to the 2D polymeric chain (see Fig. S24). This also looks like an inverted nest but more packed and one layer faces in the same direction and other in another direction if seen from tilted 'c' axis. The presence of C-H…O interaction between H14A···O10 gives rise to the 3D polymeric chain (see Fig. S25).[2] The bond length is 2.700 Å.

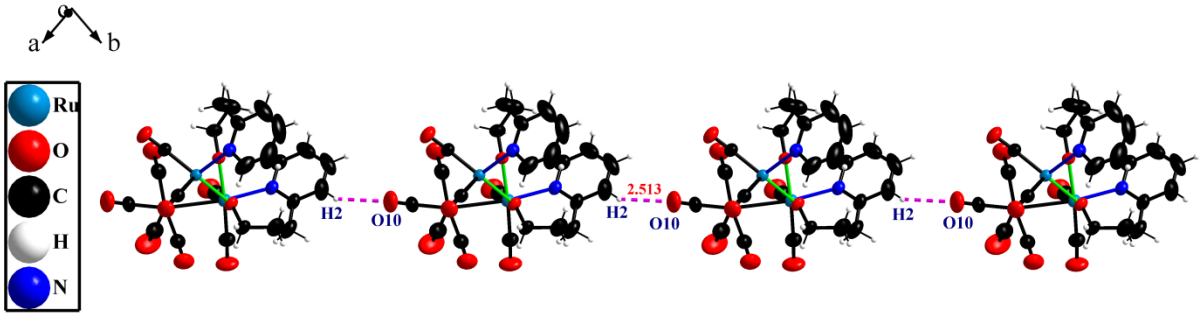

Fig. S15. 1D polymeric chain of complex **2**

The presence of C-H···O interaction between H6A···O10 and H11···O5 with the bond length 2.572 Å and 2.618 Å, respectively gives rise to the 1D polymeric chain (see Fig. S16). The H4A···O11 is hydrogen bond interactions with bond length 2.035 Å and H4A…O11 C-H…O interaction with bond length 2.414 Å if seen along 'b' axis give rise to 2D polymeric chain (see Fig. S26). Along with other interactions, the presence of π···π interaction between C8···C3 and C9···C2 give rise to the 3D polymeric chain (see Fig. S27) and the bond length is 3.389 Å and 3.386 Å, respectively.

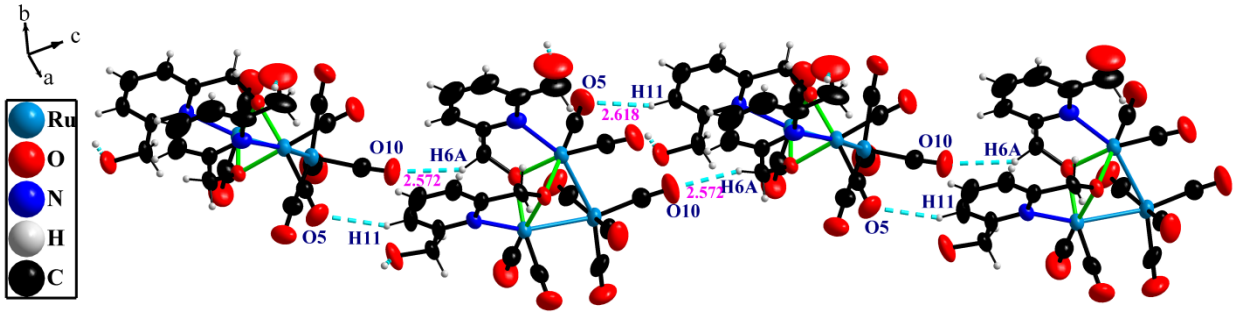

Fig. S16. 1D polymeric chain of complex **3**

Salient features and comparison of the structure 1–3

The molecule $Ru_3(CO)_{12}$ has essentially D_{3h} symmetry with a mean Ru–Ru bond length of 2·848 Å.[12] In the complexes, **1–3**, the bond distance stretched and length was more than 2.848 Å. The bond length is 3.078, 3.030 and 3.045 Å, respectively. Complex **2** has a seven-membered stable ring which involves C13–C16, O2, N2 and Ru2 (see Fig. S17).

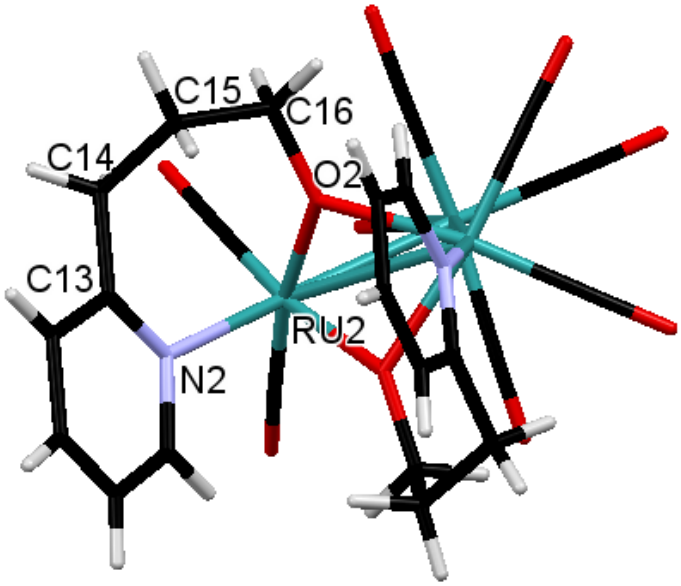

Fig. S17. Seven-members ring in complex **2** involving C13–C16, O2, N2 and Ru2

In complex **3,** the hydrogen bonding is present between H2A and O4 atoms. The bond length is 2.045 Å (see Fig. S18).

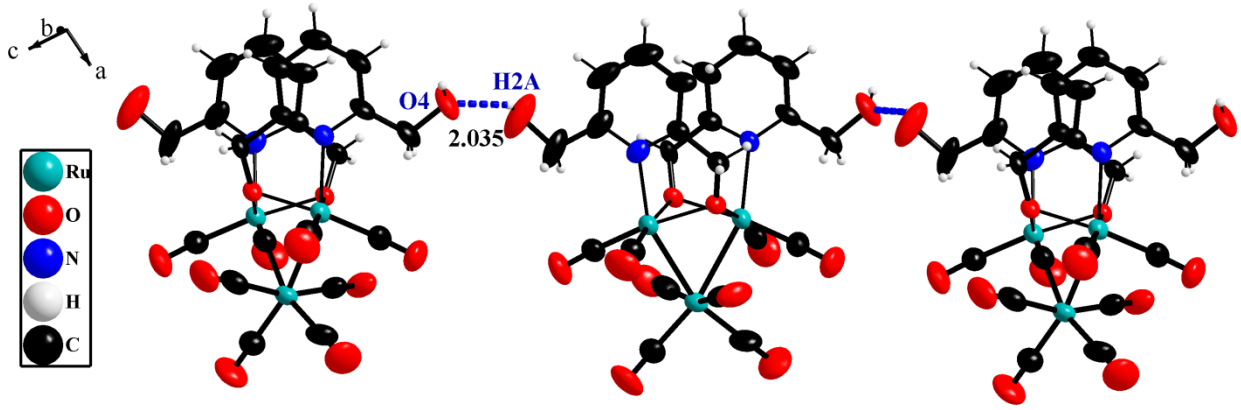

Fig. S18. Hydrogen bonding in **3** between H2A···O4 with distance 2.035 Å

Symmetry Operators

Table S2. Symmetry operators present in complex **1**

Number	Symm. Op.	Description	Detailed Description	Order	Type
1	x,y,z	Identity	Identity	1	1
2	1/2-x,1/2+y,1/2-z	Screw axis (2-fold)	2-fold screw axis with direction [0, 1, 0] at 1/4, y, 1/4 with screw component [0, 1/2, 0]	2	2
3	-x,-y,-z	Inversion centre	Inversion at [0, 0, 0]	2	-1
4	1/2+x,1/2-y,1/2+z	Glide plane	Glide plane perpendicular to [0, 1, 0] with glide component [1/2, 0, 1/2]	2	-2

Table S3. Symmetry operators present in complex **2**

Number	Symm. Op.	Description	Detailed Description	Order	Type
1	x,y,z	Identity	Identity	1	1
2	-x,-y,-z	Inversion centre	Inversion at [0, 0, 0]	2	-1

Table S4. Symmetry operators present in complex **3**

Number	Symm. Op.	Description	Detailed Description	Order	Type
1	x,y,z	Identity	Identity	1	1
2	1/2-x, 1/2+y, 1/2-z	Screw axis (2-fold)	2-fold screw axis with direction [0, 1, 0] at 1/4, y, 1/4 with screw component [0, 1/2, 0]	2	2
3	-x,-y,-z	Inversion centre	Inversion at [0, 0, 0]	2	-1
4	1/2+x, 1/2-y, 1/2+z	Glide plane	Glide plane perpendicular to [0, 1, 0] with glide component [1/2, 0, 1/2]	2	-2

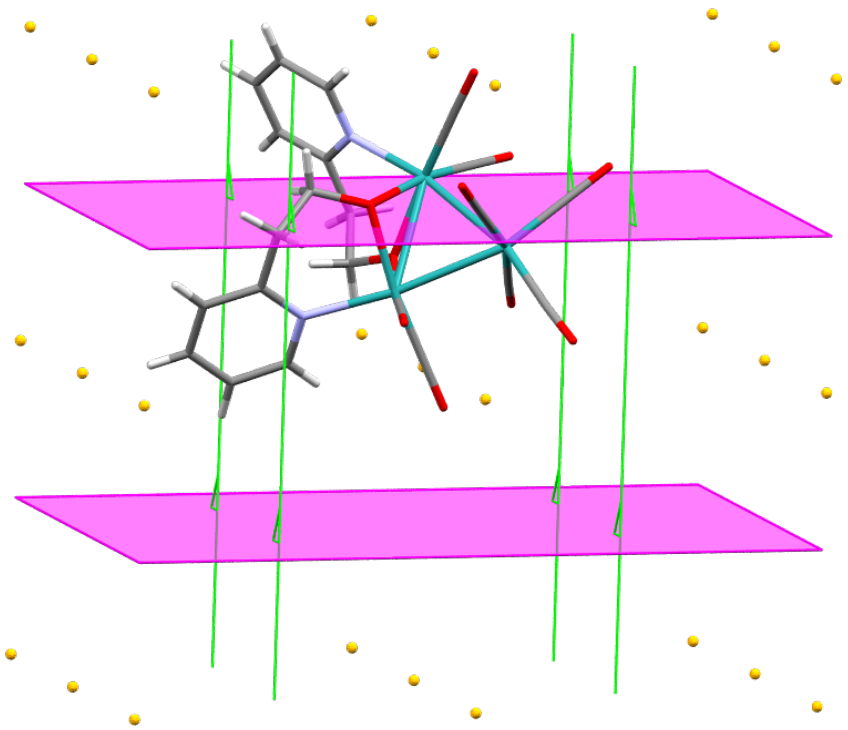

Fig. S19. Symmetry operators present in **1**

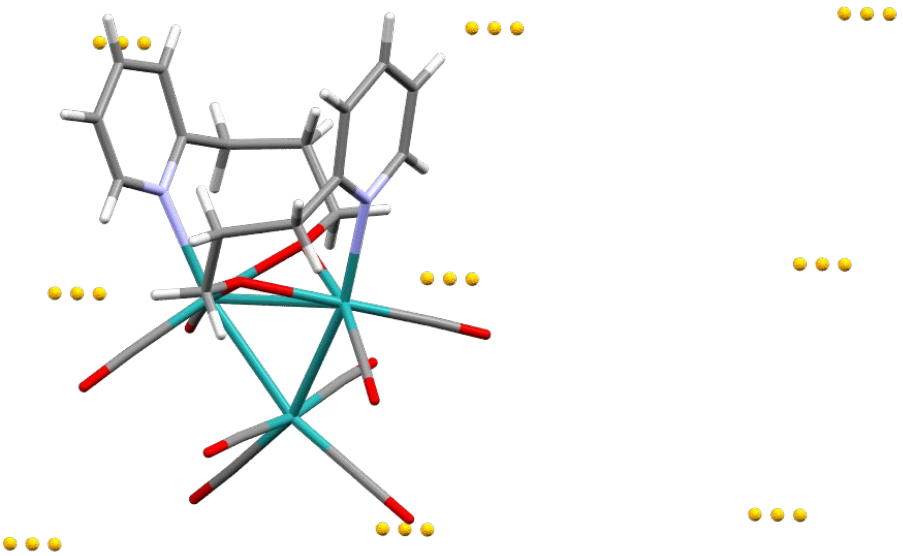

Fig. S20. Symmetry operators present in **2**

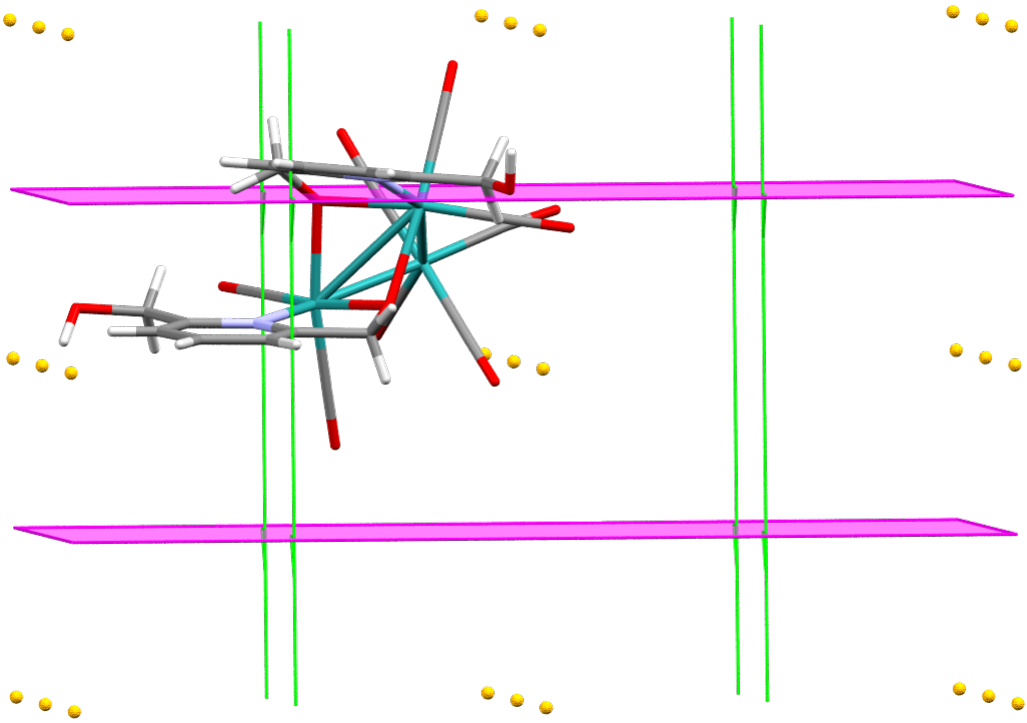

Fig. S21. Symmetry operators present in **3**

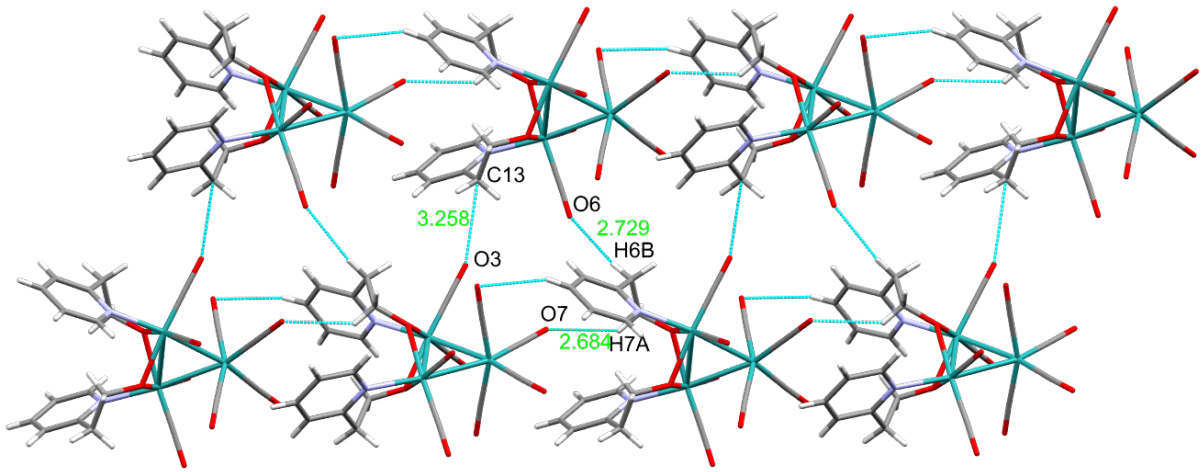

Fig. S22. 2D network of **1**along tilted c-axis

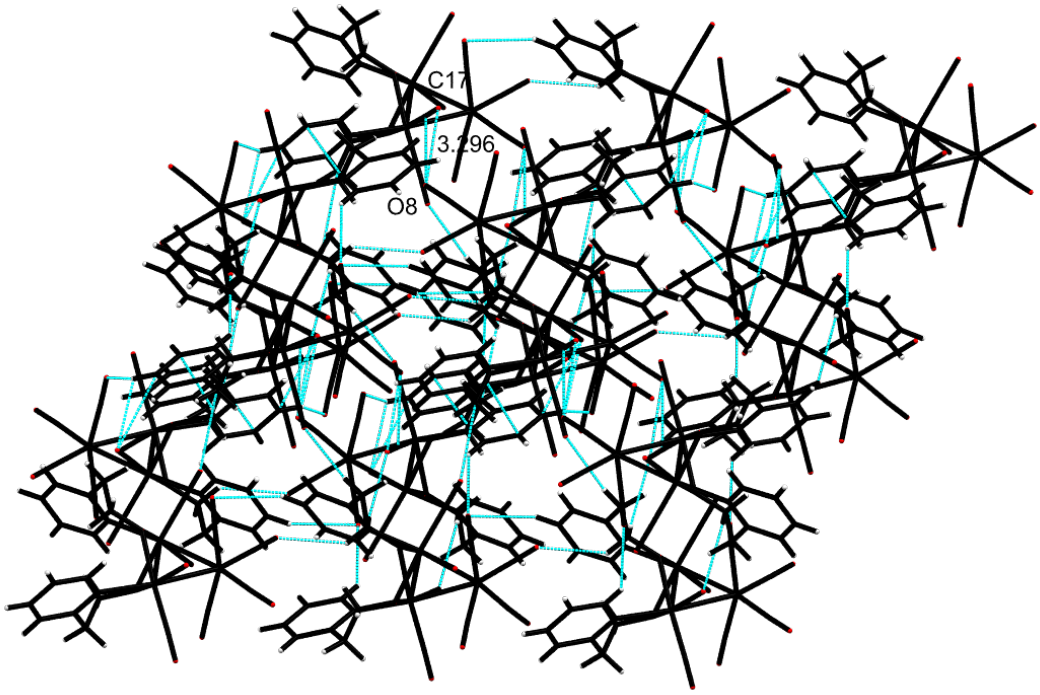

Fig. S23. 3D network of **1** along b-axis

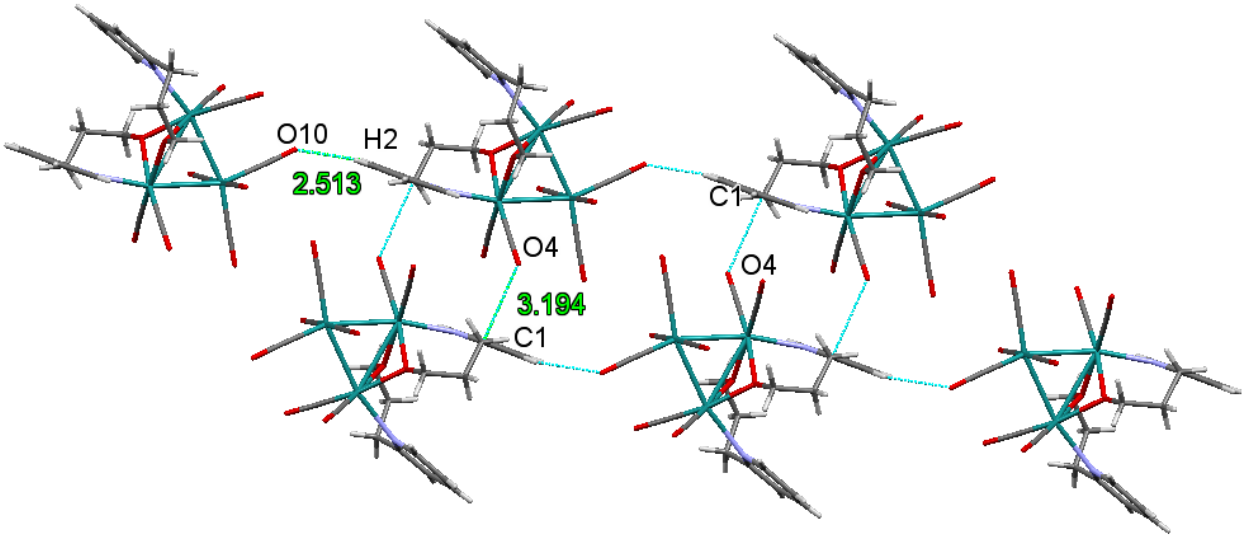

Fig. S24. 2D network of **2** along c-axis

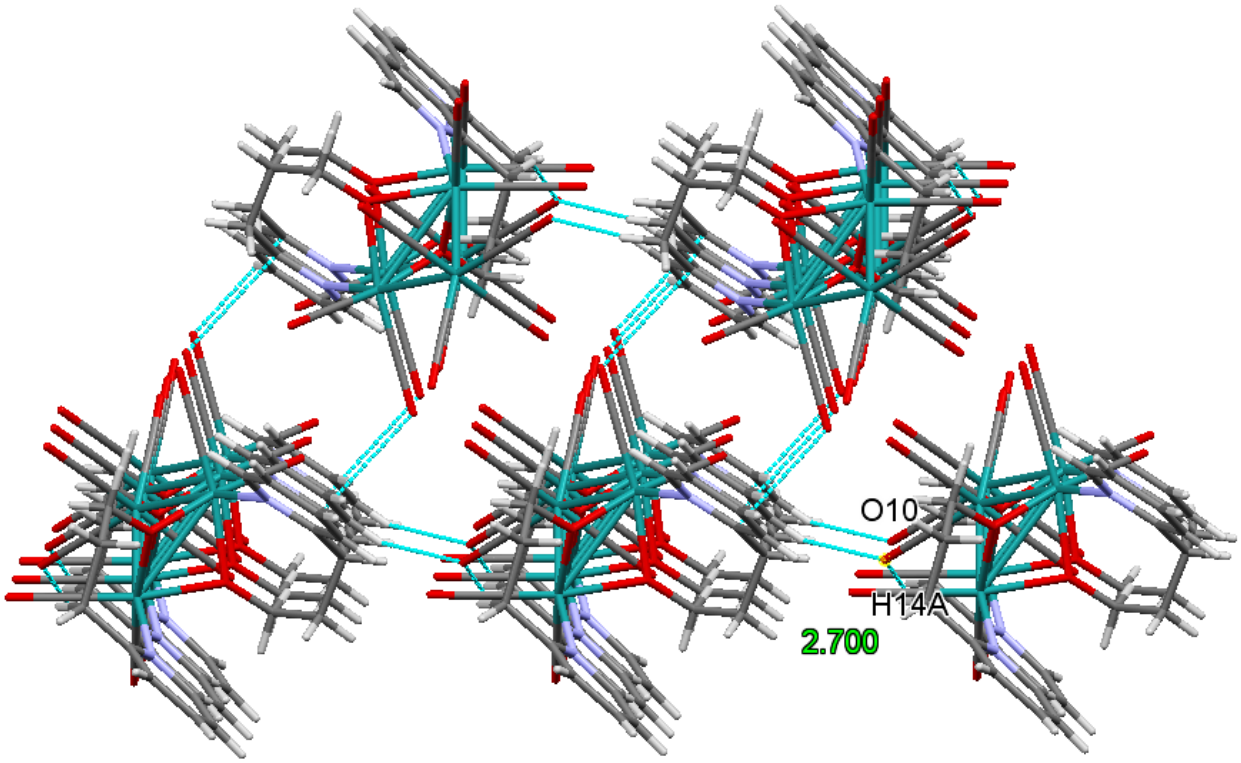

Fig. S25. 3D network of **2** along tilted a-axis

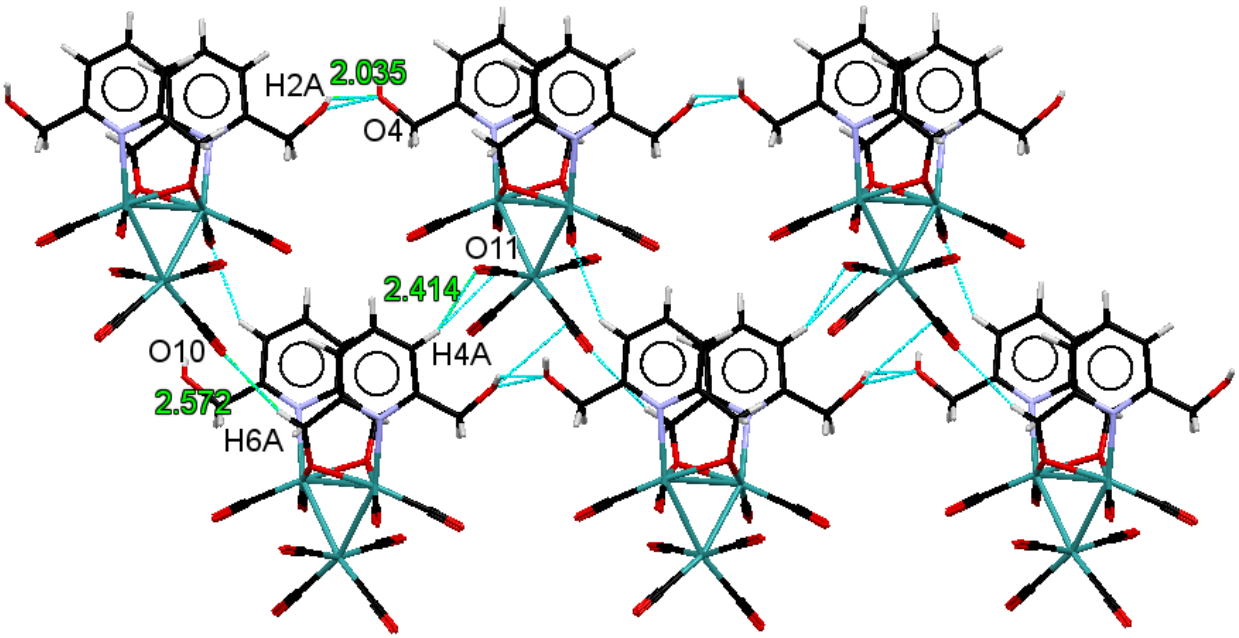

Fig. S26. 2D network of **3** along b-axis

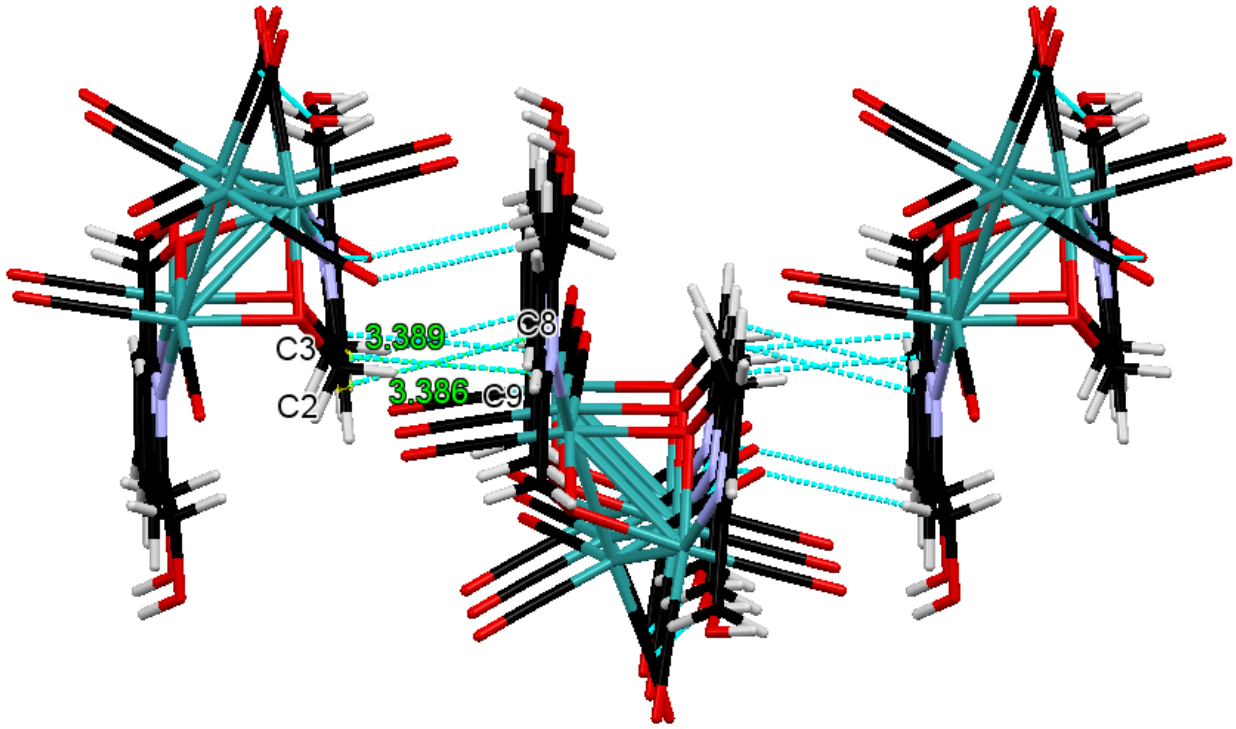

Fig. S27. 3D network of **3** along tilted a-axis

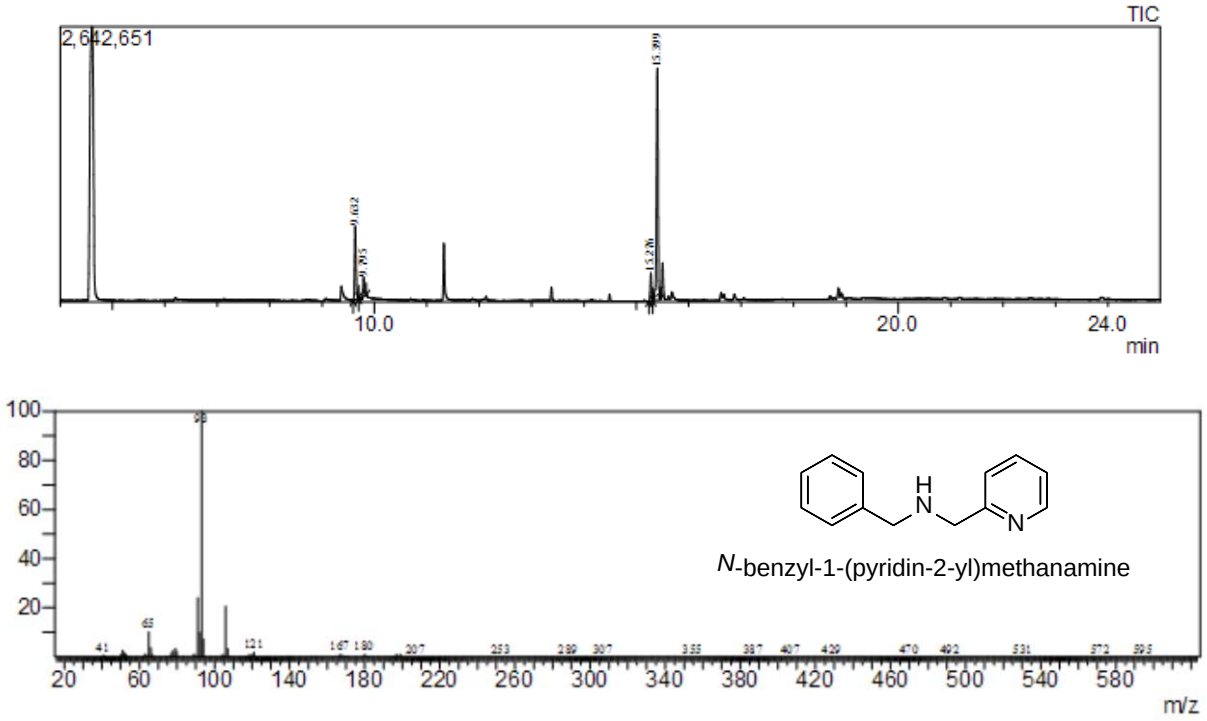

Fig. S28. GCMS of table 3, entry no. 3 (chromatogram and mass peaks)

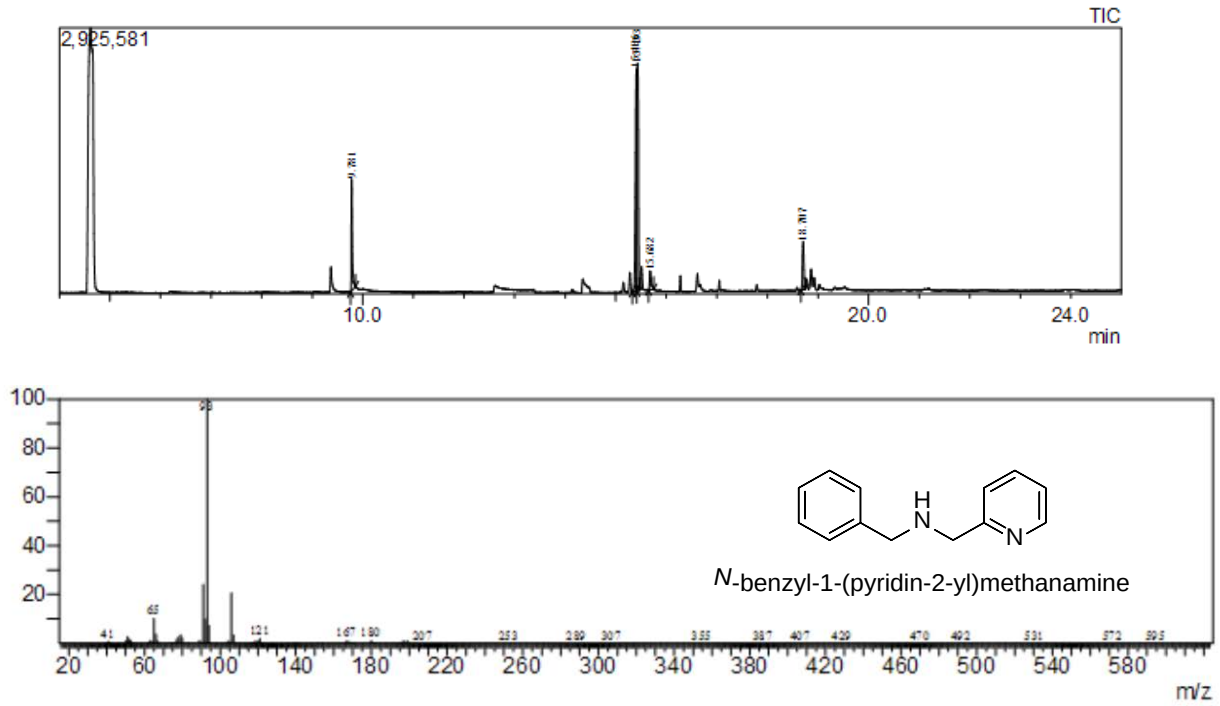

Fig. S29. GCMS of table 3, entry no. 4 (chromatogram and mass peaks)

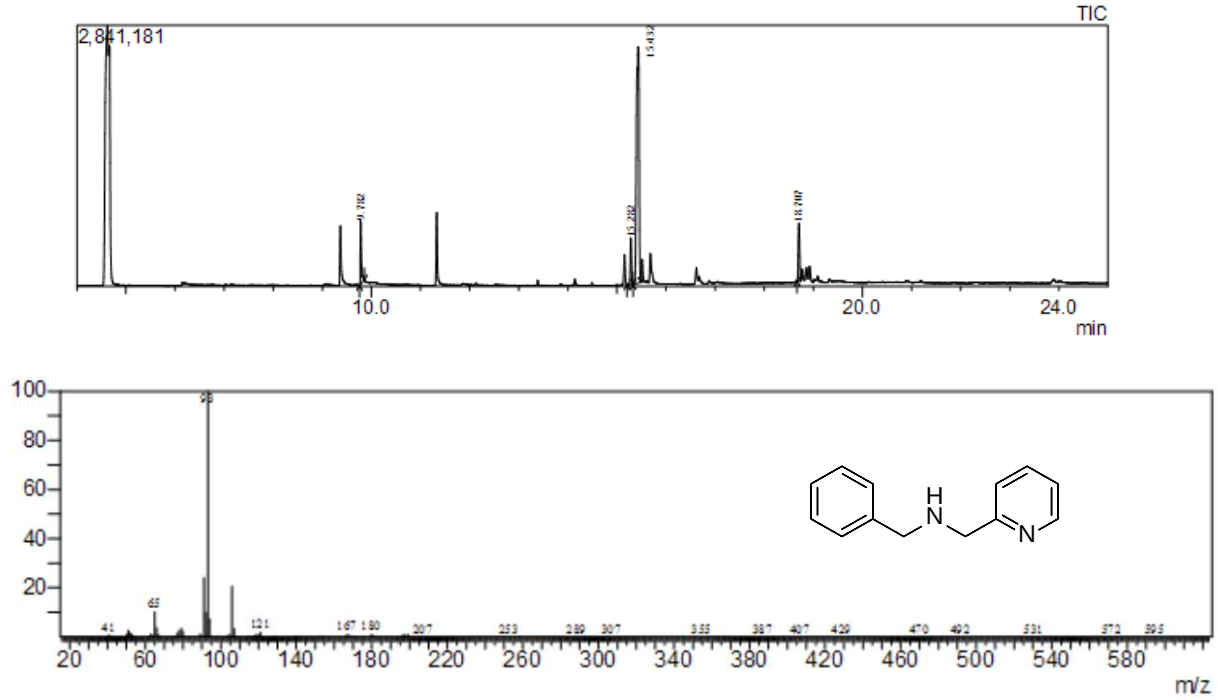

Fig. S30. GCMS of table 3, entry no. 5 (chromatogram and mass peaks)

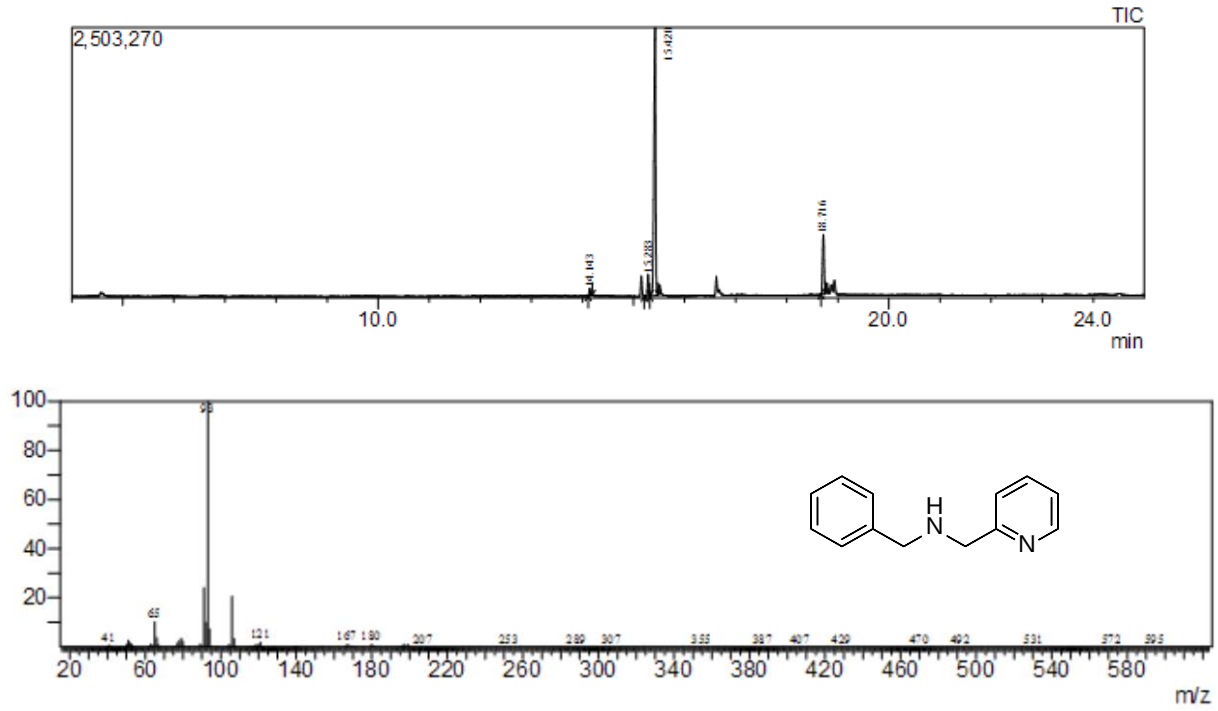

Fig. S31. GCMS of table 3, entry no. 6 (chromatogram and mass peaks)

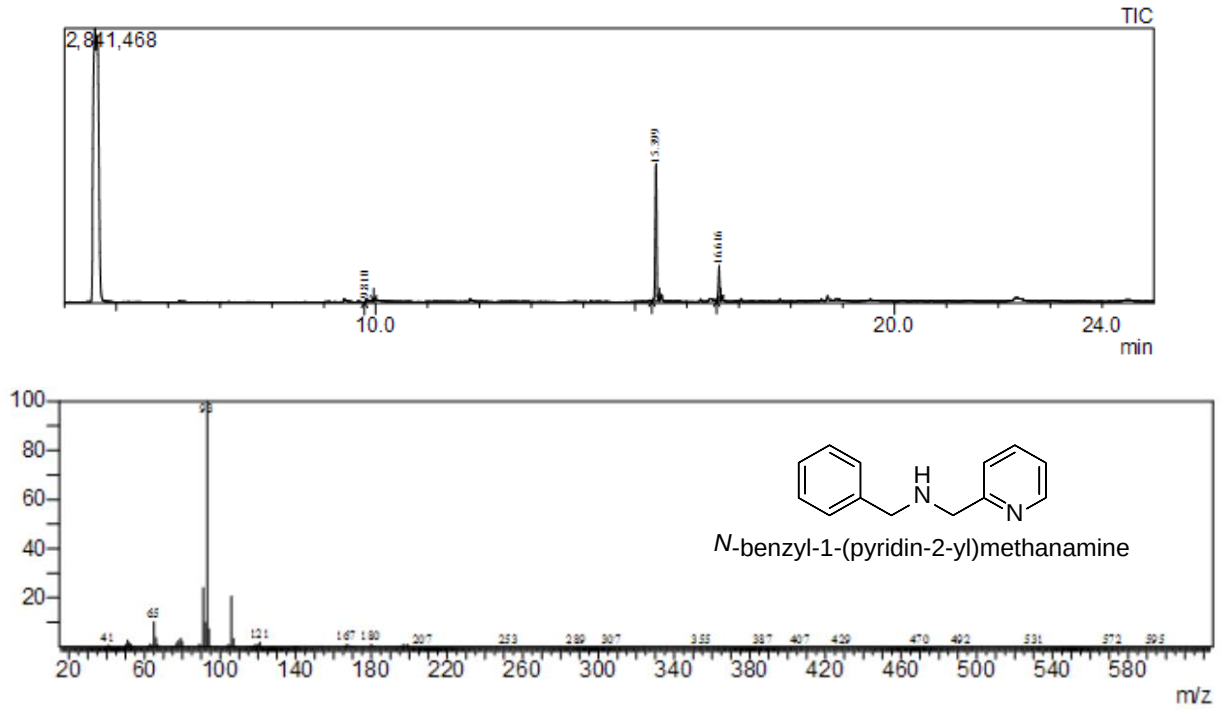

Fig. S32. GCMS of table 3, entry no. 7 (chromatogram and mass peaks)

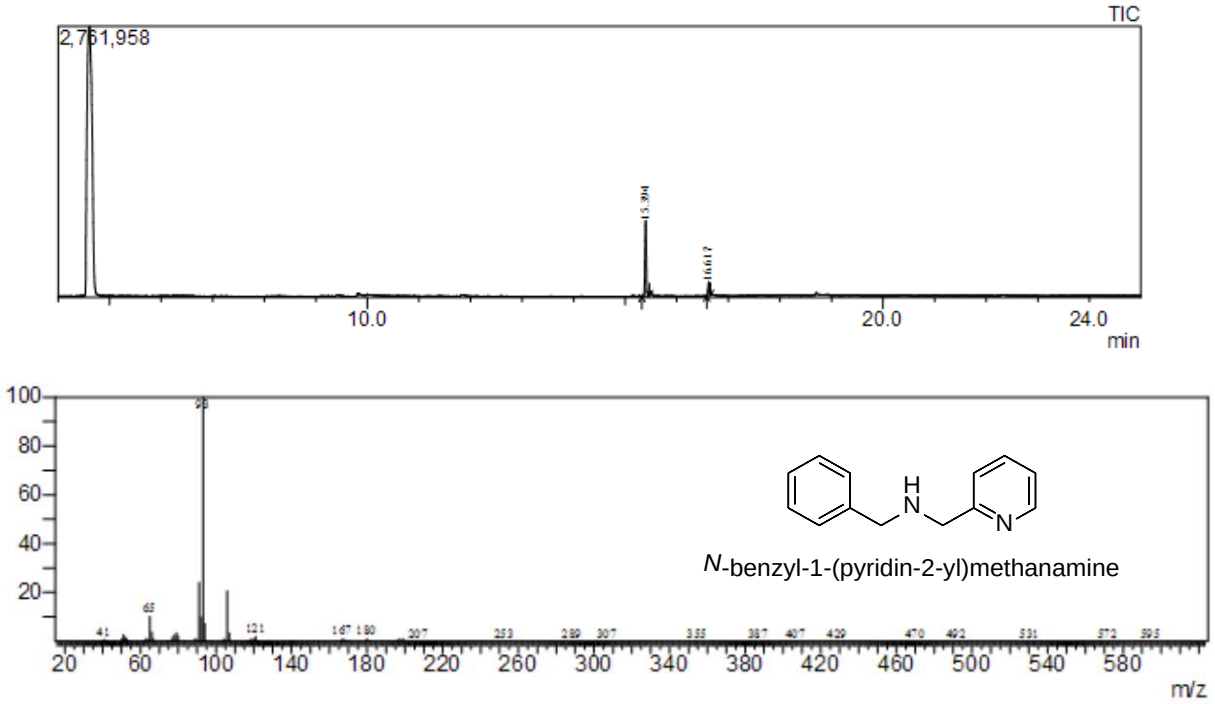

Fig. S33. GCMS of table 3, entry no. 8 (chromatogram and mass peaks)

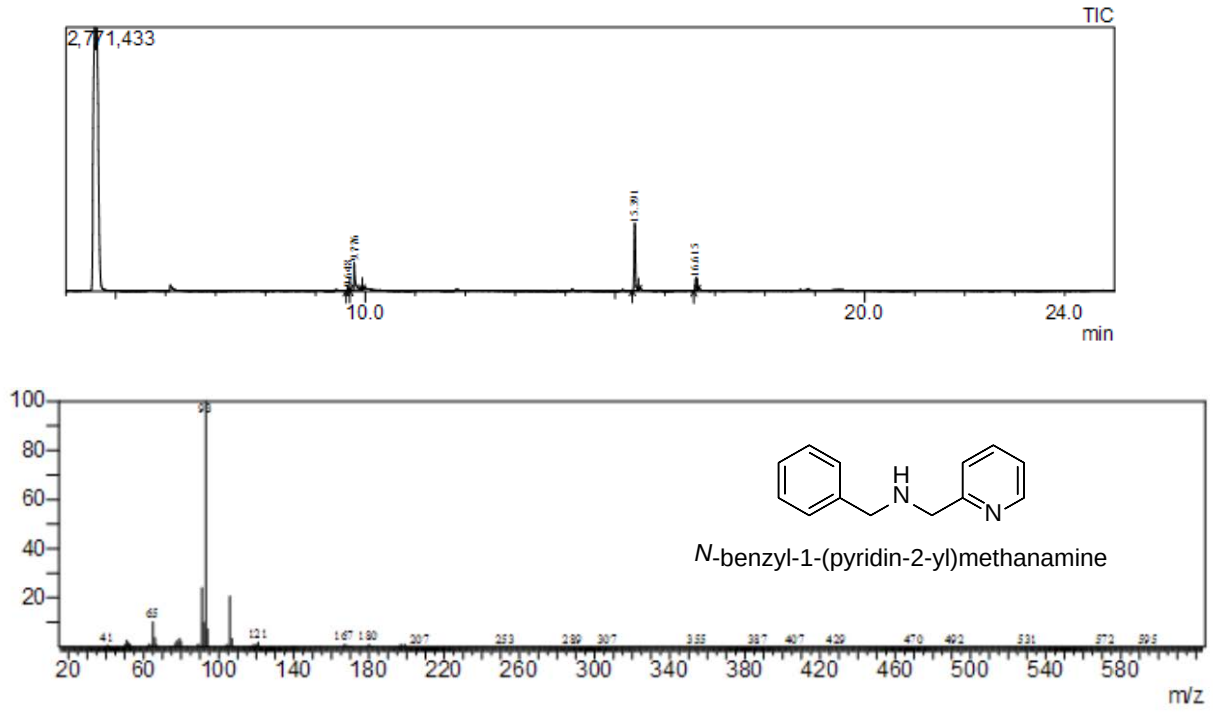

Fig. S34. GCMS of table 3, entry no. 9 (chromatogram and mass peaks)

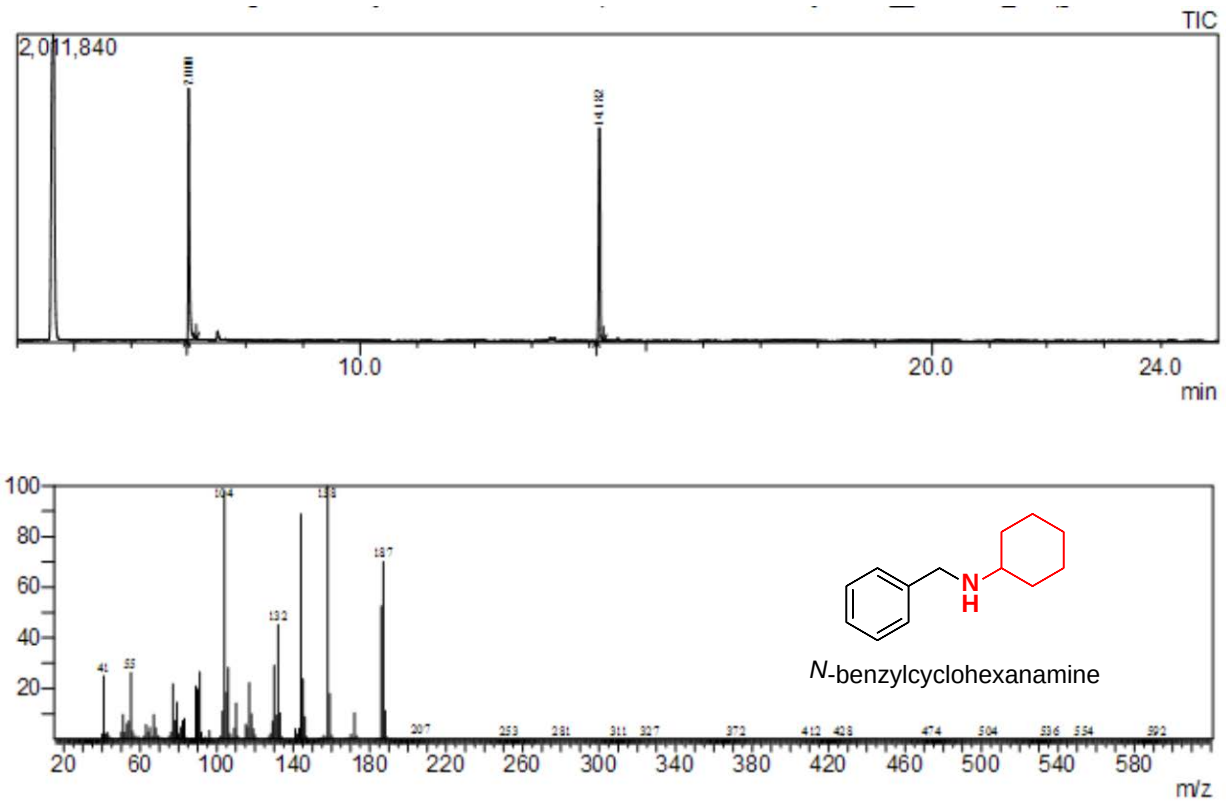

Fig. S35. GCMS of table 4, entry no. 2 (chromatogram and mass peaks)

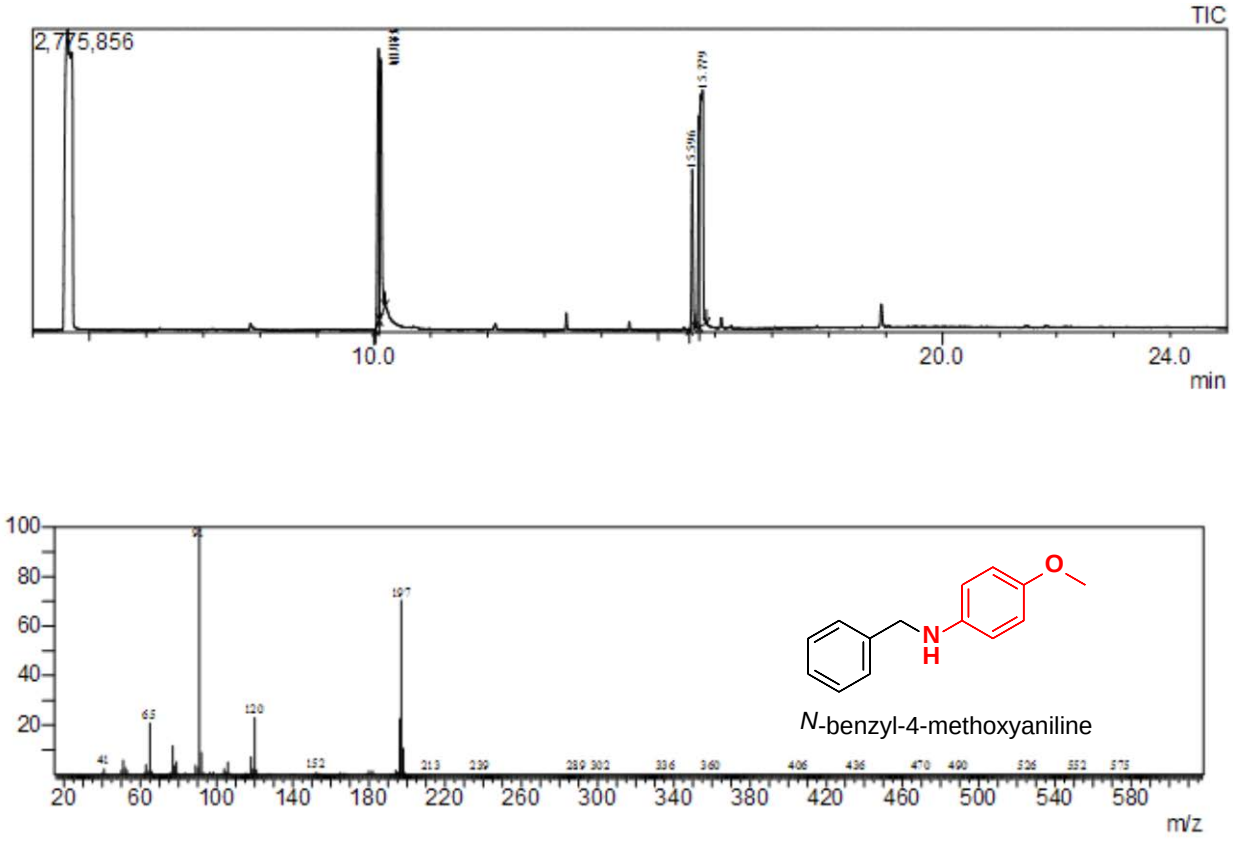

Fig. S36. GCMS of table 4, entry no. 3 (chromatogram and mass peaks)

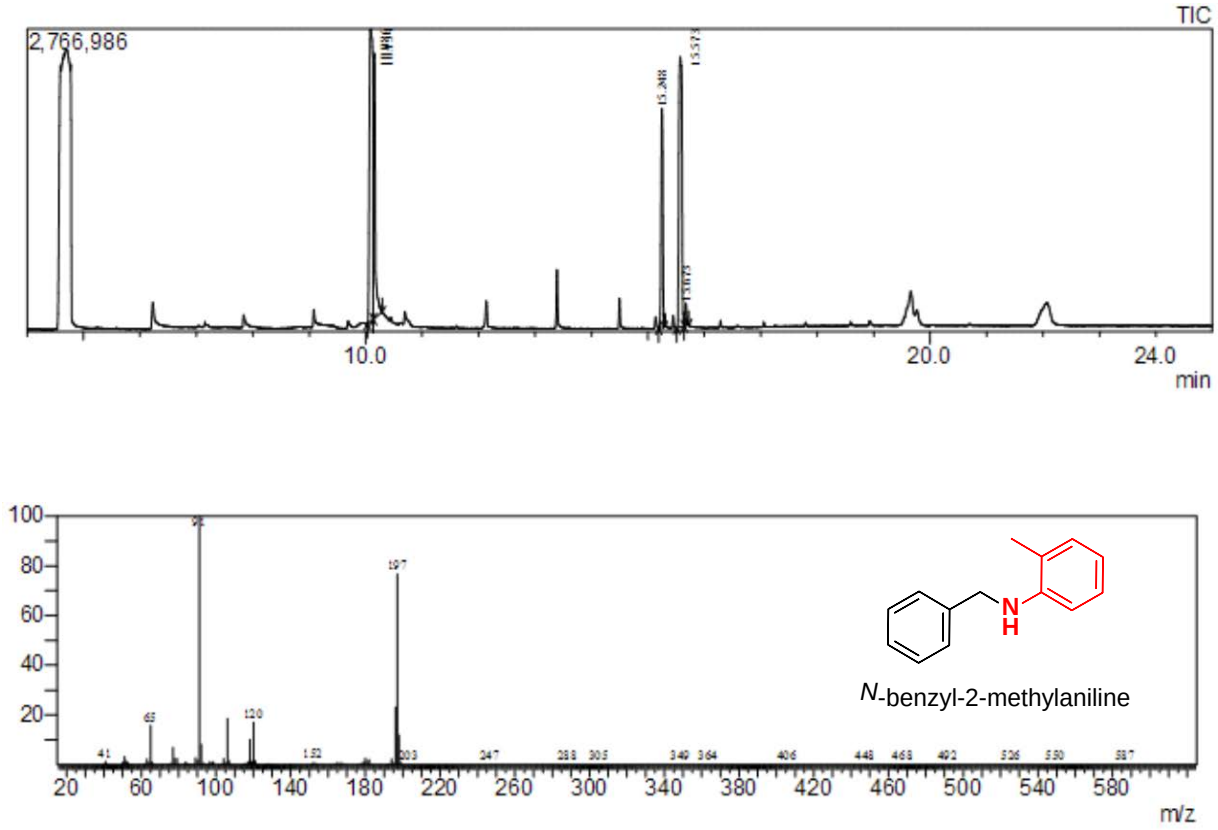

Fig. S37. GCMS of table 4, entry no. 4 (chromatogram and mass peaks)

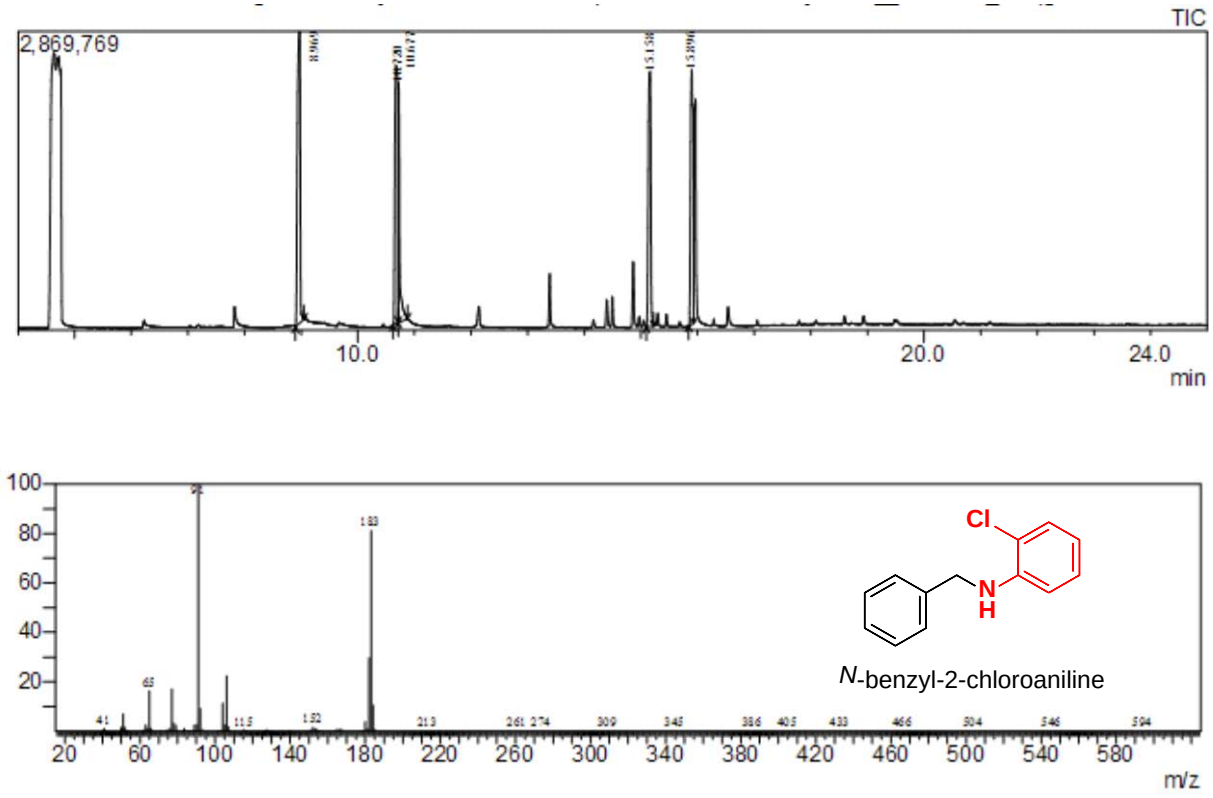

Fig. S38. GCMS of table 4, entry no. 5 (chromatogram and mass peaks)

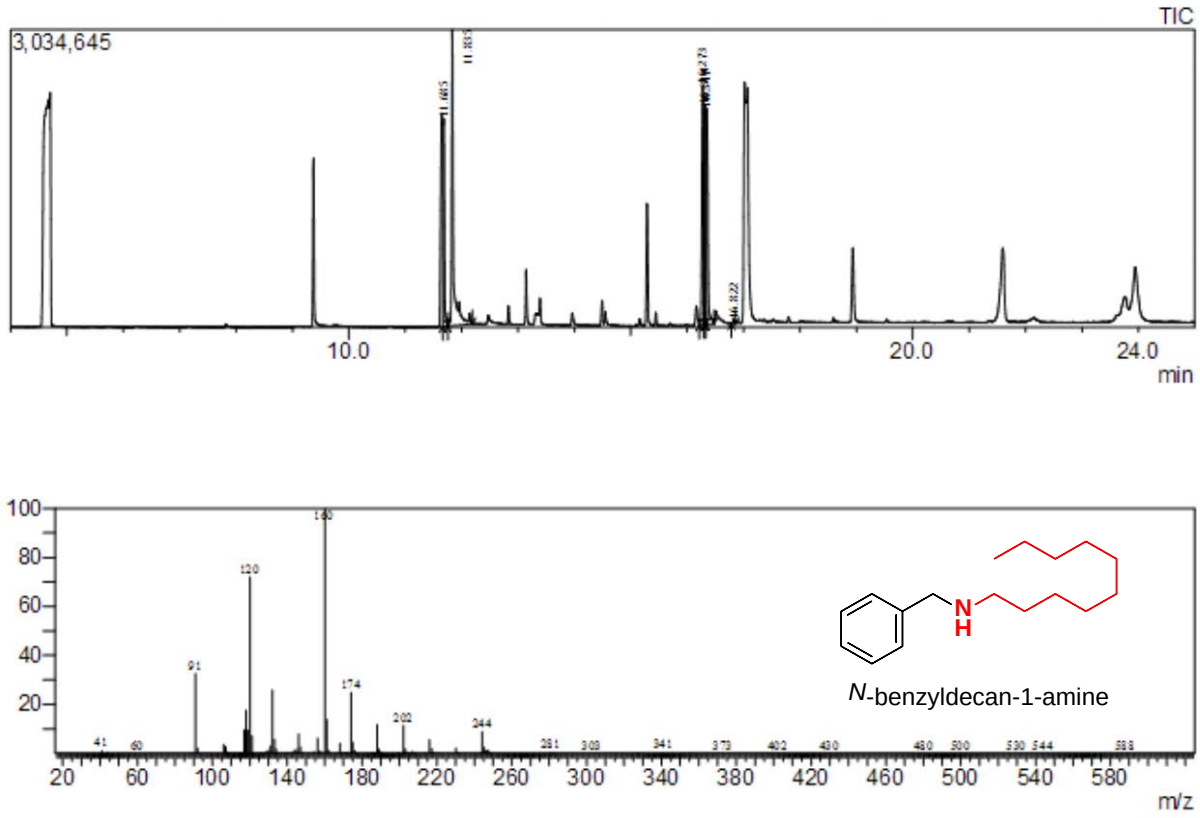

Fig. S39. GCMS of table 4, entry no. 6 (chromatogram and mass peaks)

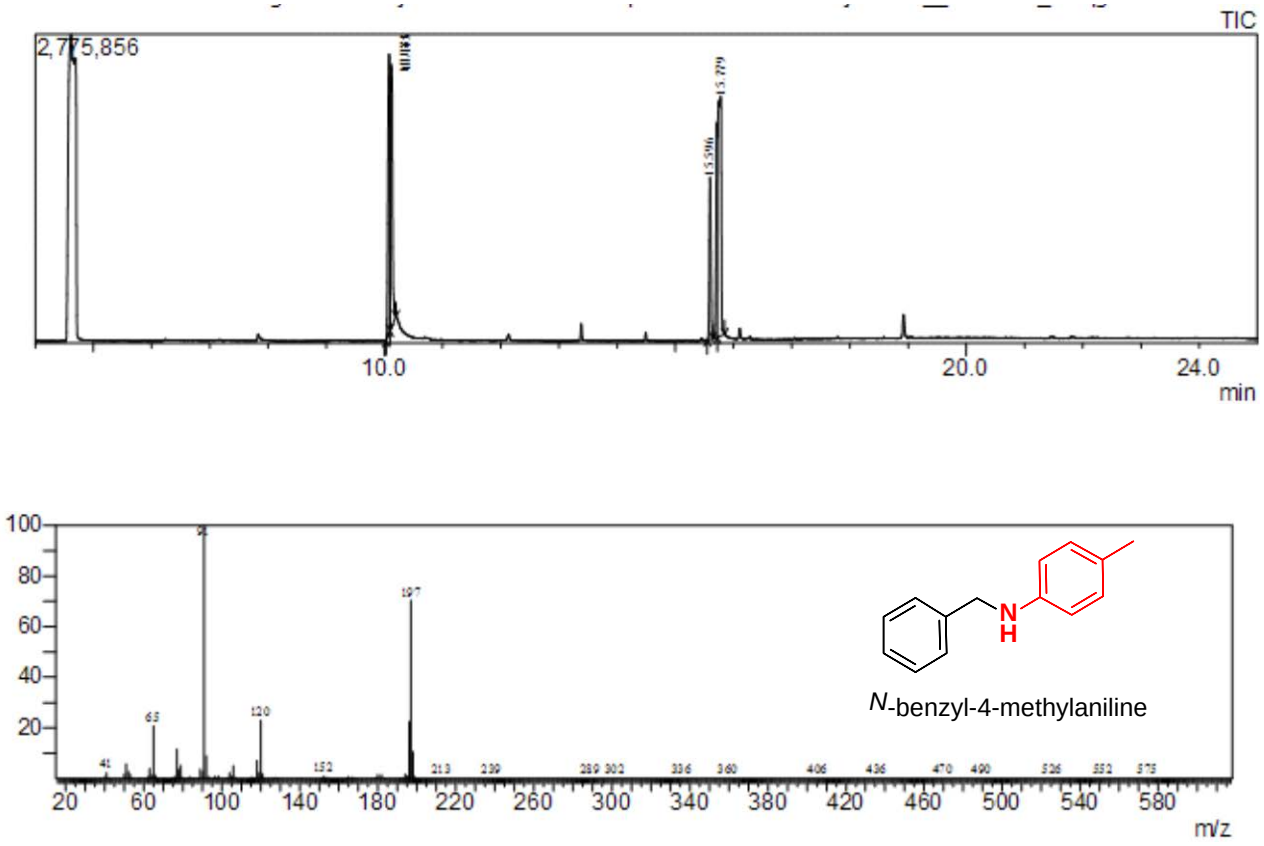

Fig. S40. GCMS of table 4, entry no. 7 (chromatogram and mass peaks)

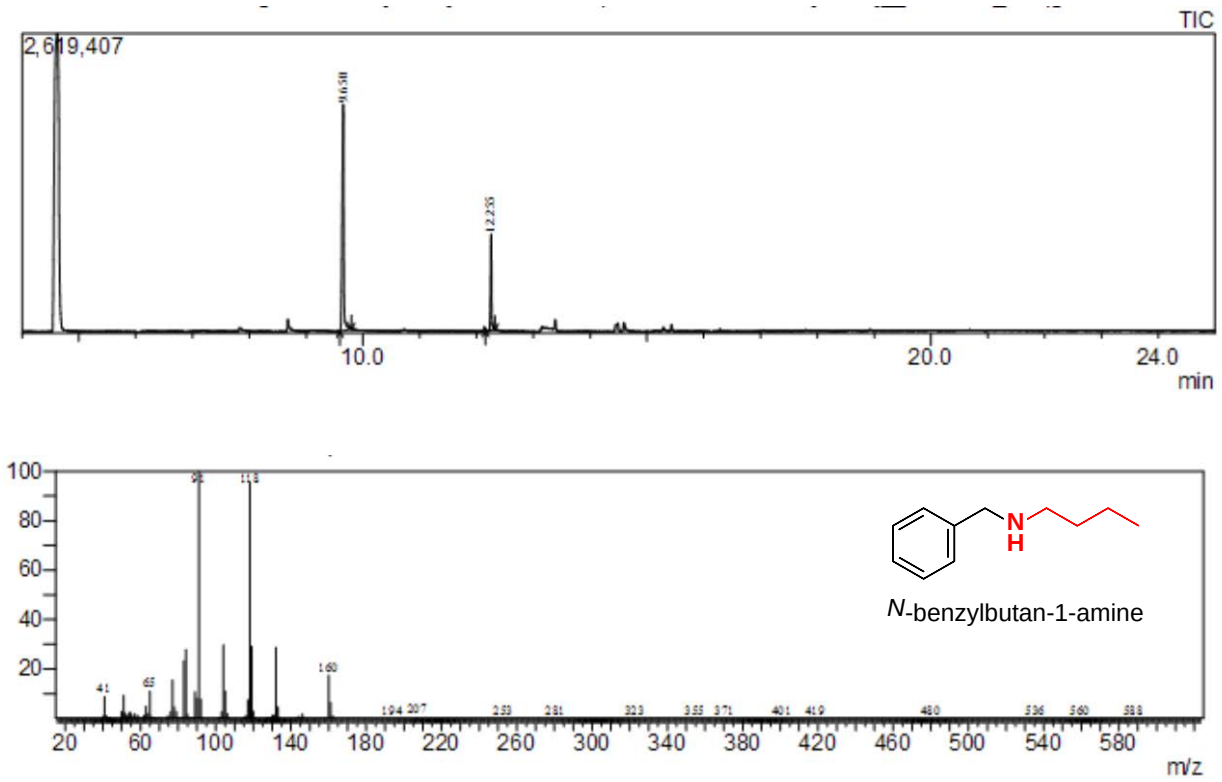

Fig. S41. GCMS of table 4, entry no. 8 (chromatogram and mass peaks)

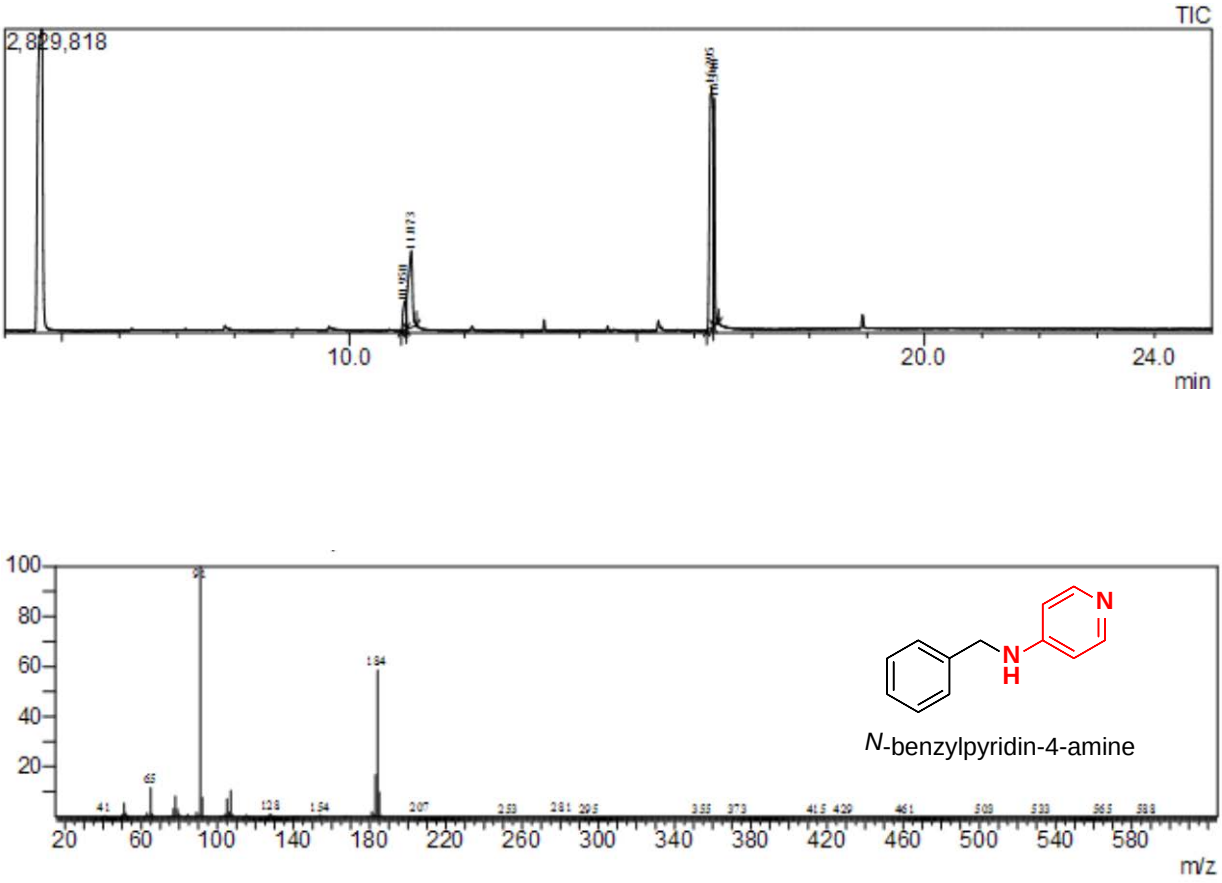

Fig. S42. GCMS of table 4, entry no. 11 (chromatogram and mass peaks)

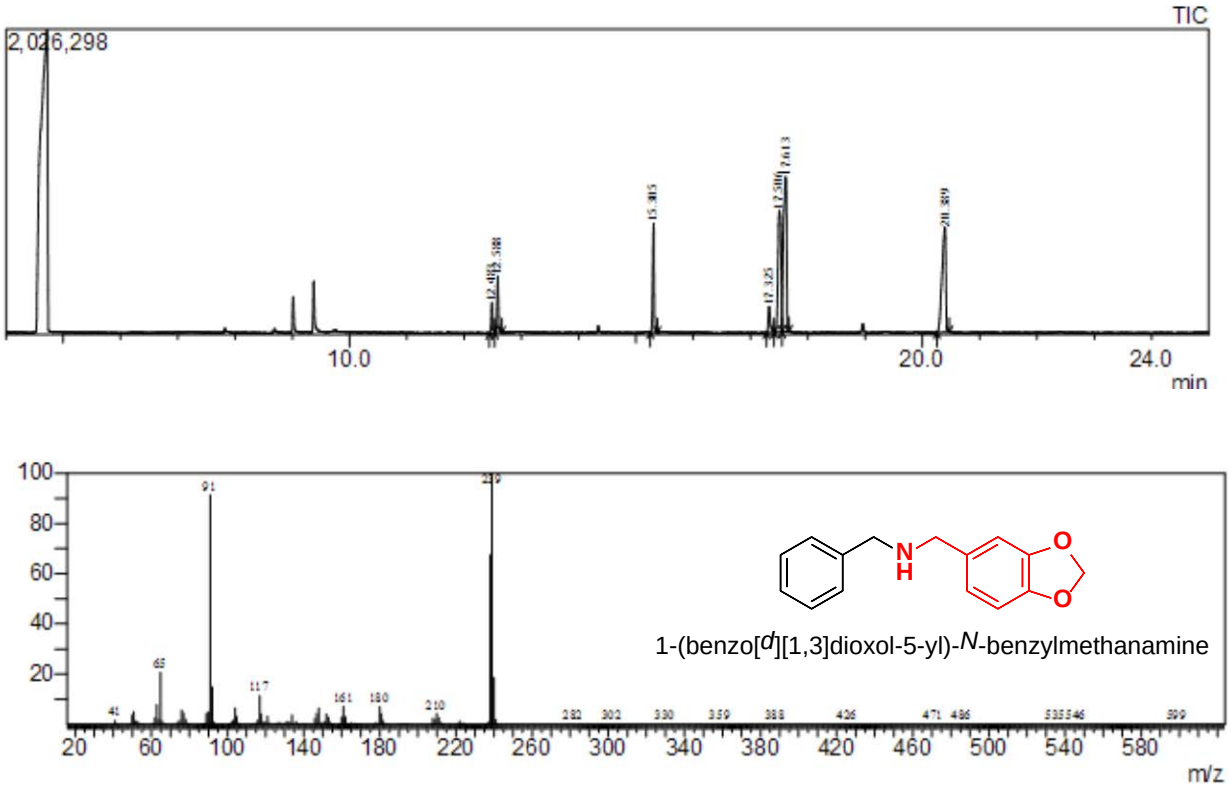

Fig. S43. GCMS of table 4, entry no. 12 (chromatogram and mass peaks)

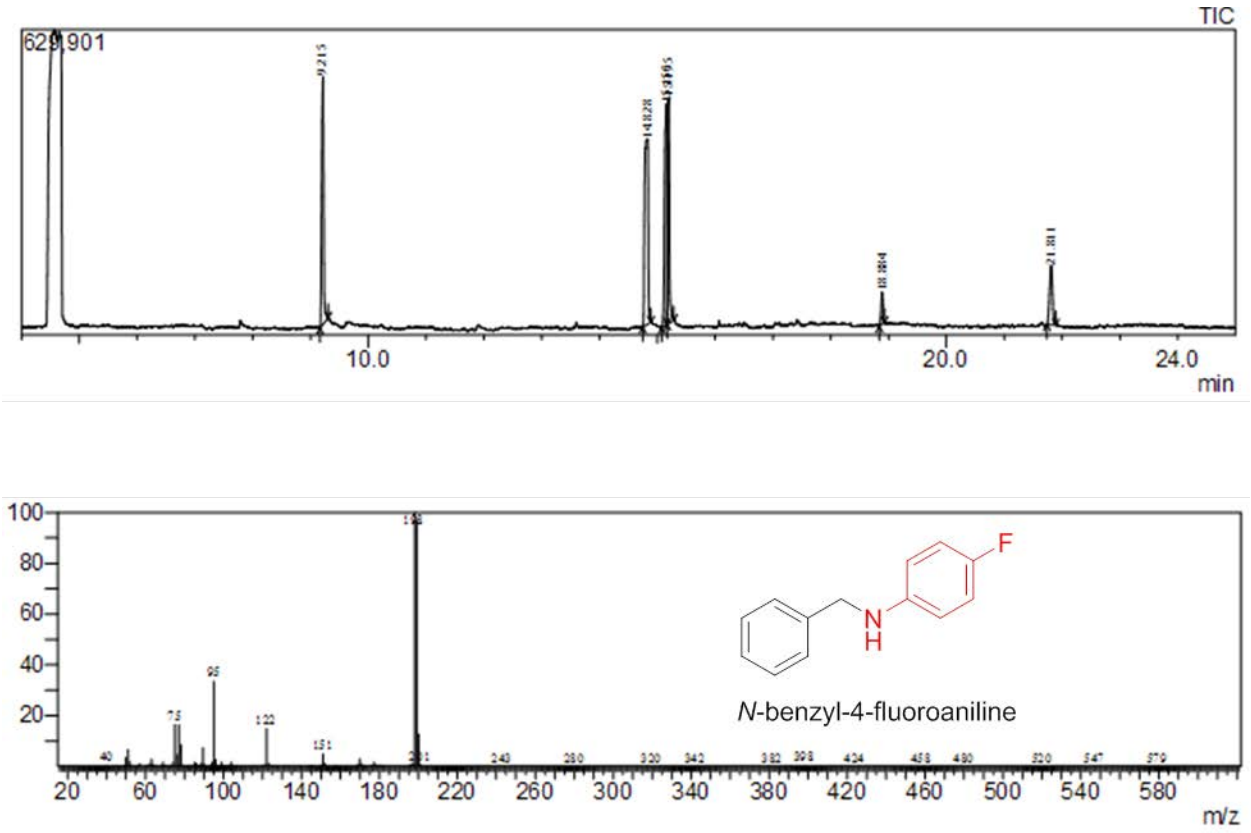

Fig. S44. GCMS of table 4, entry no. 13 (chromatogram and mass peaks)

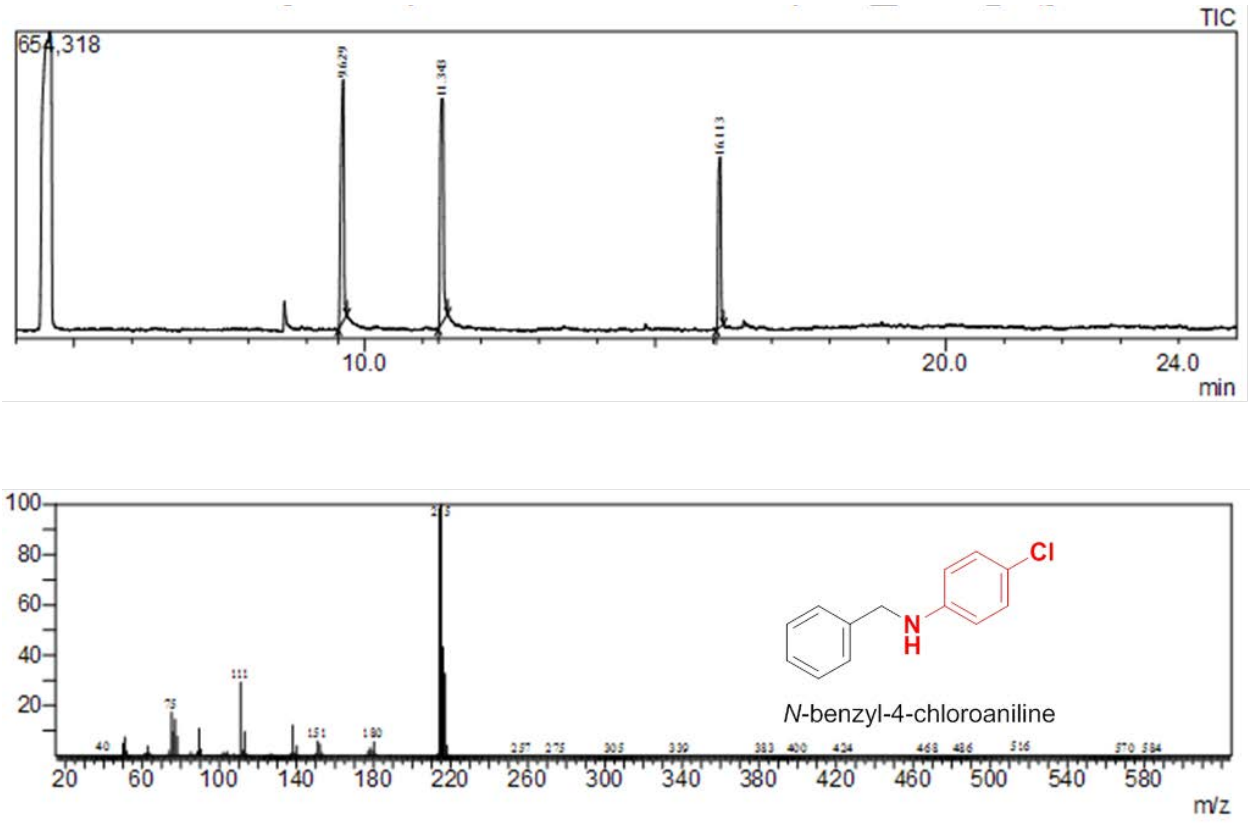

Fig. S45. GCMS of table 4, entry no. 14 (chromatogram and mass peaks)

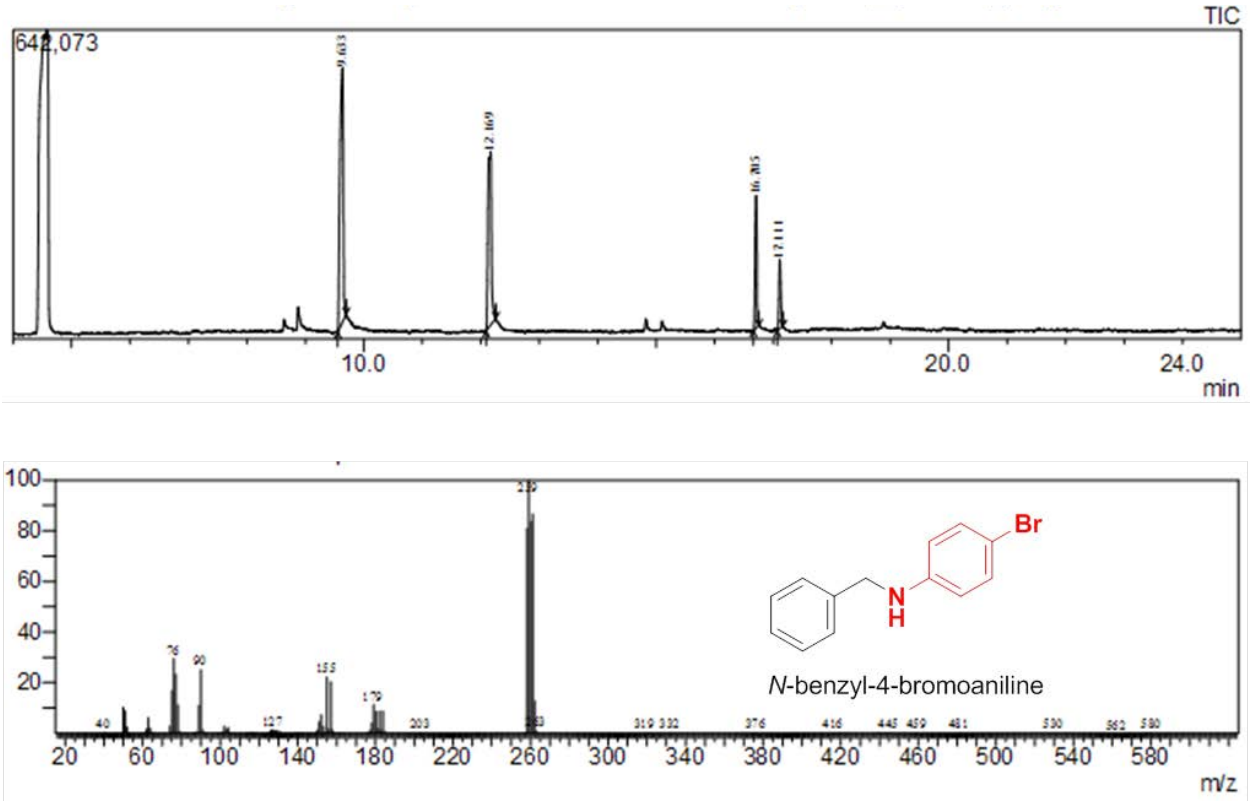

Fig. S46. GCMS of table 4, entry no. 15 (chromatogram and mass peaks)

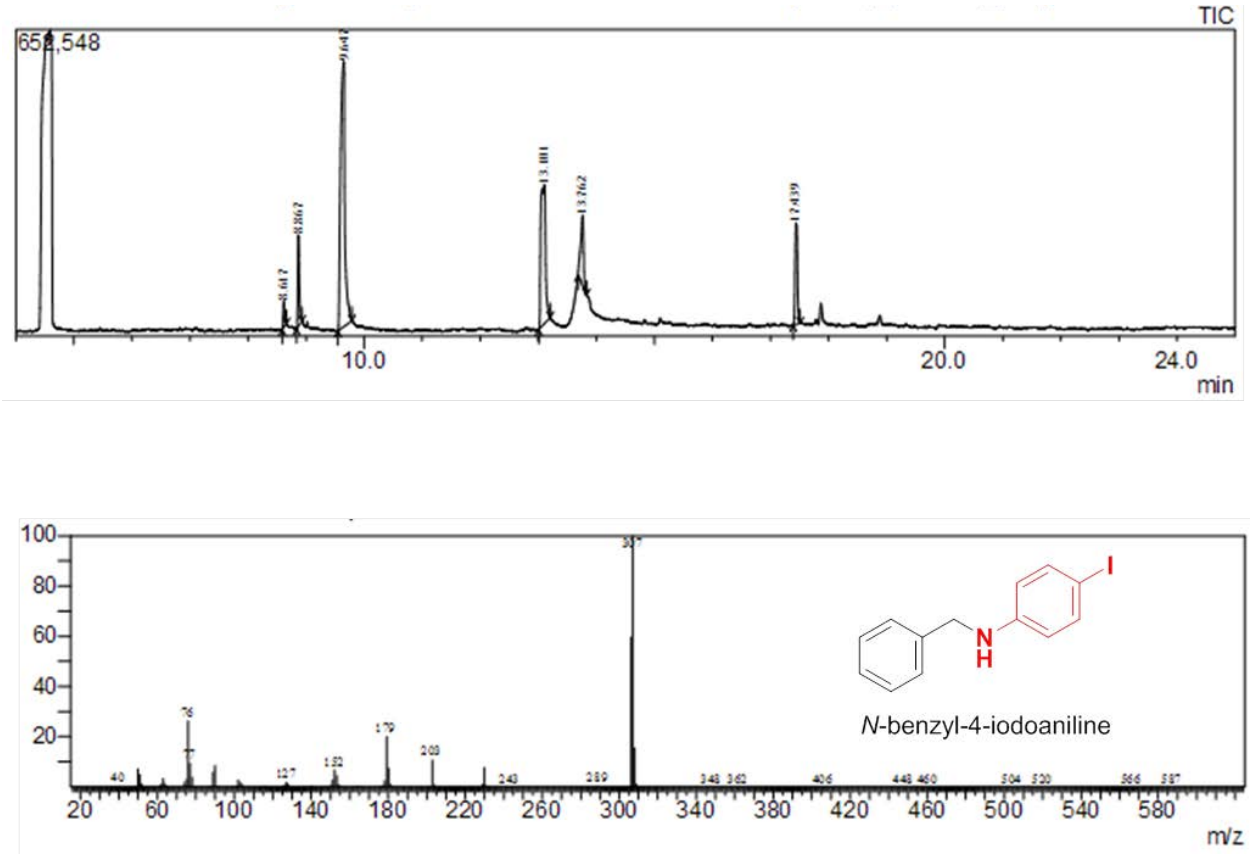

Fig. S47. GCMS of table 4, entry no. 16 (chromatogram and mass peaks)

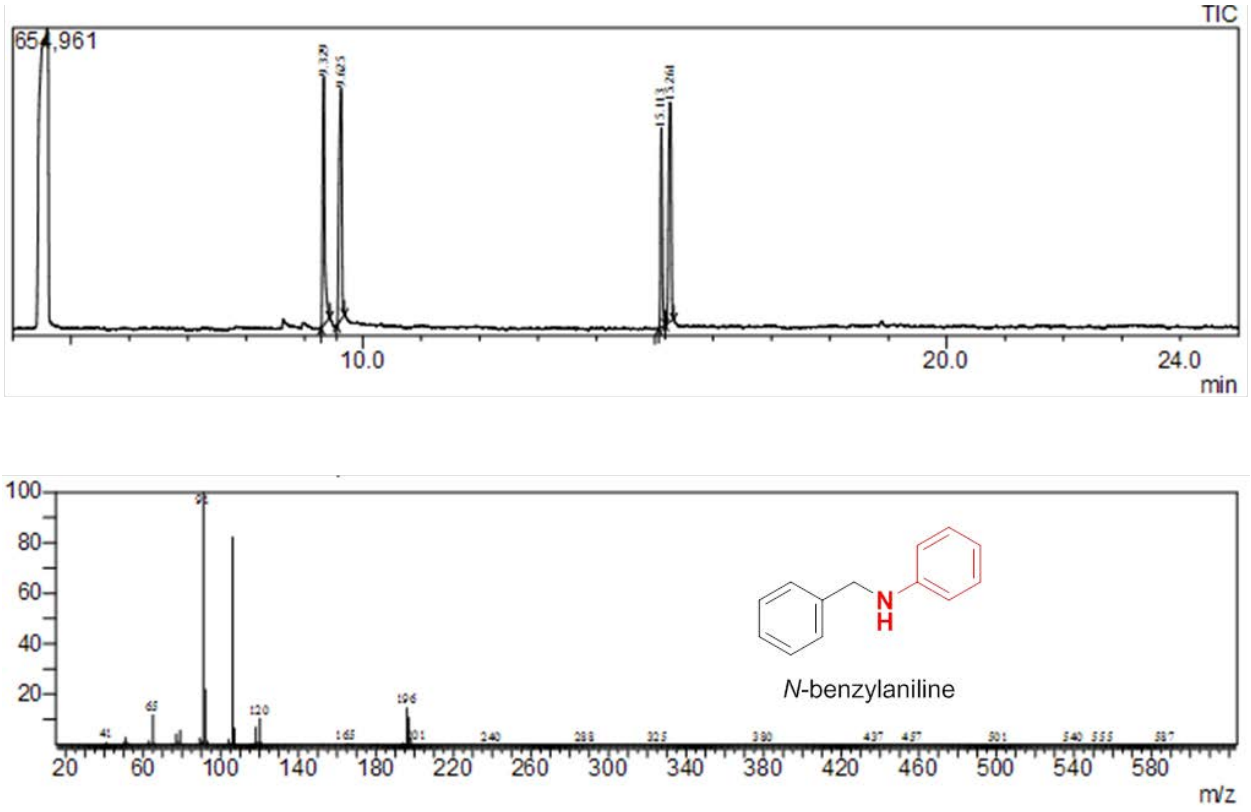

Fig. S48. GCMS of table 4, entry no. 17 (chromatogram and mass peaks)

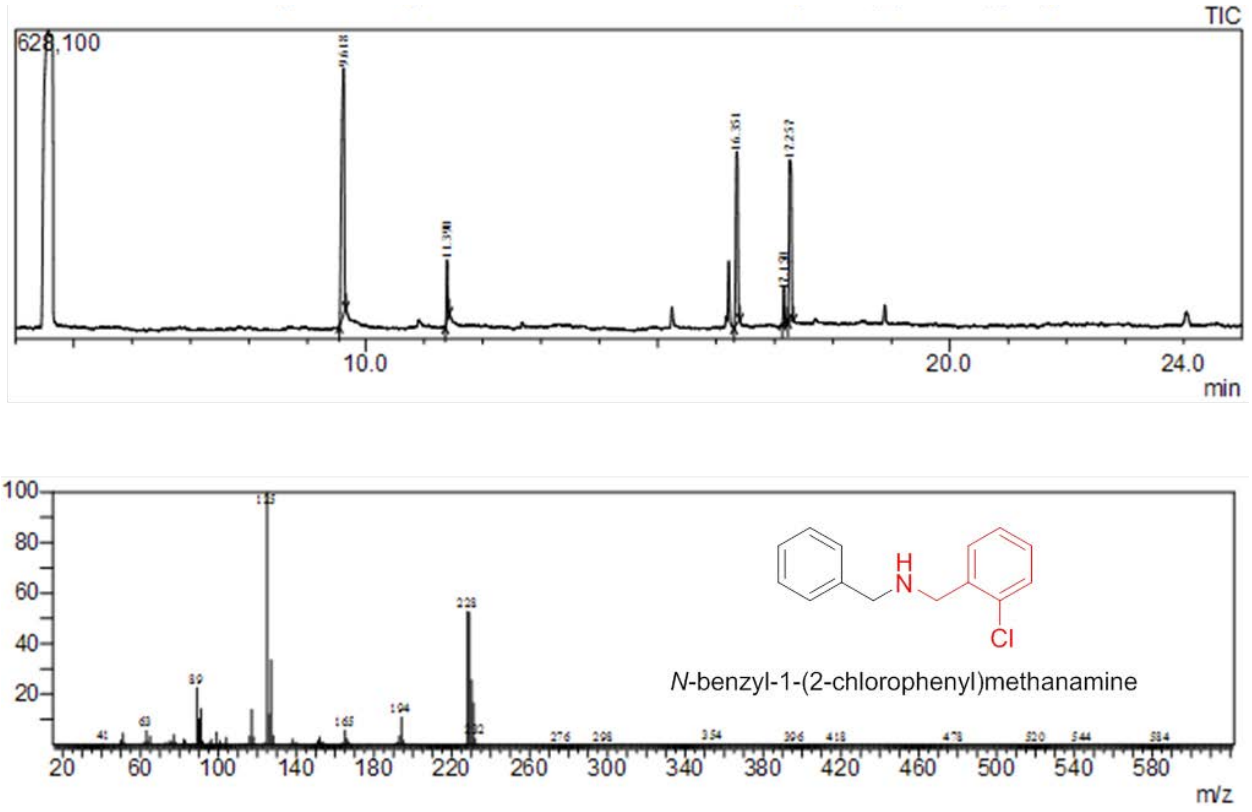

Fig. S49. GCMS of table 4, entry no. 18 (chromatogram and mass peaks)

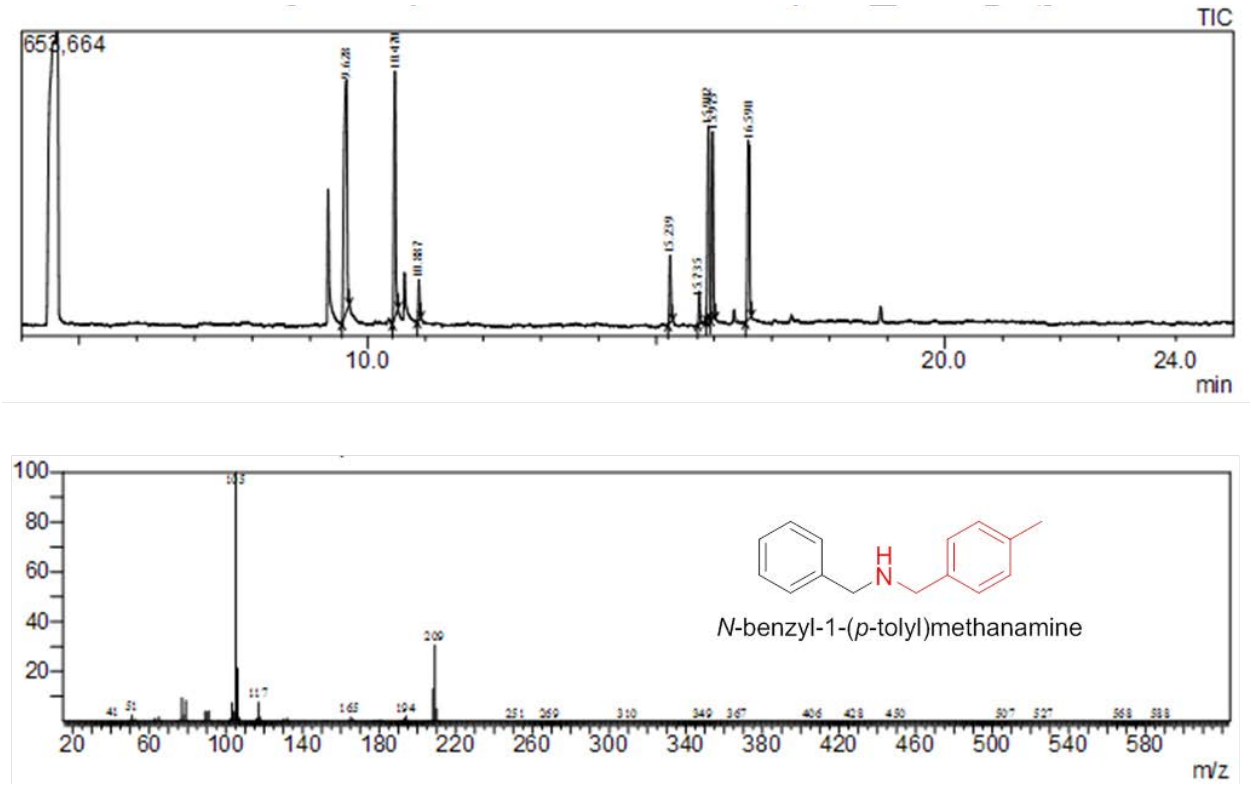

Fig. S50. GCMS of table 4, entry no. 19 (chromatogram and mass peaks)

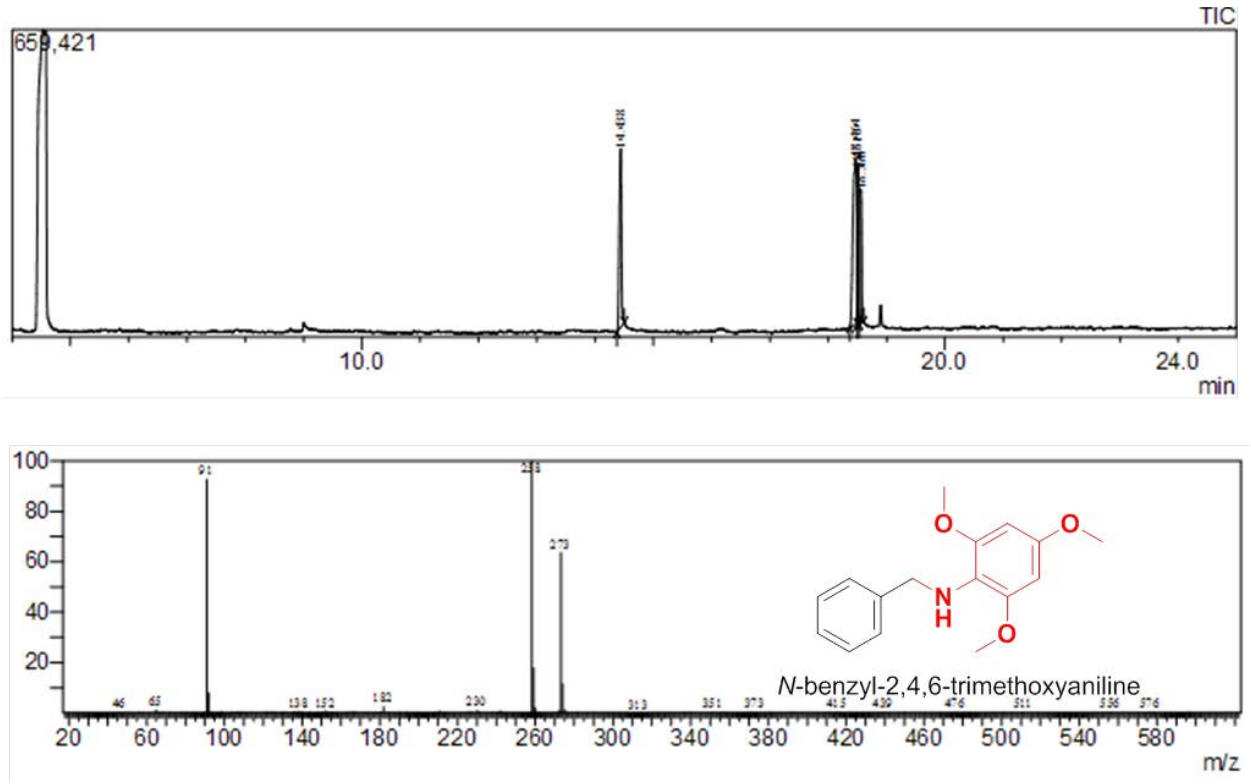

Fig. S51. GCMS of table 4, entry no. 20 (chromatogram and mass peaks)

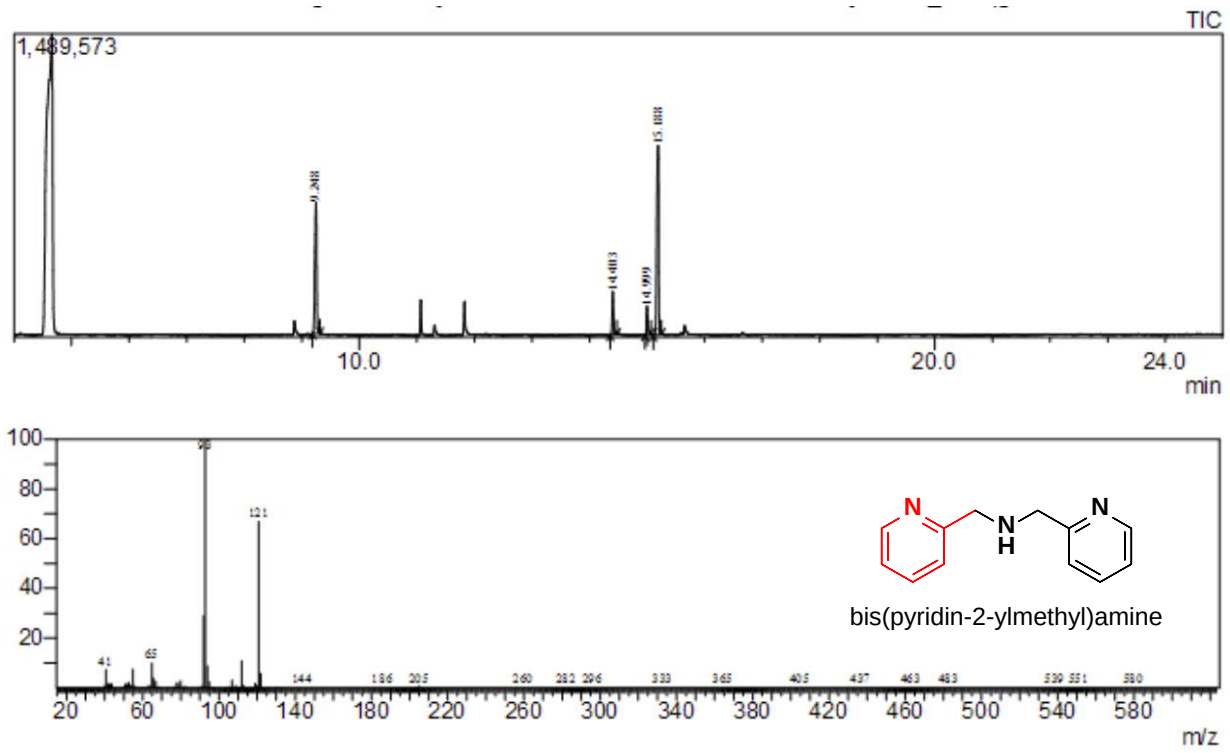

Fig. S52. GCMS of table 5, entry no. 1 (chromatogram and mass peaks)

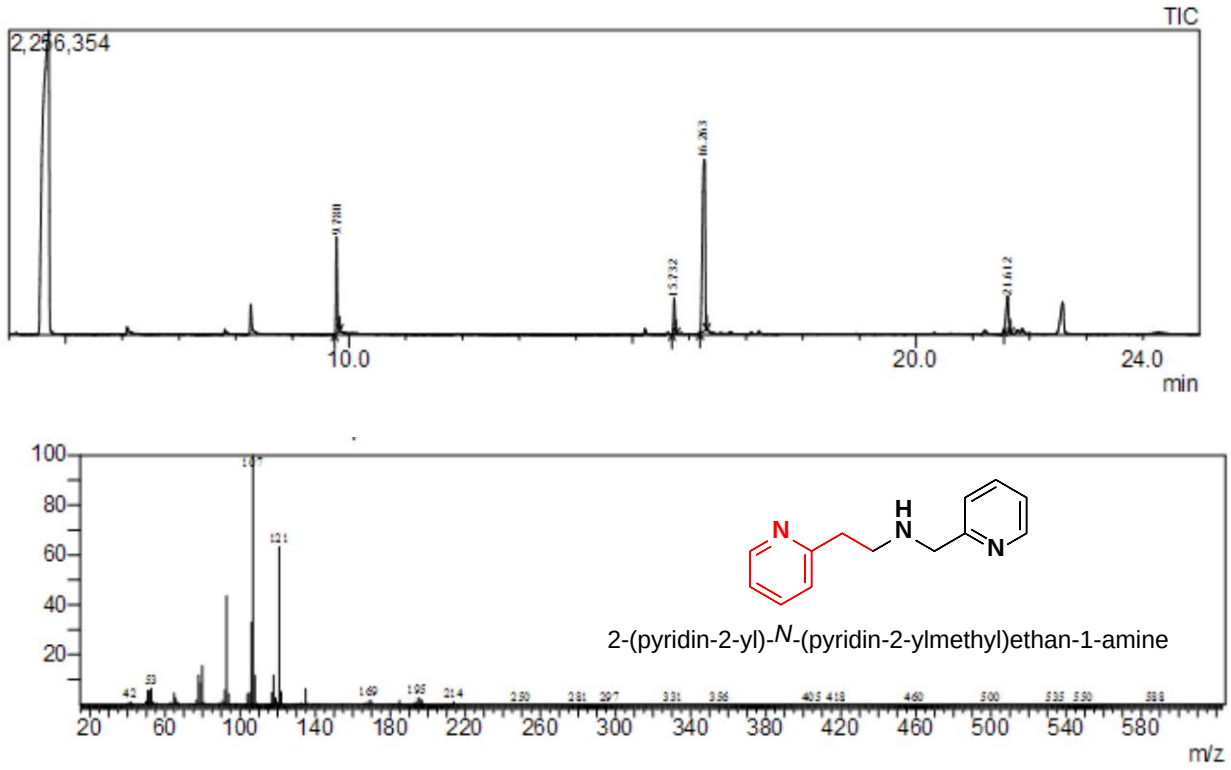

Fig. S53. GCMS of table 5, entry no. 2 (chromatogram and mass peaks)

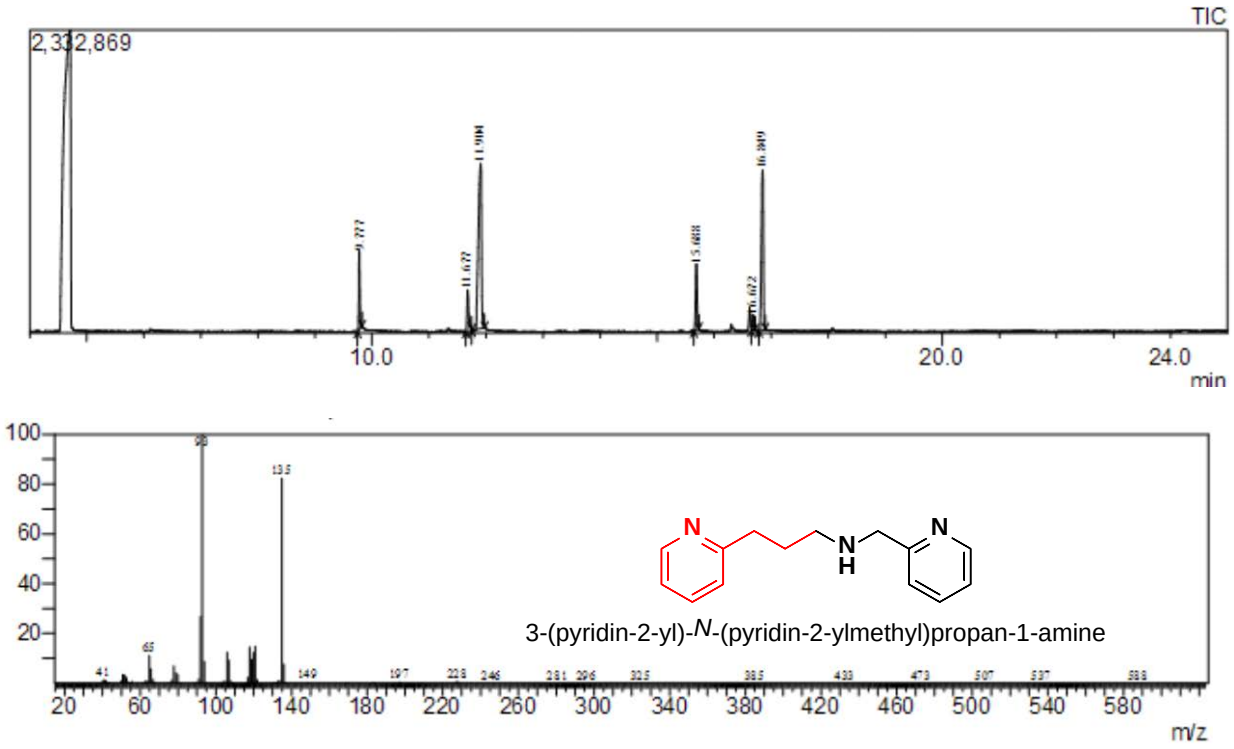

Fig. S54. GCMS of table 5, entry no. 3 (chromatogram and mass peaks)

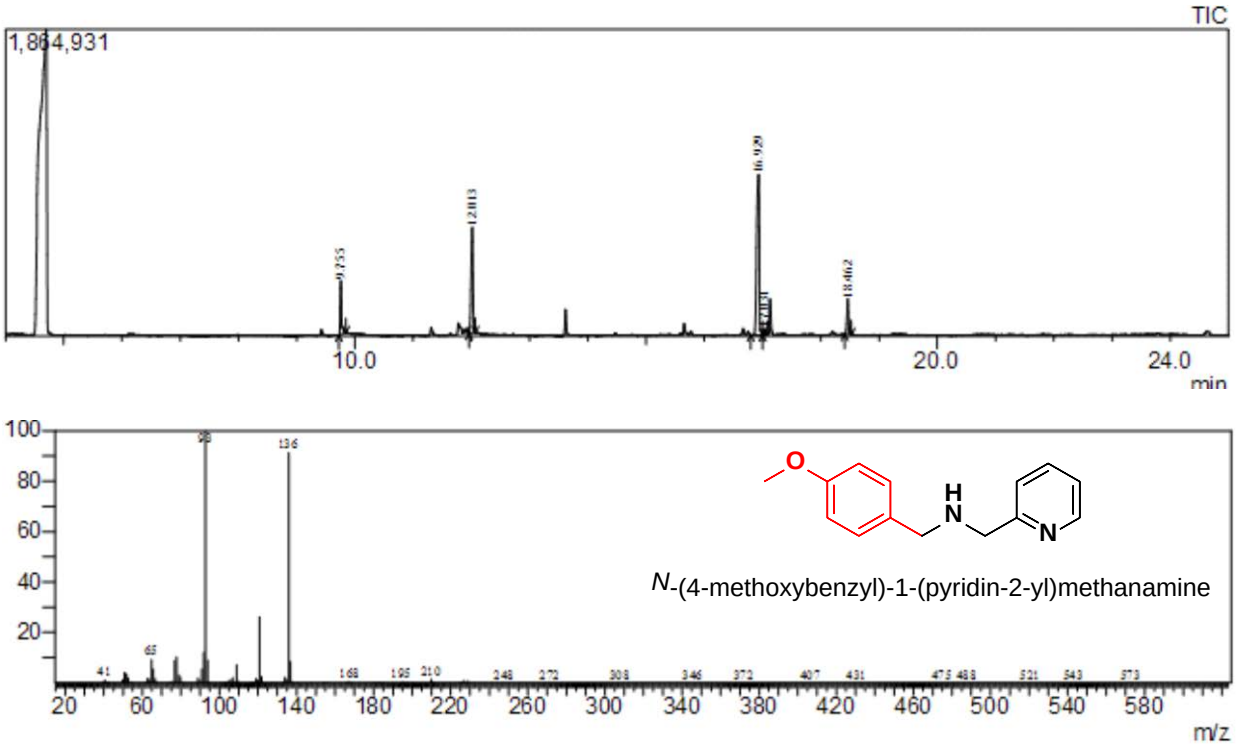

Fig. S55. GCMS of table 5, entry no. 4 (chromatogram and mass peaks)

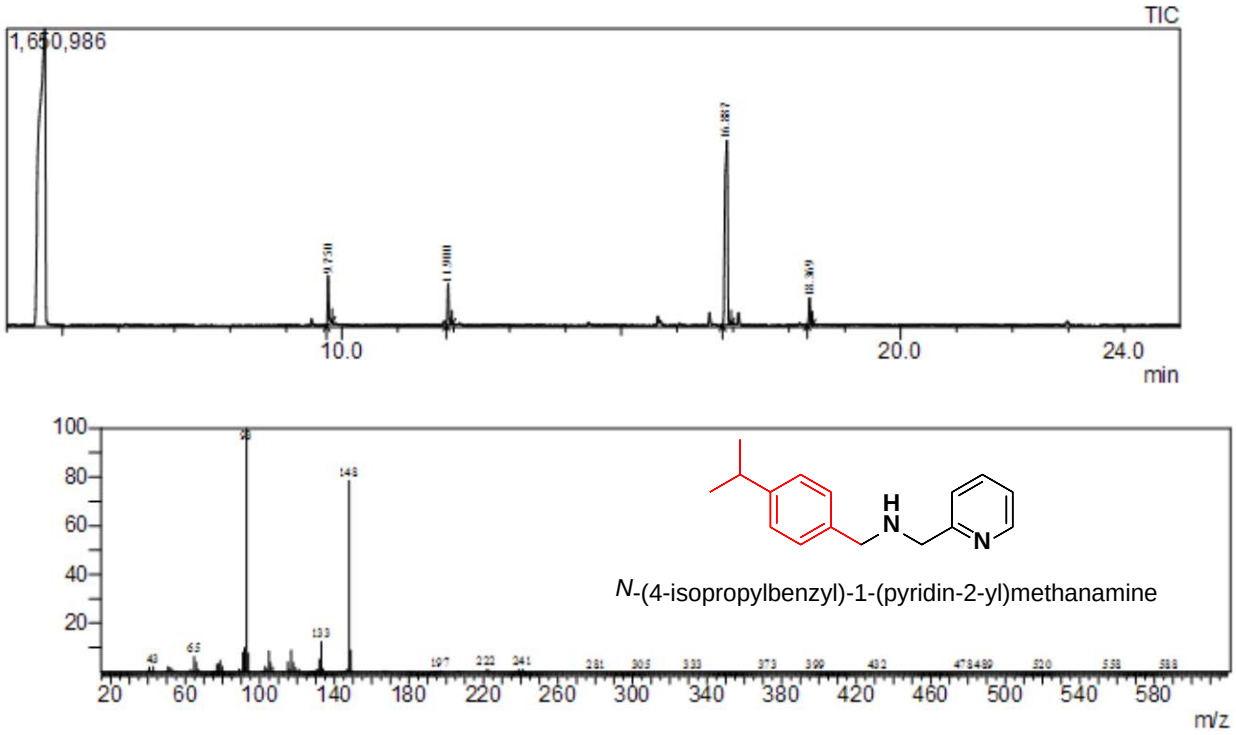

Fig. S56. GCMS of table 5, entry no. 5 (chromatogram and mass peaks)

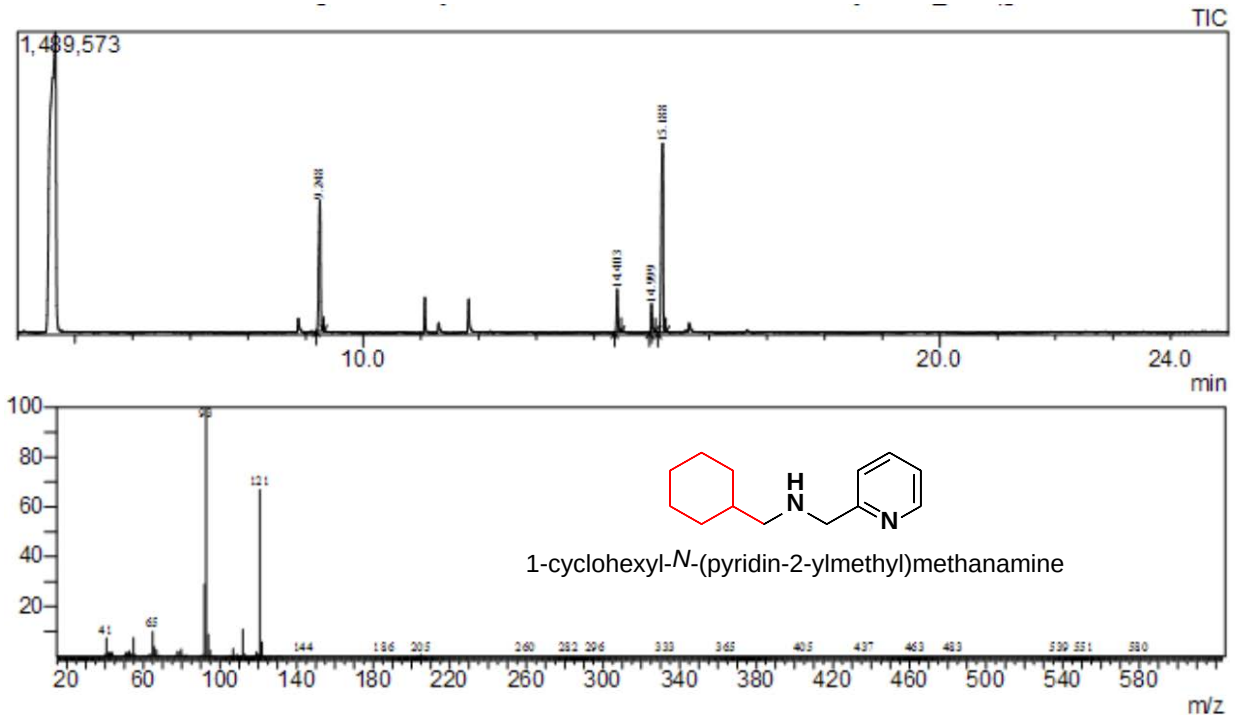

Fig. S57. GCMS of table 5, entry no. 6 (chromatogram and mass peaks)

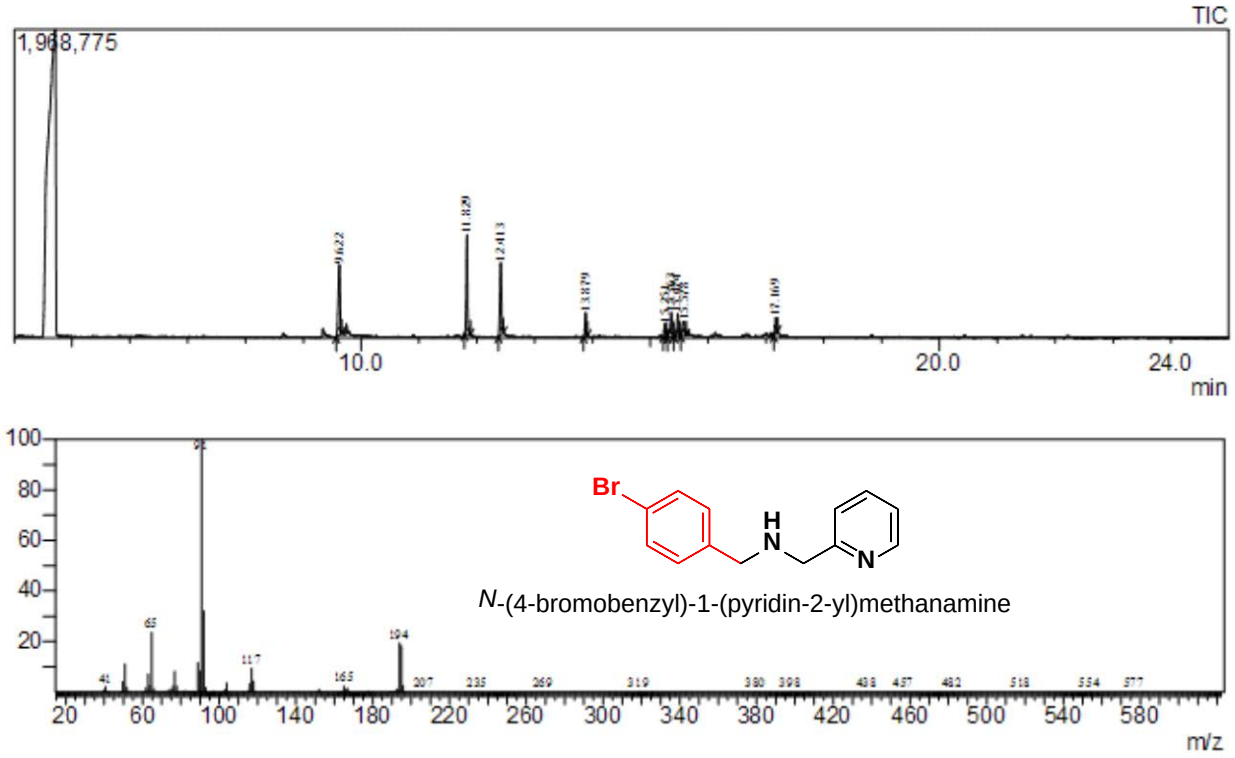

Fig. S58. GCMS of table 5, entry no. 7 (chromatogram and mass peaks)

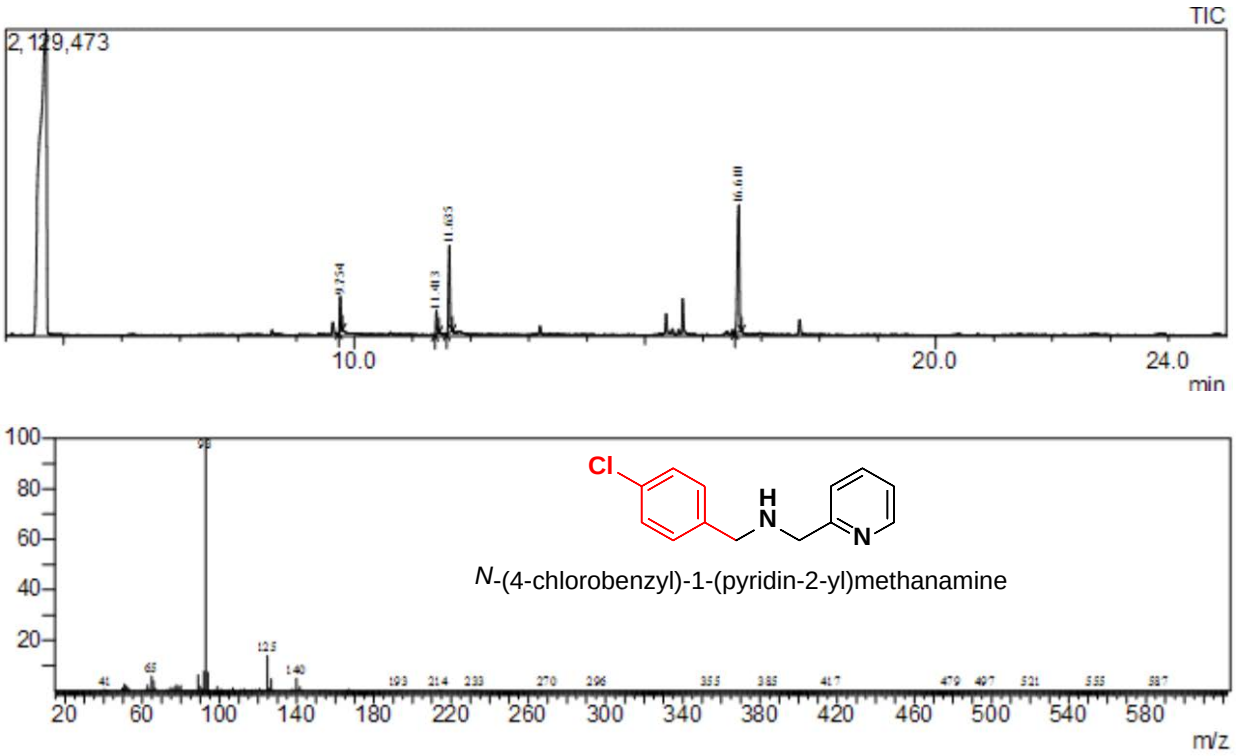

Fig. S59. GCMS of table 5, entry no. 8 (chromatogram and mass peaks)

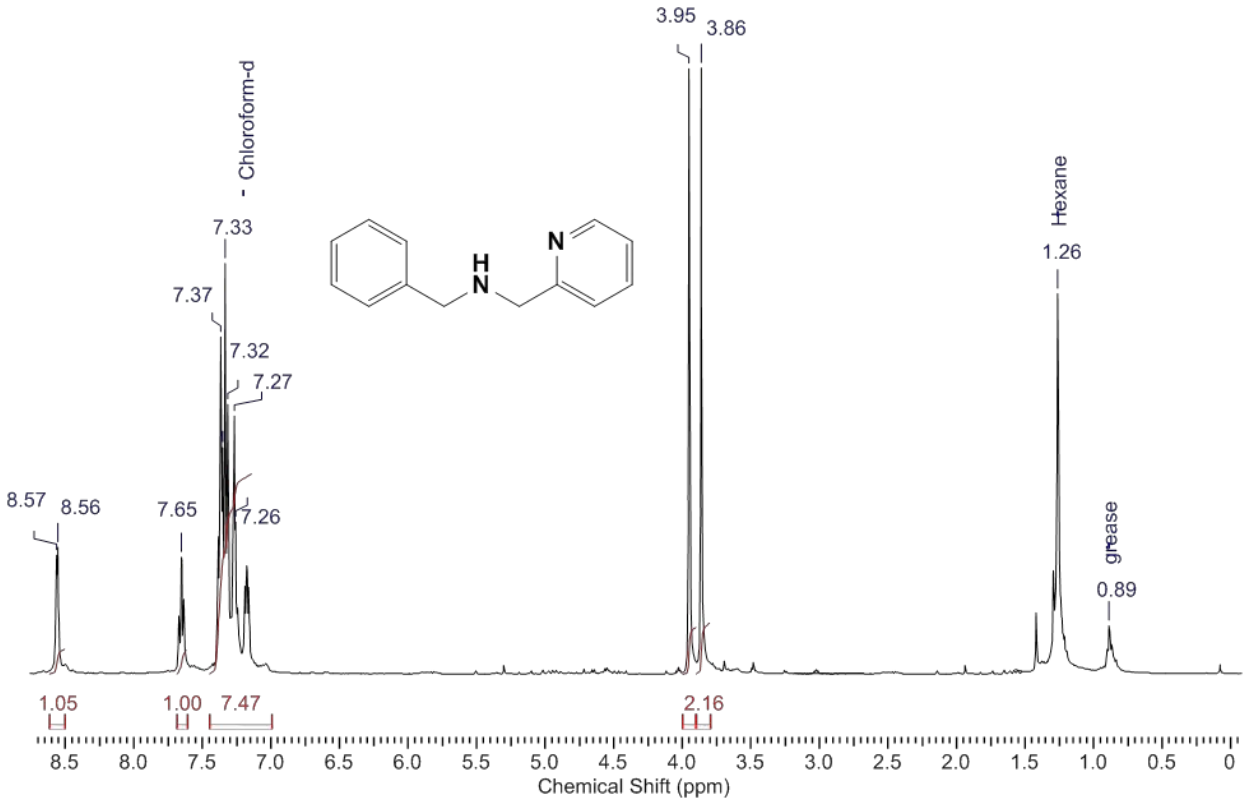

^{1}H NMR (400 MHz, $CDCl_3$): δ (ppm) = 8.56 (t, 1H), 7.65(t, 1H), 7.37–7.27 (m, 7H), 3.95 (s, 2H), 3.86 (s, 2H)

Fig. S60. ^{1}H NMR of N-benzyl-1-(pyridin-2-yl)methanamine (Table 6, entry 1)

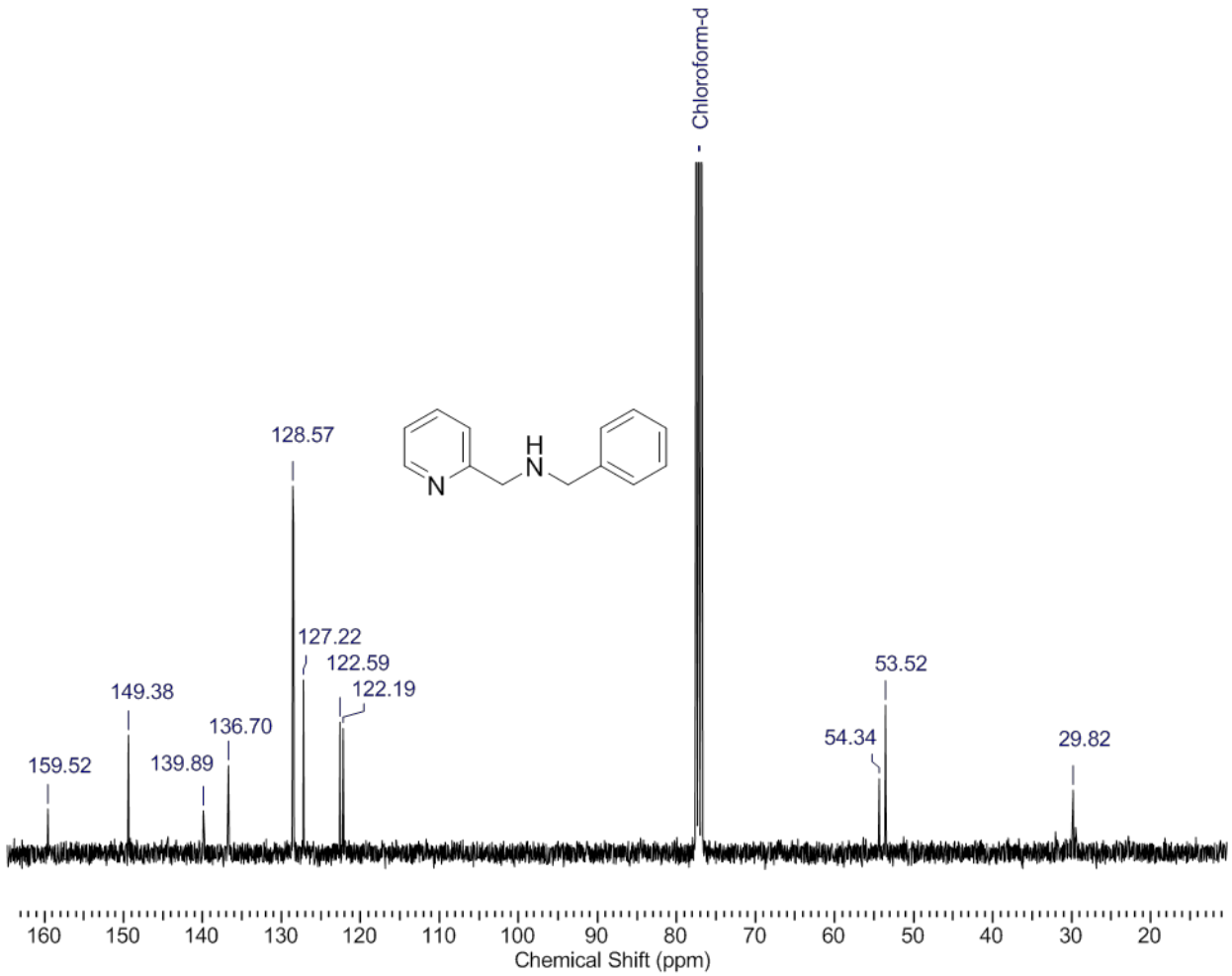

^{13}C NMR (400 MHz, $CDCl_3$): δ (ppm) = 159.5, 149.4, 139.9, 136.7, 128.6, 127.2, 122.6, 122.2, 54.3, 53.5, 29.3

Fig. S61. ^{13}C NMR of N-benzyl-1-(pyridin-2-yl)methanamine (Table 4, entry 1)

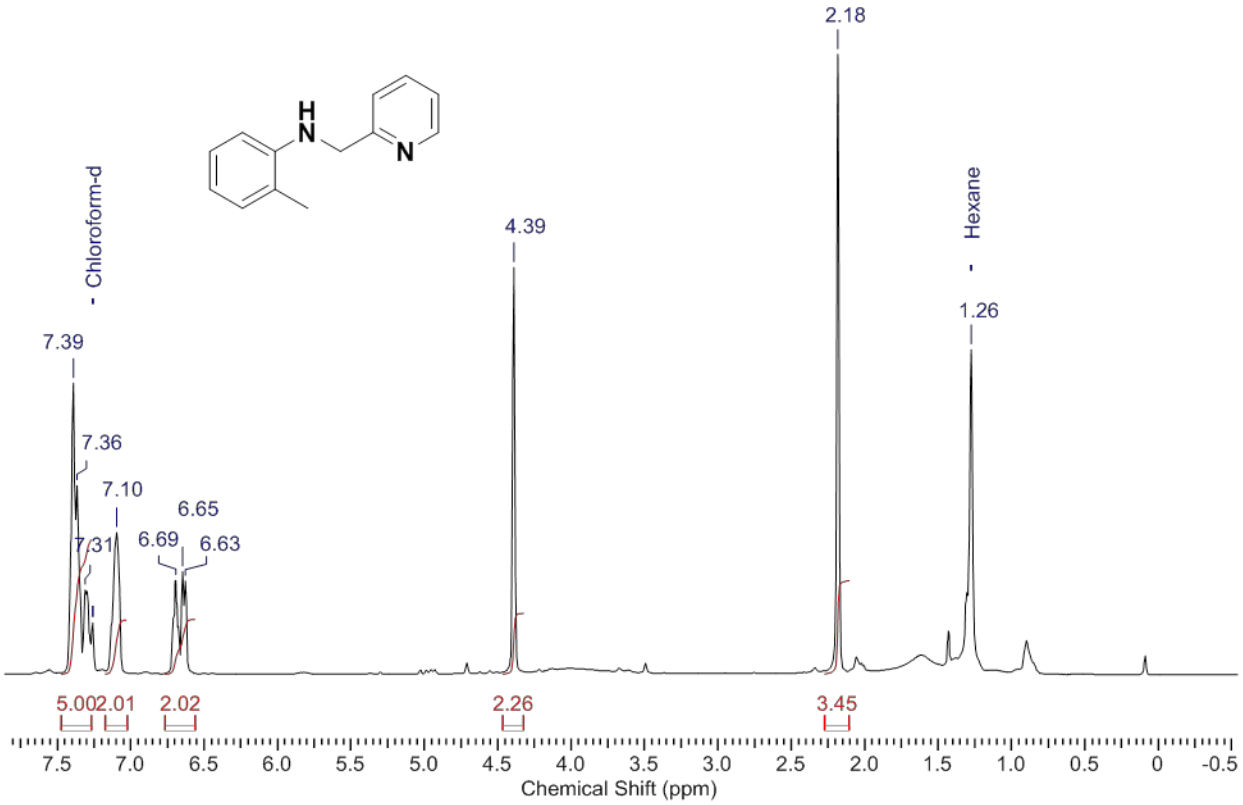

^{1}H NMR (400 MHz, $CDCl_3$): δ (ppm) = 7.39–7.31 (m, 5H), 7.10 (s, 2H), 6.69–6.65 (dt, 2H), 4.39 (s, 2H), 2.35 (s, 3H)

Fig. S62. ^{1}H NMR of o-toluidine (Table 4, entry 4)

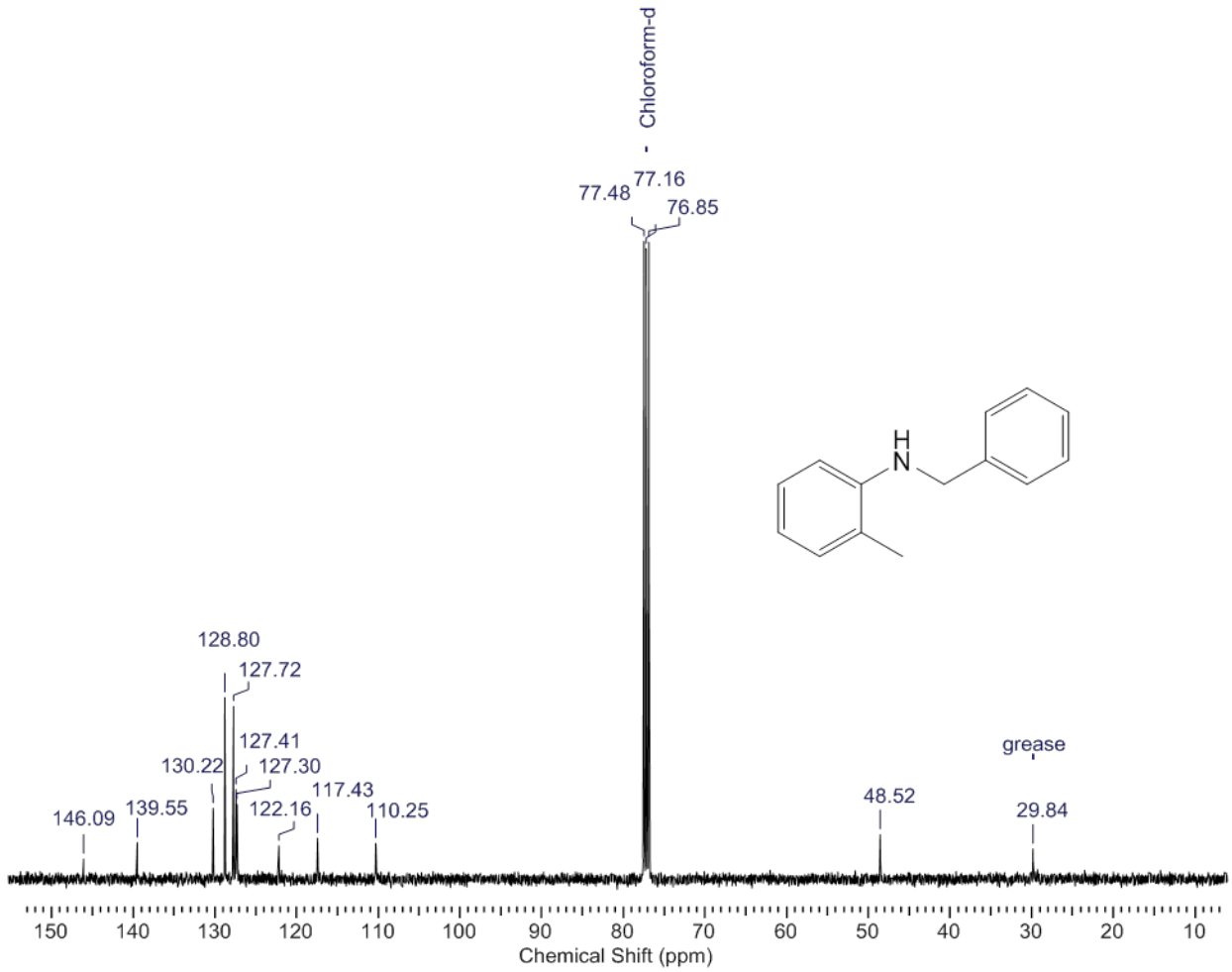

^{13}C NMR (400 MHz, $CDCl_3$): δ (ppm) = 146.0, 139.5, 130.2, 128.8, 127.7, 127.4, 127.3, 122.16, 117.4, 110.2, 48.5

Fig. S63. ^{13}C NMR of o-toluidine (Table 4, entry 4)

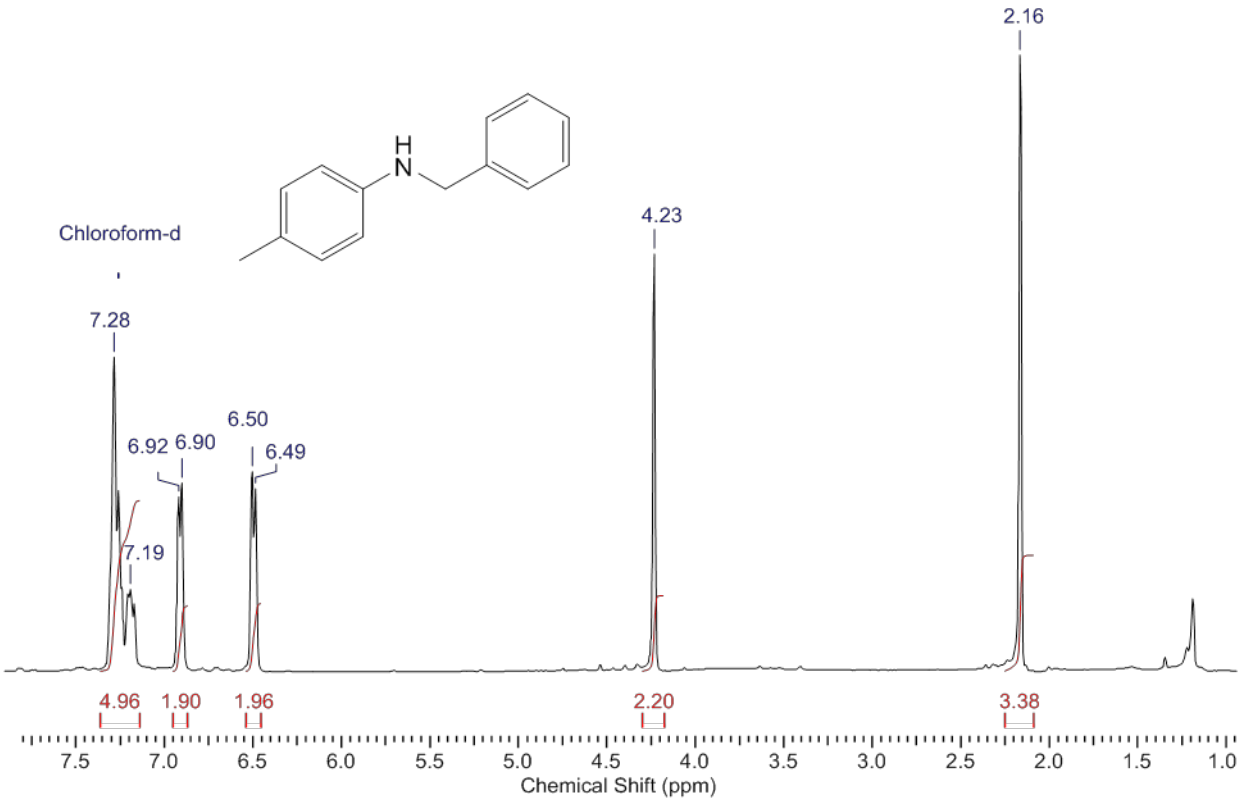

^{1}H NMR (400 MHz, $CDCl_3$): δ (ppm) = 7.28–7.19 (m, 5H), 6.92 (d, 2H), 6.50 (d, 2H), 4.23 (s, 2H), 2.165 (s, 3H)

Fig. S64. ^{1}H NMR of p-toluidine (Table 4, entry 7)

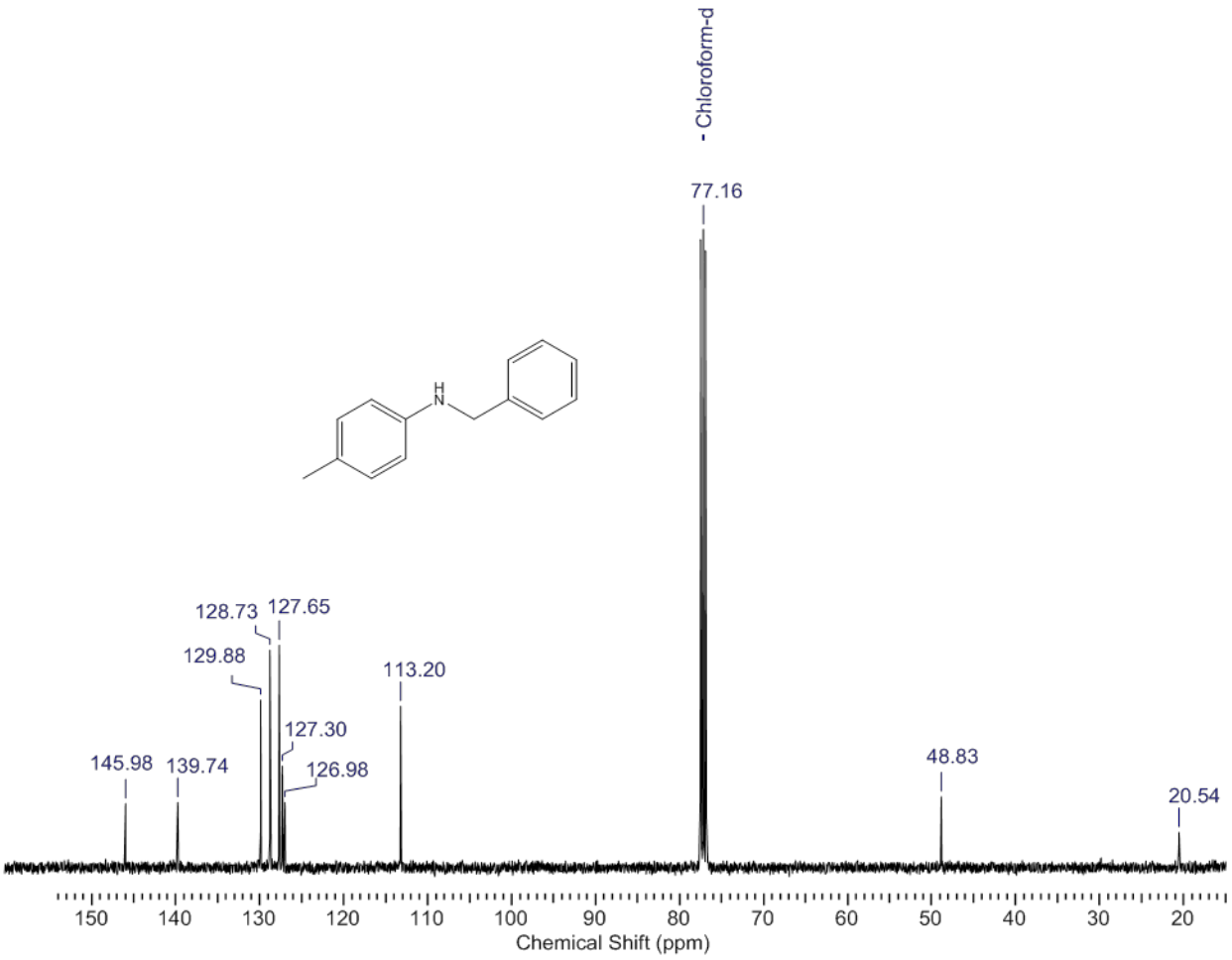

^{13}C NMR (400 MHz, $CDCl_3$): δ (ppm) = 146.0, 139.7, 129.9, 128.7, 127.7, 127.3, 127.0, 113.2, 48.8, 20.5.

Fig. S65. ^{13}C NMR of p-toluidine (Table 4, entry 7)

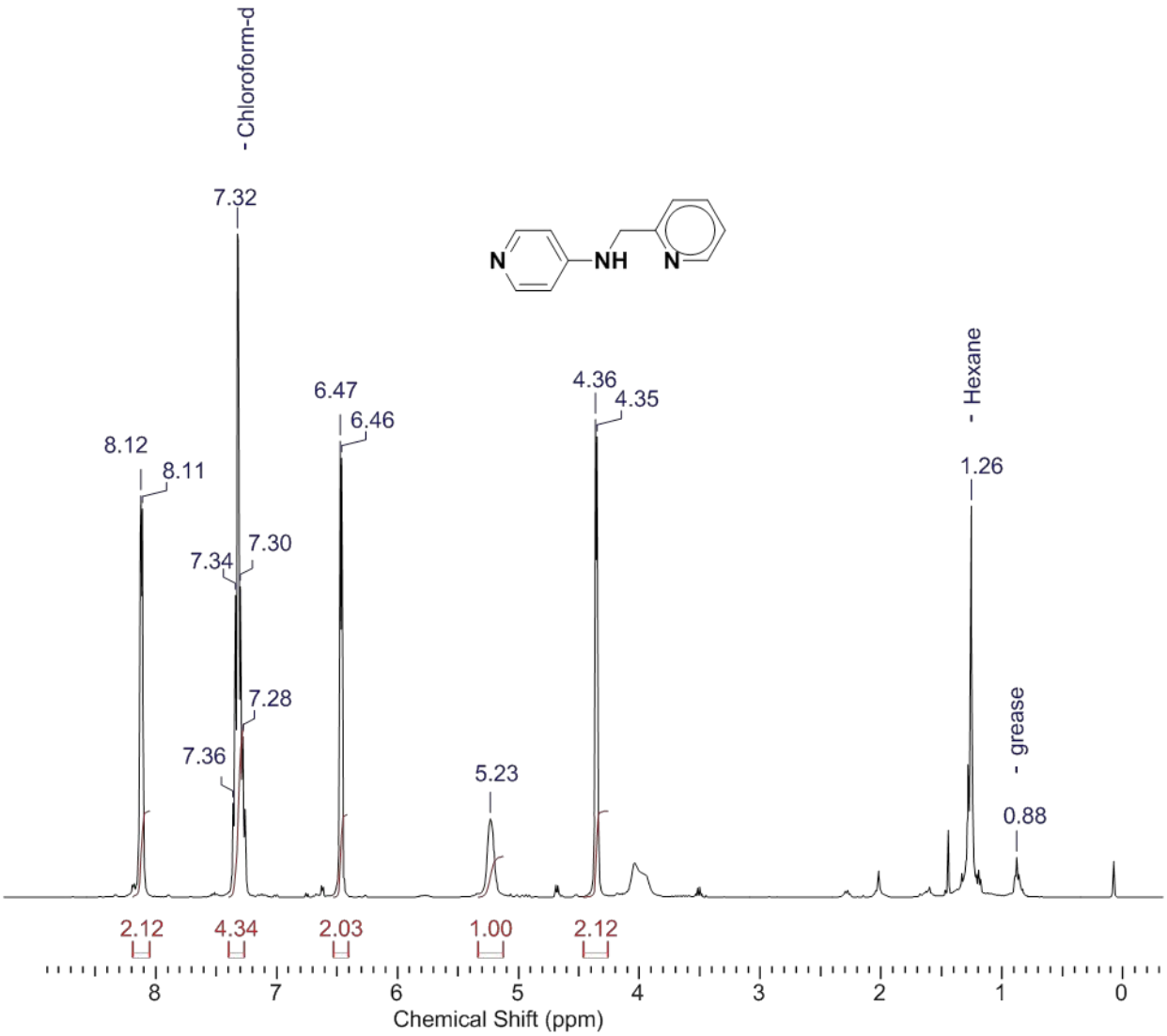

^{1}H NMR (400 MHz, $CDCl_3$): δ (ppm) = 8.12 (d, 2H), 7.32 (q, 4H), 6.47 (d, 2H), 5.23 (s, 1H), 4.36 (s, 2H)

Fig. S66. ^{1}H NMR of N-(pyridin-2-ylmethyl)pyridin-4-amine (Table 4, entry 11)

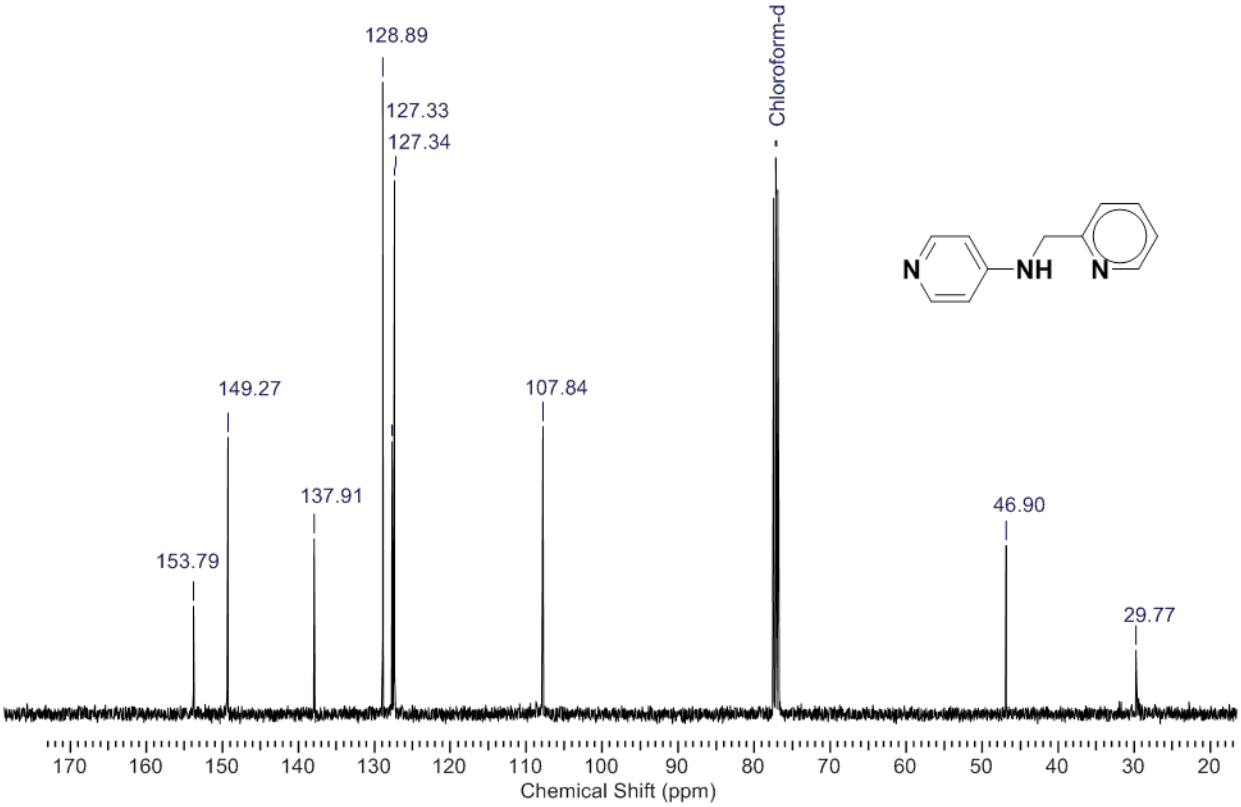

^{13}C NMR (400 MHz, $CDCl_3$): δ (ppm) = 153.8, 149.3, 137.9, 128.9, 127.3, 127.3, 107.3, 46.9, 29.8

Fig. S67. ^{13}C NMR of N-(pyridin-2-ylmethyl)pyridin-4-amine (Table 4, entry 11)

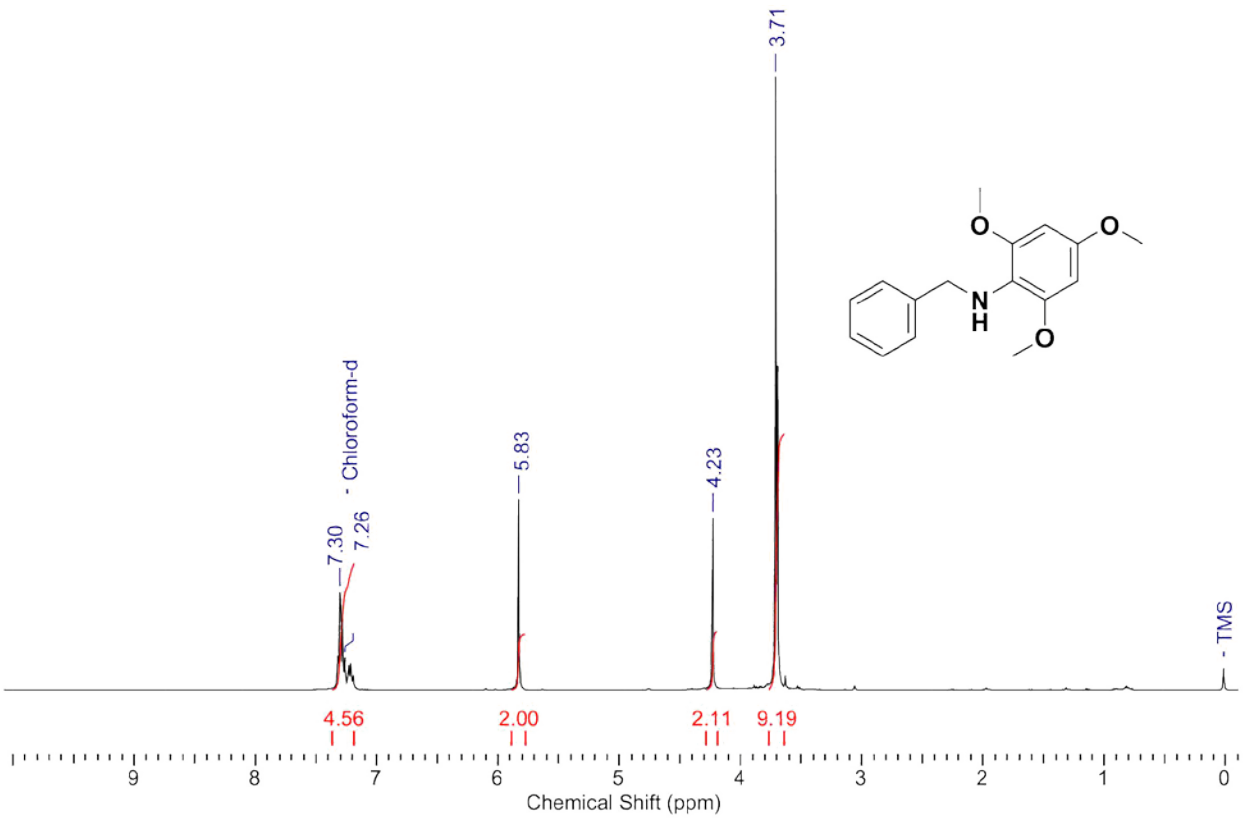

^{1}H NMR (400 MHz, $CDCl_3$): δ (ppm) = 7.32 (m, 4H), 5.83 (s, 2H), 4.23 (s, 2H), 3.71 (d, 9H)

Fig. S68. ^{1}H NMR of N-benzyl-2,4,6-trimethoxyaniline (Table 4, entry 20)

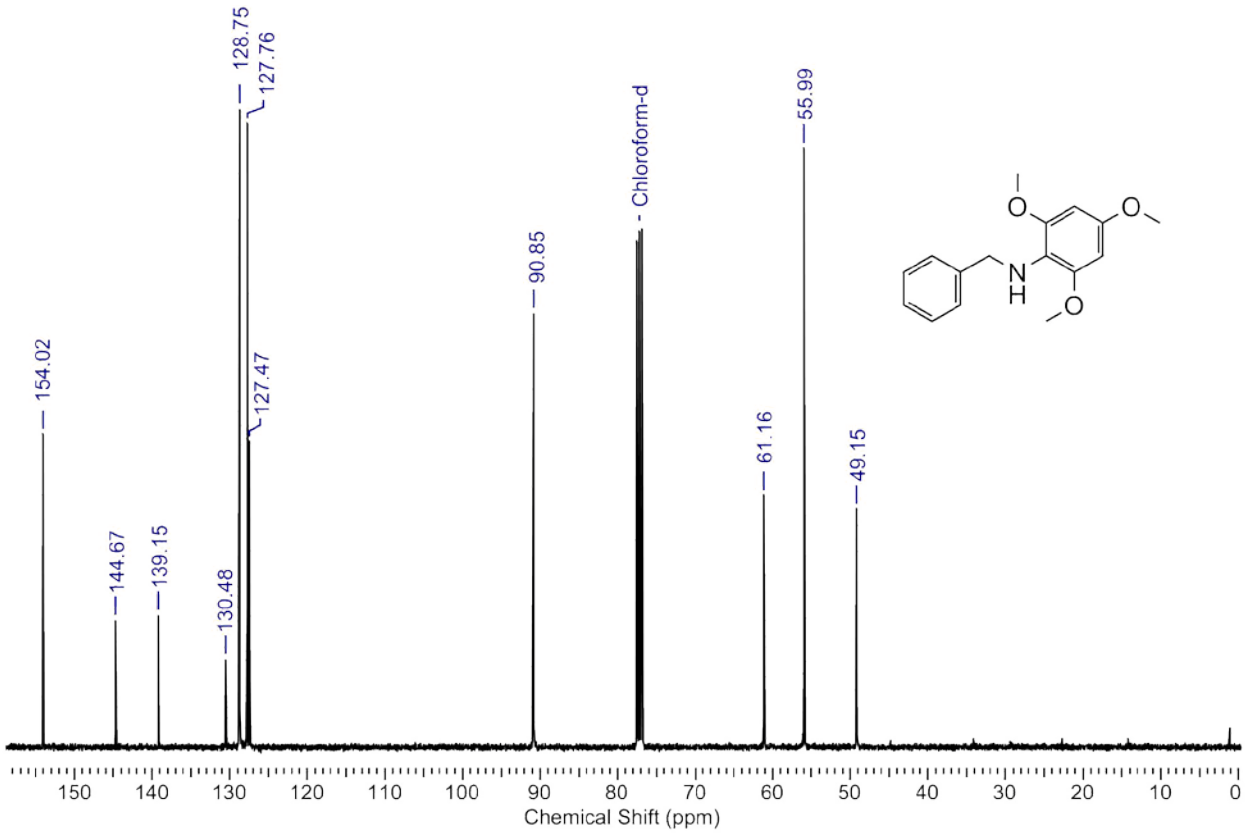

^{13}C NMR (400 MHz, $CDCl_3$): δ (ppm) = 154.0, 144.7, 139.2, 130.5, 128.75, 127.76, 127.5, 90.9, l61.2, 55.9, 49.2

Fig. S69. ^{13}C NMR of N-benzyl-2,4,6-trimethoxyaniline (Table 4, entry 20)

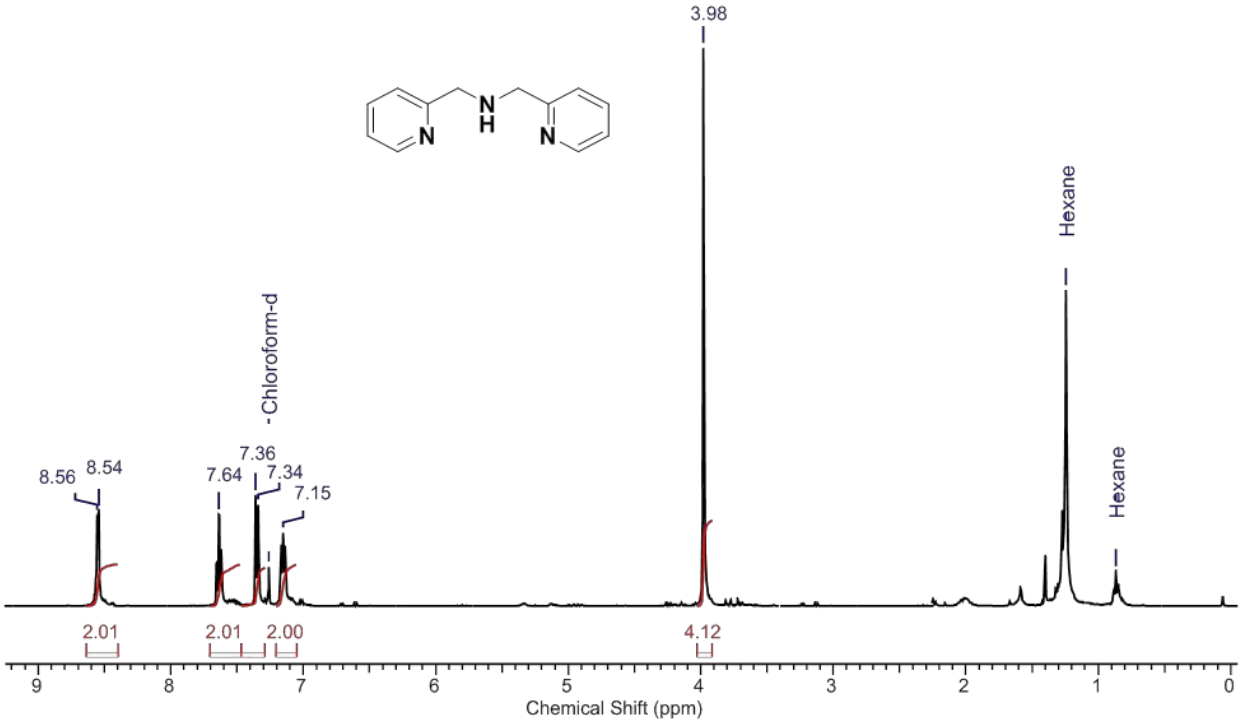

^{1}H NMR (400 MHz, $CDCl_3$): δ (ppm) = 8.56 (d, 2H), 7.64 (t, 2H), 7.36 (d, 2H), 7.15 (t, 2H), 3.98 (s, 4H)

Fig. S70. ^{1}H NMR of bis(pyridin-2-ylmethyl)amine (Table 5, entry 1)

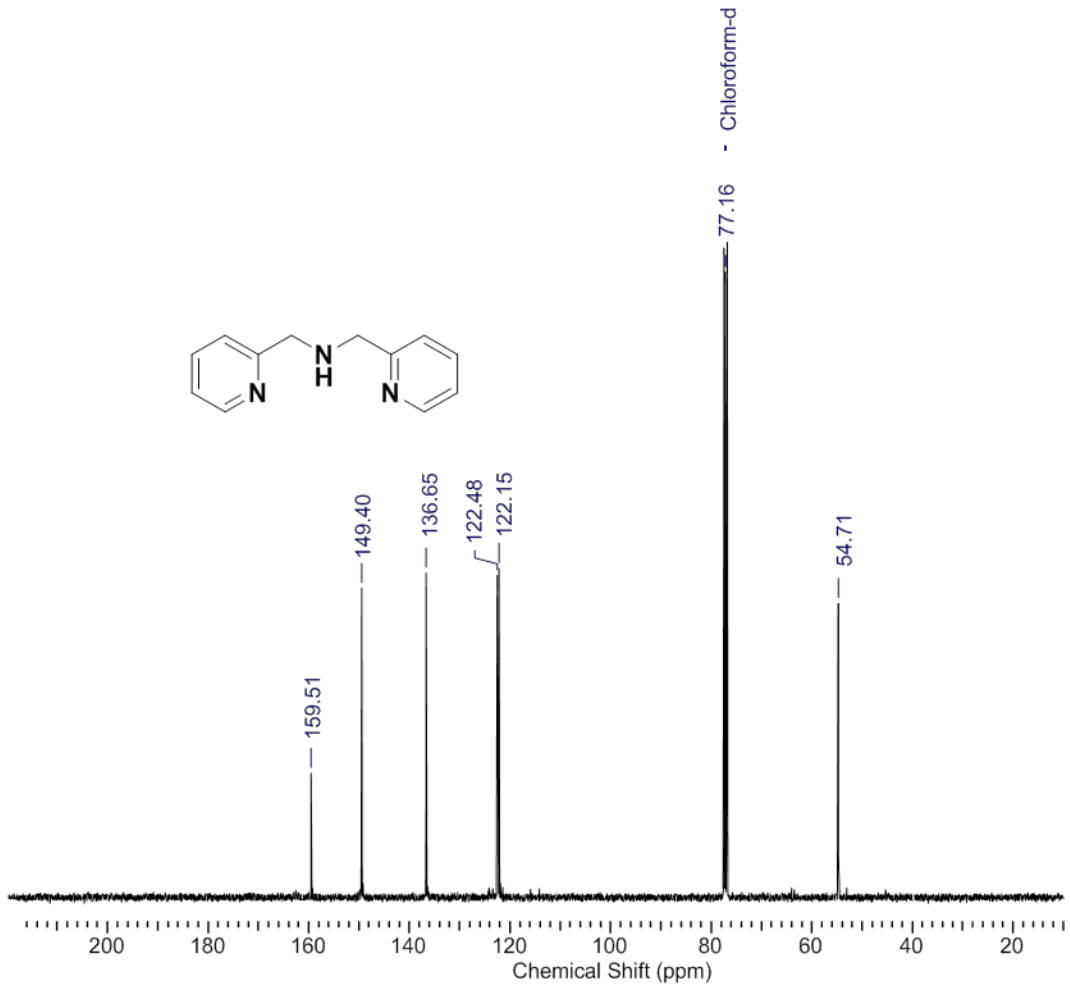

^{13}C NMR (400 MHz, $CDCl_3$): δ (ppm) = 159.5, 149.4, 136.7, 122.5, 122.2, 54.7

Fig. S71. ^{13}C NMR of bis(pyridin-2-ylmethyl)amine (Table 5, entry 1)

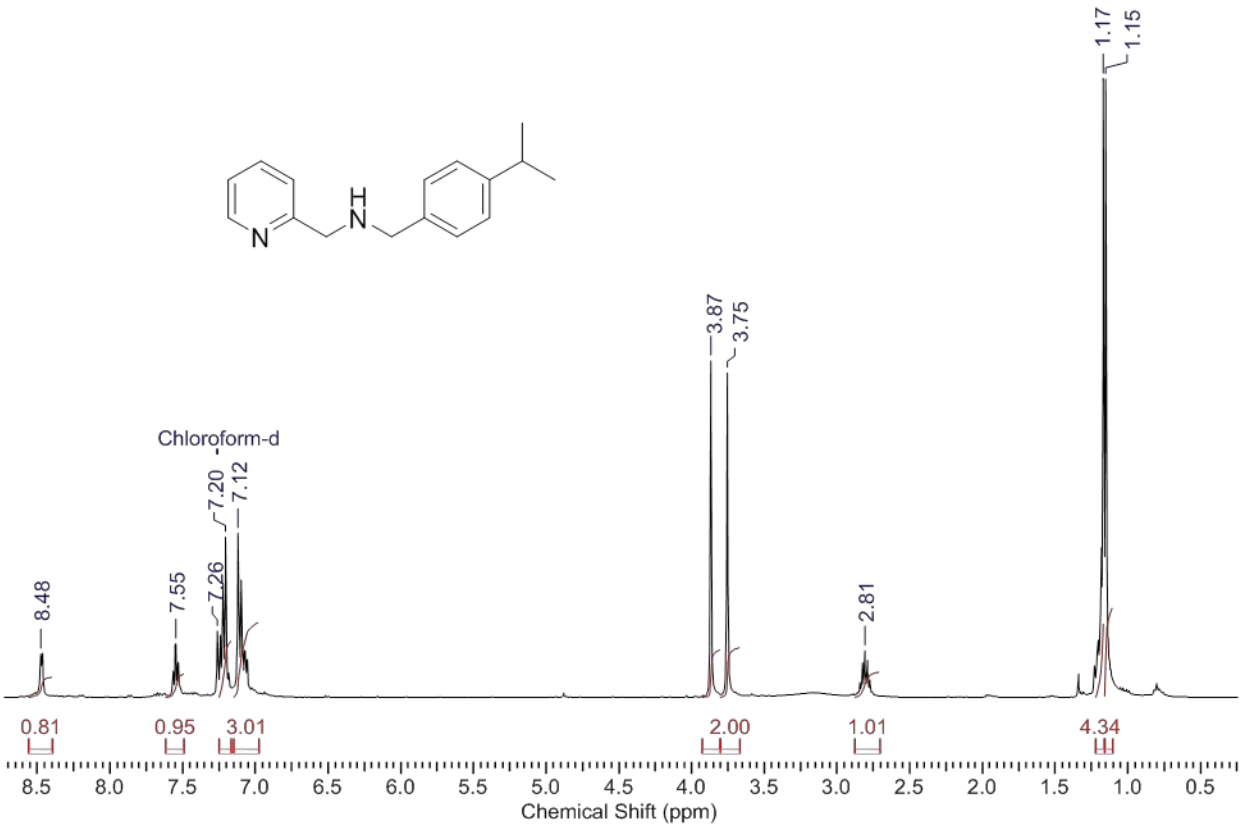

^{1}H NMR (400 MHz, $CDCl_3$): δ (ppm) = 8.48 (d, 1H), 7.55 (d, 1H), 7.20-7.12 (4H), 3.87 (d, 2H), 3.75 (d, 2H), 2.81 (m, 1H), 1.17-1.15 (m, 6H)

Fig. S72. ^{1}H NMR of N-(4-isopropylbenzyl)-1-(pyridin-2-yl)methanamine (Table 5, entry 5)

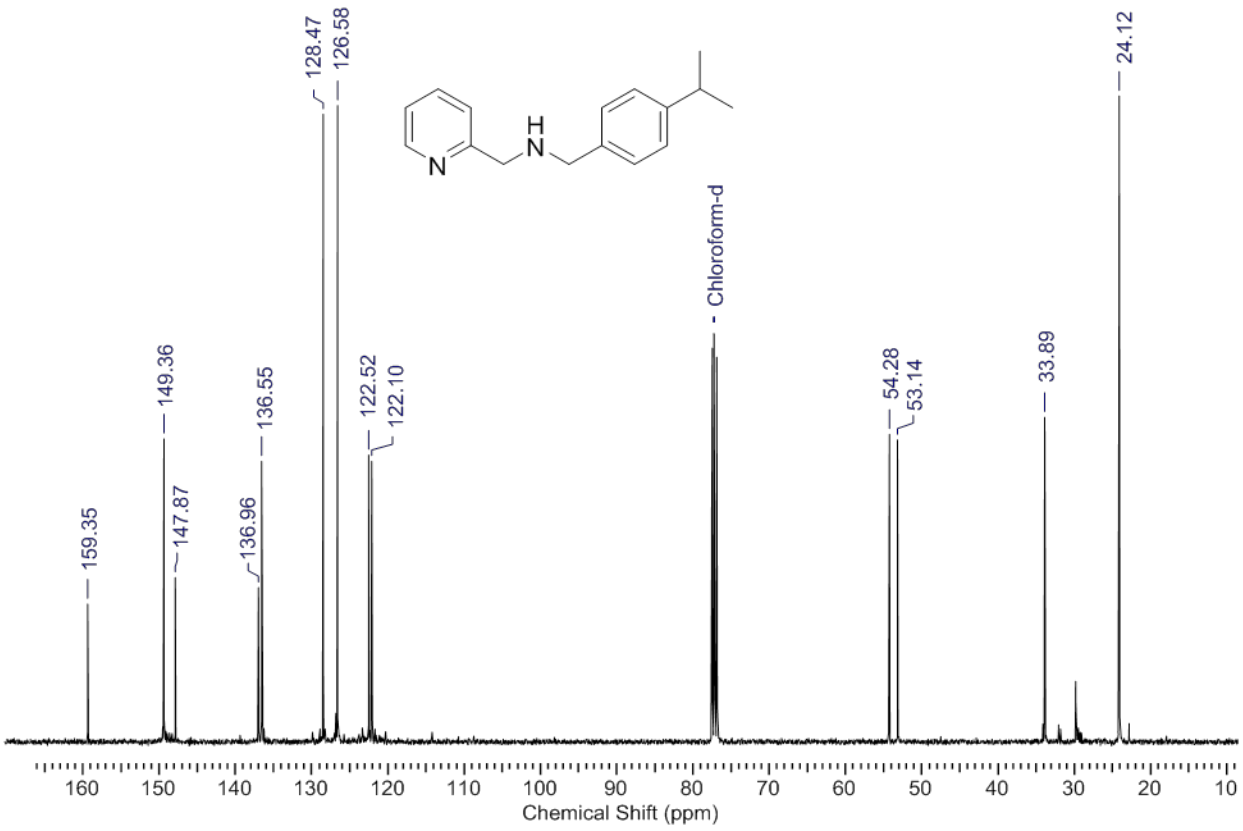

^{13}C NMR (400 MHz, $CDCl_3$): δ (ppm) = 159.4, 149.4, 147.9, 136.6, 128.5, 126.6, 122.5, 122.1, 54.3, 53.1, 33.9, 24.1

Fig. S73. ^{13}C NMR of N-(4-isopropylbenzyl)-1-(pyridin-2-yl)methanamine (Table 5, entry 5)

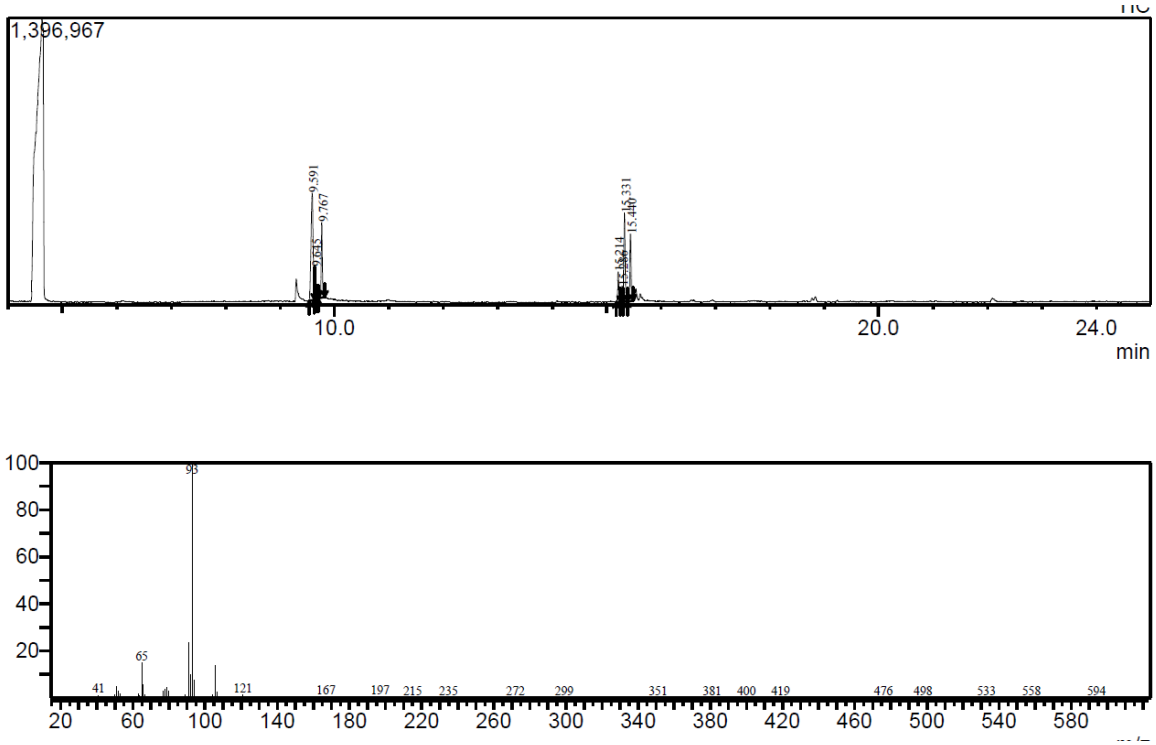

Fig. S74. Mercury Poisoning experiment of the standard reaction between benzyl alcohol and picolylamine

X-ray Crystallography

Data were collected at 293 K using graphite-monochromated Mo Kα (λ_α = 0.71073 Å). The data collection strategy was interpreted by employing the CrysAlisPro CCD software. The collection of data was done by the standard phi-omega scan techniques. The data were scaled and reduced employing CrysAlisPro RED. The direct methods using SHELXS-97 was used to solve the crystal structures and refined by the full matrix least squares method with SHELXL-97, refining on F^2.[3] Olex-1.2 software was also used for structure solutions.[4] The H-atoms were placed at geometrically constrained positions and refined using isotropic temperature factors, generally 1.2 x U_{eq} of their parent atoms. All remaining non-hydrogen atoms were refined anisotropically. All the C–H···π interactions,[5] molecular drawings,[6] and mean plane analyses were obtained by Diamond (ver. 3.1d)[7] and Mercury (ver. 3.1)[8].

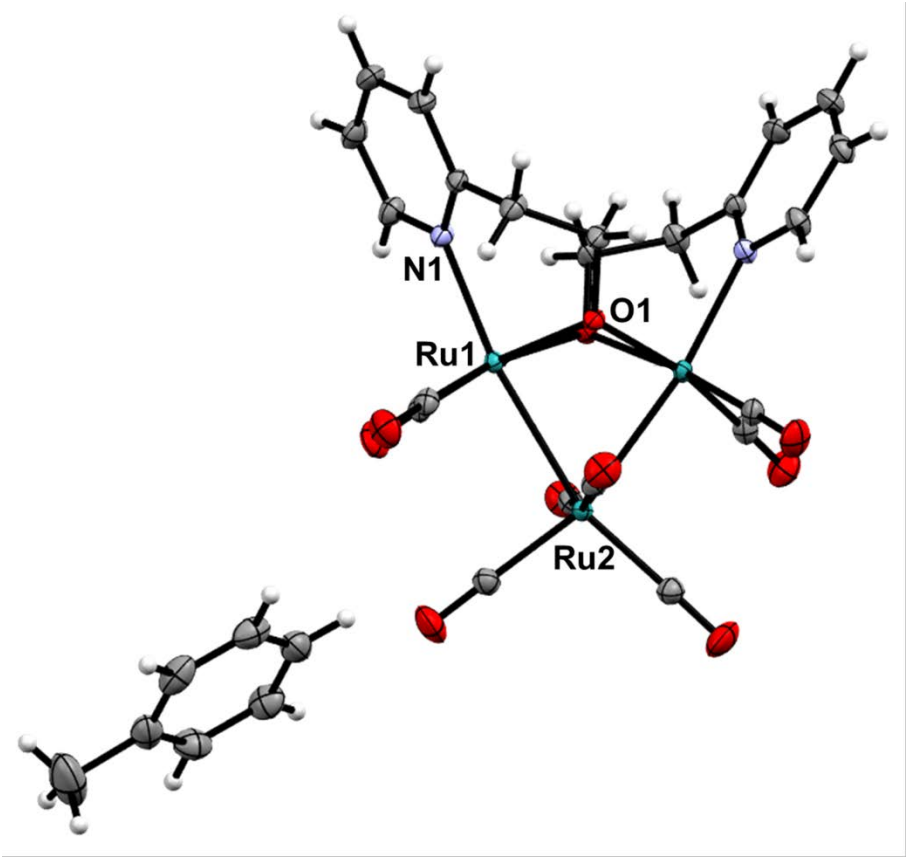

Fig. S75. Perspective view of **1**a

Table S5 Crystal data and structure refinement for **1a**

Identification code	**1a**
Empirical formula	$C_{36}H_{32}N_2O_{10}Ru_3$
Formula weight	955.84
Temperature/K	293
Crystal system	monoclinic
Space group	I_2/a
a/Å	18.6183(4)
b/Å	11.77089(19)
c/Å	17.3349(2)
α/°	90
β/°	107.9232(17)
γ/°	90
Volume/Å^3	3614.65(11)
Z	4
ρ_{calc} Mg/m^3	1.756
μ/mm^{-1}	1.297
F(000)	1896
Crystal size/mm^3	0.31 × 0.3 × 0.29
Radiation	Mo Kα (λ = 0.71073)
2Θ range for data collection/°	2.944 to 32.347
Index ranges	$-23 \le h \le 26$, $-16 \le k \le 16$, $-24 \le l \le 25$
Reflections collected	12688
Refinement method	Full-matrix least-squares on F^2
Independent reflections	5279 [R_{int} = 0.0219, R_{sigma} = 0.0226]
Data/restraints/parameters	5279/0/232
Goodness-of-fit on F^2	1.052
Final R indexes [I>=2σ (I)]	R1 = 0.0255, wR2 = 0.0650
Final R indexes [all data]	R1 = 0.0268, wR2 = 0.0661
Largest diff. peak/hole / e Å^{-3}	0.939/-1.421
CCDC No.	1539165

References

1. A. K. Saini, K. Natarajan and S. M. Mobin, *Chem. Commun.*, 2017, **53**, 9870-9873.
2. A. Chaudhary, A. Mohammad and S. M. Mobin, *Cryst. Growth Des.*, 2017, **17**, 2893-2910.
3. G. M. Sheldrick, *Acta Crystallogr., Sect. C: Struct. Chem.*, 2015, **71**, 3-8.
4. O. V. Dolomanov, L. J. Bourhis, R. J. Gildea, J. A. K. Howard and H. Puschmann, *J. Appl. Crystallogr.*, 2009, **42**, 339-341.
5. Y. V. Torubaev, K. A. Lyssenko, P. Y. Barzilovich, G. A. Saratov, M. M. Shaikh, A. Singh and P. Mathur, *CrystEngComm*, 2017, **19**, 5114-5121.
6. A. Singh, P. Kumari, A. Raghuvanshi, S. M. Mobin and P. Mathur, *Appl. Organomet. Chem*, 2018, **32**, DOI: 10.1002/aoc.4071.
7. K. B. G. H. Putz., Kreuzherrenstr. 102, 53227 Bonn, Germany, and http://www.crystalimpact.com/diamond.
8. C. F. Macrae, P. R. Edgington, P. McCabe, E. Pidcock, G. P. Shields, R. Taylor, M. Towler and J. v. d. Streek, *J. Appl. Cryst.*, , 2006, **39**, 453-457.